

Biochemical Characterisation of Photosystem I Complexes in Diatoms

Dissertation

zur Erlangung des Doktorgrades
der Naturwissenschaften

vorgelegt beim Fachbereich Biowissenschaften der
Johann Wolfgang Goethe – Universität
in Frankfurt am Main

von

Thomas Veith
aus Frankfurt am Main

Frankfurt 2009
(D30)

vom Fachbereich der
Johann Wolfgang Goethe – Universität als Dissertation angenommen.

Dekan:

Gutachter:

Datum der Disputation:

“Der Groschen ist kein Sturxbomber”

Contents

Abbreviations

viii

1 Introduction

1

- 1.1 Oxygenic photosynthesis 1
- 1.2 Structure of Photosystem I 8
- 1.3 Regulation of excitation energy distribution and electron flow 11
- 1.4 Aspects of photosynthesis in diatoms 14
- 1.5 Aims of this work 17

2 Materials and methods

20

- 2.1 Biological material 20
- 2.2 Cell culture 20
 - 2.2.1 *Phaeodactylum tricornutum* 20
 - 2.2.2 *Cyclotella meneghiniana* 21
 - 2.2.3 *Pisum sativum* 21
 - 2.2.4 *Synechocystis* sp. PCC 6803 21
- 2.3 Isolation of thylakoids 21
 - 2.3.1 *P. tricornutum* 22
 - 2.3.2 *C. meneghiniana* 22
 - 2.3.3 *P. sativum* 23
 - 2.3.4 *Synechocystis* sp. PCC 6803 23
- 2.4 Purification of pigment-protein complexes 24
 - 2.4.1 Ion exchange chromatography (IEX) 24
 - 2.4.2 Discontinuous sucrose gradient centrifugation 25
 - 2.4.3 Analytical gel filtration 25
 - 2.4.4 Concentration & washing of isolated pigment-protein fractions 26

2.5	Gel electrophoresis	26
2.5.1	Sodium dodecyl sulfate-polyacrylamide gel electrophoresis (SDS-PAGE)	26
2.5.2	Blue native-PAGE (BN-PAGE)	27
2.5.3	Coomassie staining	28
2.5.4	Silver staining	28
2.6	Protein transfer & immunodetection	29
2.6.1	Western Blot	29
2.6.2	Slot Blot	29
2.6.3	Immunodetection	30
2.7	Spectroscopy	31
2.7.1	Absorbance spectra	31
2.7.2	Determination of P700	31
2.7.3	Chlorophyll determination	31
2.7.3.1	Chlorophyll <i>c</i> containing algae	31
2.7.3.2	Higher plants	32
2.7.3.3	Cyanobacteria	32
2.7.4	Fluorescence spectra	32
2.8	High Performance Liquid Chromatography (HPLC)	33
2.9	Electron microscopy	33
2.10	Sequence comparison	34
3	Results	35
3.1	A monomeric PS I-FCP complex of <i>P. tricornutum</i>	35
3.1.1	Isolation of a PS I complex from <i>P. tricornutum</i>	35
3.1.2	Polypeptide composition of the PS I complex	36
3.1.3	Characterisation of the complex	38
3.1.4	Higher organisation of the PS I-FCP complex	45

<i>CONTENTS</i>	vii
3.1.5 Preparation yield	50
3.1.6 Analysis of the IEX fractions II and V	50
3.1.7 Purification of a PS I complex by discontinuous sucrose gradient centrifugation	52
3.2 Association of Fcp polypeptides with PS I in the diatom <i>C. meneghiniana</i>	55
3.2.1 Isolation of pigment-protein complexes	55
3.2.2 Polypeptide analysis	60
3.2.3 Further purification of PS I	62
4 Discussion	67
4.1 The monomeric PS I-FCP complex of <i>P. tricornutum</i>	68
4.2 Association of Fcp polypeptides with PS I of <i>C. meneghiniana</i>	76
4.3 Concluding remarks	84
5 Summary	86
6 Zusammenfassung	89
7 Acknowledgements	112
8 Curriculum vitae	114

Abbreviations

Å	Ångstrom
APS	ammonium persulfate
ATP	adenosine triphosphate
B1	buffer 1
BChl	bacteriochlorophyll
Bis-Tris	2-(bis(2-hydroxyethyl)amino)-2-(hydroxymethyl)propane-1,3-diol
BN-PAGE	Blue native-polyacrylamide gel electrophoresis
C	concentration [%] of bisacrylamide in relation to T, see T
cab proteins	Chl <i>ab</i> -binding proteins, see Chl
CET	cyclic electron transport
Chl	chlorophyll
cyt c_6	cytochrome c_6
Da	Dalton
DDM	<i>n</i> -dodecyl β -D-maltoside
ECL	enhanced chemiluminescence
EDTA	ethylenediaminetetraacetic acid
<i>fcp</i>	genes encoding fucoxanthin chlorophyll proteins
FCP	a complex of fucoxanthin chlorophyll proteins
Fcp	fucoxanthin chlorophyll proteins
FNR	ferredoxin:NADP ⁺ oxidoreductase, see NADP ⁺
HB	homogenisation buffer
HEPES	4-(2-hydroxyethyl)piperazine-1-ethanesulfonic acid
HPLC	high performance liquid chromatography
IEX	ion exchange chromatography
kDa	kilo Dalton, 1000 Dalton

λ	wavelength in nm
LET	linear electron transport
LHC	light-harvesting complexes
LWC	longwavelength chlorophyll
MALDI	matrix supported laser desorption/ ionisation
Mes	4-Morpholineethanesulfonic acid
MS	mass spectrometry
MW	molecular weight
NAD	nicotinamide adenine dinucleotide
NG	nonyl β -D-glucopyranoside
NADP	nicotinamide adenine dinucleotide phosphate
NPQ	non-photochemical quenching
OG	octyl β -D-glucopyranoside
<i>p.a.</i>	per analysi
PC	plastocyanin
PQ	plastoquinone
PS I	photosystem I
PS II	photosystem II
Psa	PS I subunit
Psb	PS II subunit
psi	pounds per square inch
PVDF	Polyvinylidene difluoride
Q	quinone
qE	energy dependent fluorescence quenching
qI	photoinhibition fluorescence quenching
qT	state transition fluorescence quenching
RB	resuspension buffer

RC	reaction centre
rpm	rounds per minute
rRNA	ribosomal ribonucleic acid
RT	room temperature
S	Svedberg
SB	sample buffer
SDS	Sodium dodecyl sulfate
SDS-PAGE	Sodium dodecyl sulfate-polyacrylamide gel electrophoresis
SU	subunit
T	concentration [%] of acrylamide and bisacrylamide
TEMED	N, N, N', N'-tetra-methylethylenediamine
TOF	time of flight
Tris	Tris(hydroxymethyl)aminomethane
TX 100	Triton X 100
WB	washing buffer

List of Figures

1	The light reaction of oxygenic photosynthesis	4
2	Photosystem I complexes of cyanobacteria and higher plants	9
3	General structure of a pennate diatom	14
4	IEX of solubilised thylakoids of <i>P. tricornutum</i>	36
5	Western Blot of IEX fractions III – V	37
6	SDS-PAGE & Western Blots of IEX fractions III & IV	38
7	Analytical HPLC of IEX fractions III & IV	40
8	Absorbance & fluorescence excitation spectra of IEX fractions III & IV	41
9	77 K fluorescence emission spectra of IEX fractions III & IV	42
10	Gel filtration & fluorescence excitation measurement of the IEX fraction III	44
11	Sequence comparison of PS I subunits from different organisms	46
12	BN-PAGE of the PS I-FCP complex	47
13	Gel filtration of thylakoids from <i>P. tricornutum</i> & <i>Synechocystis</i> sp.	48
14	Electron micrographs of the PS I-FCP complex	49
15	SDS-PAGE of the IEX fractions II & V	51
16	Western Blot of IEX the fractions II - V	51
17	Absorbance spectra of IEX fractions II & V	52
18	Discontinuous sucrose gradient centrifugation of solubilised thylakoids from <i>P. tricornutum</i>	53
19	Fluorescence emission of sucrose gradient fractions band 1 & 2	54
20	Discontinuous sucrose gradient centrifugation of solubilised thylakoids from <i>C. meneghiniana</i>	56
21	Absorbance and fluorescence emission spectra of the sucrose gradient fractions B, C, & D	57

22	77 K fluorescence emission and excitation spectra of the sucrose gradient fractions B, C, & D	58
23	Gel filtration of the sucrose gradient fraction D	59
24	SDS-PAGE and Western Blots of the sucrose gradient fractions B, C, & D	61
25	Discontinuous sucrose gradient centrifugation of re-solubilised fraction D	62
26	SDS-PAGE and Western Blots of purified fractions derived from re-solubilisation of fraction D and further separation by sucrose density centrifugation	63
27	HPLC diagram of pigment-protein fractions derived from sucrose gradient centrifugation	65
28	Absorbance spectra of the re-solubilised fractions NGOG _{1/2} & TX _{1/2} . .	66

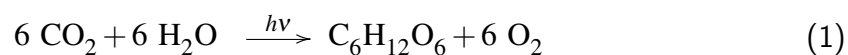
List of Tables

1	Molecular weight markers	27
2	Analytical HPLC of IEX fractions III & IV	39
3	Analytical HPLC of pigment-protein fractions derived from sucrose gradient centrifugation	64

1 Introduction

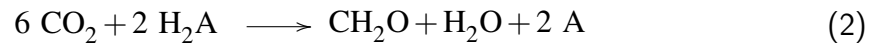
1.1 Oxygenic photosynthesis

The utilisation of sunlight as an energy source to drive the synthesis of carbohydrates from carbon dioxide and the generation of oxygen out of water as a “by-product” is described by the term “oxygenic photosynthesis”. Around 2.5 billion years ago oxygenic photosynthesis induced the change from an anoxygenic into an oxygen containing atmosphere. The generation of oxygen is essential for respiratory processes and causative for the UV protection by the ozone layer [1]. Concerning natural resources human civilisation gains its energy from recent and ancient oxygenic photosynthesis that led to e.g. fossil fuels. The net chemical reaction of oxygenic photosynthesis can be expressed by the following equation.



Photosynthesis research dates back to the 18th century when Charles Bonnet and Joseph Priestley made their discoveries. C. Bonnet observed bubbles being released from submerged leaves which were illuminated. J. Priestley discovered that an illuminated sprig of mint was capable of saving the life of a mouse being trapped in an enclosed chamber. Another milestone in early photosynthesis research was the discovery of Theodor W. Engelmann in the late 1800s who observed that aerophilic bacteria accumulate in the red and blue regions of dispersed sunlight (e.g. the chlorophyll action spectrum) used to illuminate cells of the filamentous green algae *Spirogyra*. The major discoveries in photosynthesis research were made in the last century of which some examples will be presented here. The first description of photosynthesis as a redox reaction by Cornelis B. van Niel who compared anoxygenic photosynthetic bacteria with oxygenic plants

culminated in the following formula:



and thus founded equation 1. The discovery of the “Enhancement effect” by Emerson and co-workers [2] created the basis of the two light systems (photosystem I and II, explained below) in photosynthesis by showing that the combination of red light and far red light increased the rate of photosynthesis more than the sum of both individual lights. Furthermore Robert Hill should be mentioned who discovered that the oxidation of water and the fixation of CO_2 are separate processes [3] and laid the grounds for the so called “z-scheme” for two light reactions [4]. However, within the scope of this work it is impossible to mention all the research on photosynthesis that has been done during the last 100 years (a nice review on the history of photosynthesis research can be taken from [5]).

The light reaction of oxygenic photosynthesis provides reduction equivalents in form of $\text{NADPH} + \text{H}^+$, and ATP to drive the dark reaction, the so called “Calvin-Benson-Bassham Cycle” [6] which leads to the fixation of CO_2 and the synthesis of triose-phosphates needed for the generation of sucrose or starch in eukaryotes. Both reactions are carried out in the chloroplast. It is generally accepted that the chloroplast derived from an endosymbiosis event [7]. 16S and 18S rRNA studies, as well as genome and protein sequence analysis proved the correlation between the chloroplast and cyanobacteria. It is assumed that a cyanobacterial-like prokaryote was engulfed by a eukaryote and subsequently developed into an organelle, capable of oxygenic photosynthesis. The separation of cyanobacteria from other bacteria is estimated to be around 2.6 billion years ago which is correlated with the rise of oxygen in the atmosphere. The endosymbiosis event occurred about 1.58 billion years ago and marks the divergence of animals, fungi, and plants [8]. Surprisingly, the plastids of the three eukaryotic lineages glaucophytes, rhodophytes (red lineage), and chlorophytes (green lineage, leading to the evolution of

higher plants) developed out of a single endosymbiosis event [9]. During the development of the plastid the prokaryotic genome was reduced - today approximately 100 out of 2500 proteins are still encoded in the "plastome" [10]. All the other genes are located in the nucleus of the (former) host and the proteins have to be imported from the cytoplasm into the chloroplast.

Chloroplasts are surrounded by two lipid bilayers enclosing a complex membrane lamellar system, the thylakoids. In contrast to mitochondria the second bilayer of chloroplasts is involved in metabolite transport. Whereas in mitochondria the site of oxidative phosphorylation is situated at the inner bilayer, photophosphorylation occurs in the thylakoid membrane of chloroplasts. Thylakoids carry *inter alia* the components of the light reaction. In higher plants and green algae thylakoids are organised into lamellar stacks, called grana thylakoids, and unstacked membrane regions, called stroma thylakoids. The whole thylakoid membrane system is interrelated and surrounds an internal space, the lumen. The space between the thylakoid membrane and the second bilayer is referred to as stroma. The light reaction is dependent mainly on four protein complexes, photosystem II (PS II), cytochrome b_6f , PS I, and the ATP synthase (see figure 1). As already mentioned, the main features in oxygenic photosynthesis are conserved between chloroplasts and cyanobacteria. PS II and PS I are huge protein complexes that are associated with non-covalently bound pigments, chlorophyll (Chl) *a* and carotenoids, that are capable of harvesting light and transfer its energy into the reaction centres (RCs). Both RCs contain specialised RC Chls, which upon excitation perform a charge separation and thus function as primary electron donors. According to their absorbance characteristics the RC II pigments are named P680 and RC I pigments are named P700. In case of PS II the primary electron is transferred via an accessory Chl and a pheophytin molecule to a tightly bound plastoquinone (PQ), Q_A . From there a mobile PQ, Q_B , is subsequently reduced. To reduce the oxidised $P680^+$, which possesses the highest redox potential

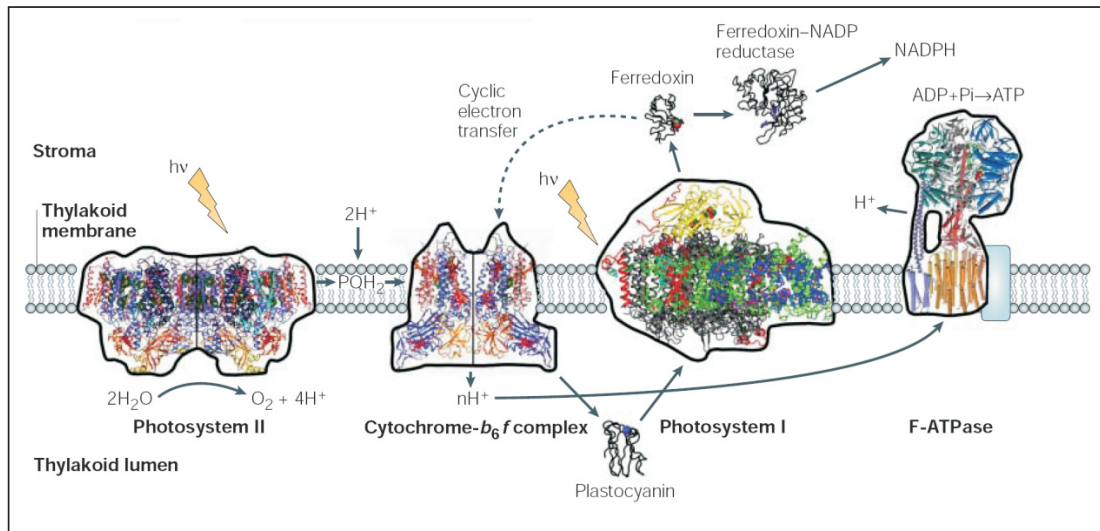


Figure 1: **The light reaction of oxygenic photosynthesis.** In this figure available structural data for the membrane-protein complexes driving the light reaction of oxygenic photosynthesis have been included in a general scheme of the thylakoid membrane. The relative sizes of the complexes were adjusted to plant photosystem I (PS I). Reactions and electron pathways are indicated including a cyclic electron-transfer pathway (dashed line). A lightning bolt symbolizes the light quanta ($h\nu$) that are absorbed by PS II and PS I. The image was taken from [11].

observed in nature (> 1 V), an electron is taken up from a nearby tyrosine, Y_Z . Y_Z then gets reduced by a manganese cluster, situated at the luminal site, which after four rounds of charge separation, oxidises two water molecules and produces 1 molecule of oxygen. Before that, after two rounds of charge separation, Q_B is reduced twice and capable of proton uptake at the stromal site. The Q_BH_2 is released into the lipid bilayer and replaced by another oxidised PQ out of a membrane quinone pool. Thus PS II can be defined as a water-PQ oxidoreductase. In the next step of the electron transfer chain the reduced PQH_2 (the former Q_BH_2) is oxidised at the Q_o site of the cytochrome b_6f complex, thereby the two protons are released into the lumen. One of the two uptaken electrons is transferred through the Rieske iron-sulphur protein and cytochrome f to reduce the water-soluble plastocyanin (PC). The other electron gets transported through two haem groups (bL and bH) of cytochrome b_6 and reduces a PQ bound to the Q_i

site, located at the stromal site. After a second reduction round the PQ located at Q_i takes up two protons and is released into the pool of reduced PQH_2 molecules. This mechanism is referred to as the Q cycle. The vectorial transport of H^+ by PQ induces a proton gradient over the thylakoid membrane which is used by the ATP-synthase. The cytochrome b_6f complex can be defined as a PQ-PC oxidoreductase. Upon charge separation at P700 (PS I), the oxidised special pair Chls are reduced by PC which moved from the cytochrome b_6f complex to PS I. The electron released by P700 is transferred over a row of co-factors named A (Chl *a*), the first stable electron acceptor A_0 (Chl *a*) with an extremely negative redox potential of -1.000 mV, A_1 (phylloquinone), and three iron-sulfur clusters (F_X , F_A , and F_B) to ferredoxin at the luminal site of PS I. A_0 , and A_1 represent pairs of co-factors like P700 itself. Thus electrons can migrate via two possible ways towards the iron-sulfur clusters, i.e the A- and the B-branch. The reduced ferredoxin plays a role in several biochemical processes e.g. desaturation of fatty acids, assimilation of nitrate and the generation of $NADPH+H^+$ ([11, 12] and references therein). Because the transport of electrons from water to ferredoxin has a unique direction, the whole process described is referred to as linear electron transport (LET). In contrast to cyanobacteria, PS II of higher plants and green algae is located in the grana thylakoids, whereas PS I is located in the stroma. This separation is thought to prevent a loss in efficiency of PS II, since PS I contains the lower energy pigments and needs less time until charge separation occurs. Thus, in case of mixed PS I and PS II populations, most of the excitons are supposed to be transferred towards PS I [13]. In case of cyanobacteria this is circumvented by the installation of huge light-harvesting antenna systems solely associated with PS II (see below).

As already introduced above, photosynthetic RCs are divided into two groups: type I RCs that direct electrons through a series of iron-sulfur-clusters, whereas type II RCs transfer electrons to a mobile quinone (Q). In contrast to cyanobacteria and photosyn-

thetic eukaryotes, anoxygenic photosynthetic bacteria contain only one type of RC and only one PS. As an example green sulfur bacteria and heliobacteria possessing type I RCs and purple bacteria possessing type II RCs should be mentioned. Among other differences bacteriochlorophylls (BChl) are used instead of Chls. Therefore, due to changed absorbance characteristics the RC BChls of purple bacteria are named P870 (BChl *a*) or P960 (BChl *b*). Another difference is the use of e.g. sulfur containing compounds instead of water as electron donor. Since water is not oxidised, no oxygen is evolved. Interestingly, both anoxygenic RC types have functional and structural similarities with PS I and PS II, indicating a common ancestry. In addition RC II of purple bacteria was the first membrane protein to be crystallised and whose structure was resolved by x-ray structure analysis in 1984. The resolved structure laid the grounds also for the understanding of structure and function of PS II [14–16].

Despite the conservation of the pigment protein complexes involved in the electron transport chain in the thylakoid membrane, the structure of the light harvesting systems differ considerably. Whereas cyanobacteria and red algae possess membrane extrinsic light harvesting systems, called phycobilisomes, several eukaryotic algae and higher plants contain membrane intrinsic light harvesting complexes (LHCs). The phycobilisomes form rod-like structures, composed of water-soluble phycobiliproteins that covalently bind bilin chromophores (open chain tetrapyrroles) via cysteine residues. The rods are built of hexameric discs containing α and β polypeptides. Three types of phycobiliproteins can be discriminated: phycocyanin, allophycocyanin, and phycoerythrin, which differ in their protein sequence and the pigments bound. The latter usually binds phycoerythrobilin and is located at the end of the rod structure. Phycocyanin binds phycocyanobilin and is located between the phycoerythrin and the phycobilisome core. Whereas phycocyanin and phycoerythrin are usually located in rods radiating into the stromal surface, allophycocyanin forms the core of the phycobilisomes in close proximity

to the surface of PS II. Because of the membrane extrinsic phycobilisomes cyanobacteria do not possess grana stacks as observed in higher plants. In contrast, the membrane intrinsic LHCs of higher plants and eukaryotic algae bind the pigments Chl *a*, Chl *b* as well as carotenoids non-covalently. In the green lineage LHCs can be divided roughly into two groups, LHC II functioning as PS II antenna and LHC I as PS I antenna. The latter is encoded by the genes *lhca1-4* and forms a crescent shape composed of two heterodimers around the PS I complex in higher plants [17]. However, in case of green algae, a number of up to 10 different LHC I proteins are supposed to be associated with PS I [18, 19]. The LHC II proteins are encoded by the genes *lhcb1-6*. *Lhcb1* and *2* belong to the most abundant proteins in the thylakoids of the green lineage. Joined by the minor *Lhcb3* protein the three form a trimeric complex, the major LHC II. The three other genes encode three monomeric proteins, CP29, CP26, and CP24. The latter are more closely associated with the PS II core complex [20–23].

The light harvesting antennas described, absorb light energy which cannot be used directly by Chl *a* molecules associated with the PSs. The arrangement of phycobilisomes with pigments absorbing at the shortest wavelength (phycoerythrobilin) at the distal and the longer wavelength absorbing pigments at the proximal part of the antenna, leads to an resonance energy transfer from the antennae into the RC II by a nonradiative mechanism commonly known as “Förster transfer” [24, 25]. According to the Planck equation $E = hc/\lambda$ light quanta with short wavelengths contain a higher energy level than the light quanta with longer wavelengths. For this reason pigments absorbing light quanta with shorter wavelengths reach a higher excited state and light energy can be transferred downhill into the RCs [14]. Though having a fundamental different structure, LHCs transfer light energy to the RCs by the same mechanism. Because LHCs bind Chl *b* and a different subset of carotenoids the spectrum of light used for photosynthesis is increased in comparison to the spectrum used by the PSs.

1.2 Structure of Photosystem I

PS I is a huge membrane protein complex consisting of 12 protein subunits in cyanobacteria [26] and 15 protein subunits in higher plants [27]. In the latter, PS I supercomplexes with (at least) four light harvesting complex (LHC I) subunits are formed. This supercomplex was crystallised in 2004 at a resolution of 4.4 Å and though containing “only” 12 of the core subunits (plus the LHC I) approximately 200 cofactors are coordinated [17, 28]. Whereas plant PS I is of monomeric nature, cyanobacteria contain PS I trimers. The cyanobacterial PS I structure was determined to a resolution of 2.5 Å (see figure 2) [26] and the molecular weight of PS I trimers was calculated to be 1 056 000 Da. The cyanobacterial PS I represents one of the largest membrane protein complexes whose structure was determined. Each monomer contains 96 chlorophylls (101 in higher plants), 22 carotenoids, three Iron-sulfur [4Fe4S] clusters, and two phylloquinone molecules [12, 29]. Based on the crystal structures, theoretical modeling revealed strong conservation between higher plant and cyanobacterial PS I cores not only concerning the protein but also antenna pigments and carriers in the electron transport chain. Thus approximately one billion years of evolution did not change the main structure of such a huge and complicated membrane protein complex as PS I [31]. A characteristic of PS I of higher plants, algae, and cyanobacteria is the presence of so called “longwavelength Chls” (LWC). LWCs are antenna Chls which absorb at wavelengths longer than 700 nm, i.e. comprising of a lower excited state as P700. They are located in the PS I core (cyanobacteria) and/or in peripheral light-harvesting antennae (higher plants, green algae). They comprise of an unknown but efficient uphill energy transfer at physiological conditions towards P700 and thus broaden the spectrum usable for PS I. Another function of LWCs could be the dissipation of energy under over-excitation of PS I [32]. The two largest and most important subunits (SUs) of PS I are PsaA and PsaB. They harbour most of the cofactors of the electron transport chain already described in the previous section but also bind the biggest part of the antenna Chls (85). This is in contrast to

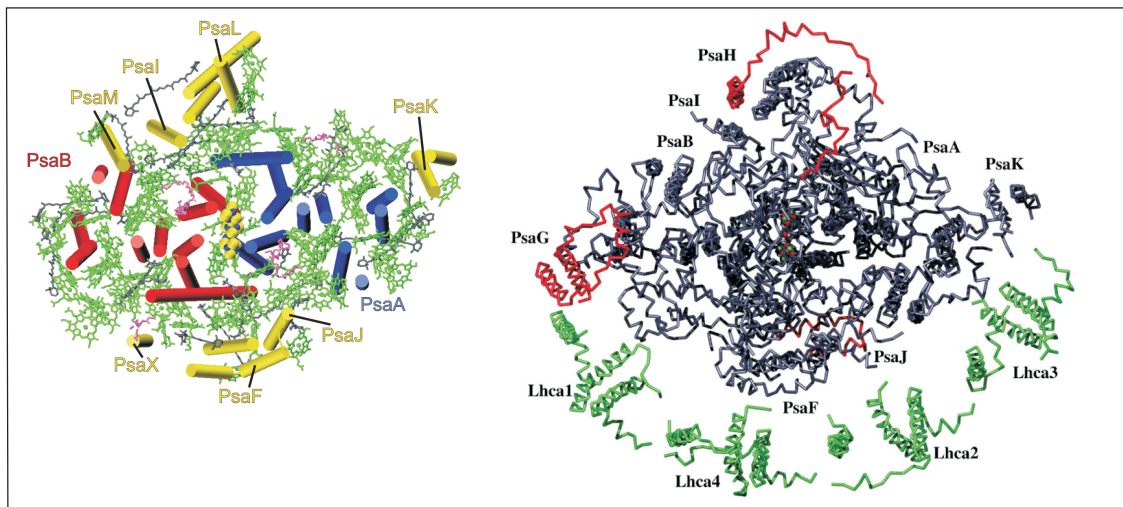


Figure 2: **Photosystem I complexes of cyanobacteria and higher plants.** On the left the structure of cyanobacterial PS I monomers based on the crystal structure published in 2001 [26] is shown as seen from the stroma. The trimerization site can be found on the top of the picture. PsaA is shown in blue, PsaB in red, the small subunits with transmembrane helices in yellow, the stromal subunits in white, chlorophylls in green, carotenoids in grey, lipids in mauve, and iron-sulfur clusters with yellow/blue spheres. The picture was taken from [30]. On the right side the corresponding structure of plant Photosystem I is presented, taken from [17]. The LHC I is shown in green (Lhca1-4) and structural elements within the RC not present in the cyanobacterial counterpart are colored red. Conserved features of the RC are in grey. The three iron-sulfur clusters are depicted as red (Fe) and green (S) balls. The SUs of both structures are indicated.

PS II where the cofactors are exclusively bound by the RC subunits D1 and D2 but the inner antenna Chls are coordinated by the SUs CP43 and CP47 [12]. Both PsaA and -B comprise of a molecular mass above 80 kDa, each containing 11 α -helices which form a heterodimer with a pseudo-twofold symmetry perpendicular to the membrane. α -Helices 7 to 11 (g to k) build the RC domain and coordinate 25 antenna Chls plus 6 Chls of the RC. α -Helices 1 to 6 (a to f), i.e. the N-terminal domain, coordinate 54 Chls and are arranged in “trimers of dimers”, similar to the core antenna of PS II (CP43 and CP47). A characteristic of the special pair chlorophylls of the RC (P700) is that they do not consist of two Chl *a* molecules but of one Chl *a* and a Chl *a'*. The Chl *a'* represents a Chl *a* epimer at the C13 position of the chlorin ring system and is located at the A-branch

[12, 26, 33]. Whereas the Chl *a'* is coordinated by three hydrogen bonds, the Chl *a* at the B-branch forms no hydrogen bonds to the protein environment. This asymmetry is supposed to induce differences in the redox potentials of the two pigments and might explain that the B-branch is preferred by the unpaired electron of P700⁺ [12]. Currently it is discussed whether not the special pair Chls represent P700 but the intermediate Chls termed A [34]. Furthermore, PsaA and -B provide the binding site for PC via two loop regions at the luminal site of the membrane [35]. Here it should be mentioned that in cyanobacteria and eukaryotic algae PC can be replaced by cytochrome *c*₆ (cyt *c*₆, also called cyt *c*₅₅₃) depending on the availability of iron and copper. Though being of a complete different structure (four α -helices and a heme for cyt *c*₆ and a β -barrel with eight β -strands plus a type-I blue copper centre for PC) both comprise of identical masses (10 kDa), similar isoelectric points and a midpoint redox potential of 350 mV at pH 7.0 [36]. In higher plants and green algae an elongated N-terminal domain of subunit PsaF provides a modified binding of PC with a faster electron transfer compared to cyanobacteria [37, 38]. In cyanobacteria as well as higher plants SUs PsaC, -D, and E provide the docking site for ferredoxin. PsaC also binds the two final [4Fe4S] clusters *F_A* and *F_B*. Again differences between higher plants and cyanobacteria are observed. Whereas the ferredoxin:NADP⁺ oxidoreductase (FNR) interacts with subunit PsaE in higher plants, in cyanobacteria ferredoxin moves away from PS I [38, 39]. Under iron deplete conditions also ferredoxin can be replaced by flavodoxin in cyanobacteria and algae [40, 41]. Beside the organisation into trimers (cyanobacteria) and monomers (higher plants), several additional and unique subunits can be found in both lineages. In cyanobacteria the subunits PsaM and PsaX are supposed to play a role in the stabilisation of the core antenna system similar to other smaller PS I subunits [26]. However, up to now, PsaX is found only in thermophilic cyanobacteria and might therefore play a special role [35]. In contrast, higher plants contain the additional subunits PsaG, -H, -N, -O, and -P. Whereas PsaG and N are supposed to be involved in the PC binding

at the luminal surface, PsaH, -O, and -P seem to play a role in the binding of LHC II under state transitions (see below), together with other subunits [27].

1.3 Regulation of excitation energy distribution and electron flow

Fluctuation of light intensities and quality can lead to the preferential excitation of one of the two PSs. For LET the rate of operation of both PSs has to be balanced. One short-term adaptation process of higher plants and green algae called “state transition” leads to a movement of antenna complexes from one PS to the other. LHC II antenna contains more Chl *b* than the LHC I antenna and thus broadens the spectrum of absorbed light. If PS II is preferentially excited, an over-reduction of the PQ pool occurs, followed by the binding of PQH₂ to the cytochrome *b₆f* complex. Subsequently, kinases are activated which lead to the phosphorylation of LHC II and induces its delocalisation from the grana. Phosphorylation occurs at threonine residues located at the stroma exposed N-termini of LHC II [42]. Thereupon, the affinity to PS II is decreased. Finally, LHC II associates with PS I. This state is referred to as state 2. The removal of LHC II occurs under preferential excitation of PS I leading to an oxidation of the PQ pool. The following association of LHC II and PS II is termed state 1. To summarise, state 1 is obtained in darkness or upon illumination with wavelengths of light ≥ 700 nm, whereas state 2 occurs at light qualities ≤ 650 nm. Transition from state 1 to state 2 can be followed by measuring the Chl fluorescence of PS II which decreases upon the removal of the LHC II antennae. This state transition quenching is referred to as qT and belongs to processes of non-photochemical quenching (NPQ, explained below). Beside the movement of LHC II also the general structure of the thylakoids is affected. The stacks of grana thylakoids are mainly dependent on electrostatic forces, i.e. cation mediated interaction of proteins in opposing membranes. Upon phosphorylation (i.e.

increase of negative charges) and removal of LHC II from PS II during state transition, one of the main forces that keeps the grana membranes attached is reduced. Hence, the number and size of grana thylakoids decrease [27, 38, 43–45]. The comparison between state transitions in green algae and higher plants revealed that in green algae around 80 % of LHC II migrates from PS II to PS I, whereas in higher plants only 10 – 20 % of LHC II is transferred. This observation might be explained by the fact that grana stacking in green algae is less pronounced and the LHC II kinases have a higher accessibility [46].

Another adaptation process involving PS I is the so called “cyclic electron transport” (CET). In contrast to the LET, electrons delivered by PS I are used for reduction of either the PQ pool or a direct transfer to the Q_i site of the cytochrome b_6f complex. Three possible pathways are discussed: Reduction of the PQ pool via a NADH dehydrogenase of the respiratory chain (cyanobacteria) or a special ferredoxin:plastoquinone oxidoreductase, and the direct transfer of electrons from ferredoxin towards the Q_i site mediated by the FNR. The function of the CET seems to be dual. Because no $\text{NADPH} + \text{H}^+$ is generated but the proton gradient across the thylakoid membrane is preserved, ATP is still synthesised. Since during CO_2 fixation in the Calvin-Benson-Bassham Cycle more ATP than $\text{NADPH} + \text{H}^+$ is needed, CET is thought to create a balance. Beside that, the ΔpH gradient across the thylakoid membrane is also influenced by CET [47]. In case of increased CET the lumen gets acidified due to the constant proton pumping at the cytochrome b_6f complex. Acidification of the lumen activates another regulatory process, the energy dependent quenching (qE). qE diminishes the over-excitation of PS II by heat dissipation which can be monitored by a decrease in fluorescence (fluorescence quenching). This process involves the de-epoxidation of xanthophyll pigments. Low pH activates a de-epoxidase which associates with the thylakoid membrane and converts violaxanthin (2 epoxide groups) via antheraxanthin (1 epoxide group) to zeaxanthin (no epoxide). A direct de-excitation of Chl *a* by zeaxanthin (and probably antheraxanthin)

is supposed because the lowest singlet excited state of the latter is below that of $^1\text{Chl}^*$. Another factor involved is the PsbS protein which probably binds zeaxanthin but its actual function is still a matter of debate [48]. qE is only one mechanism of NPQ, which can be generally defined as processes leading to fluorescence quenching that are not involved in primary photochemistry [49]. Besides qE also qT (state transition, see above), and qI (photo-inhibition) should be mentioned. However, apart from its impact on photoprotection and balancing of the electron transfer in photosynthesis, it is discussed that CET might occur constantly in stroma regions “far off” the grana margins, whereas LET is located near grana stacks. Steric hindrance in the grana stacks would promote LET because the FNR has no accessibility towards the cytochrome b_6f complex. In stroma thylakoids the distance for PQH_2 to reach the cytochrome b_6f complex might be too large and therefore CET is induced. [46, 47].

As already mentioned above, iron deplete conditions lead to the exchange of ferredoxin by flavodoxin in cyanobacteria. Flavodoxin is encoded on the *isiAB* (iron stress induced) operon, more precisely by the *isiB* gene. The *isiA* gene encodes the *isiA* protein also referred to as CP43' because of its homology with CP43, the RC II antenna protein. However, *isiA* is not associated with PS II but forms a ring system of 18 subunits around the trimeric PS I complex of cyanobacteria as has been shown by single particle analysis [50, 51]. Thus under iron starved conditions supercomplexes with intrinsic antenna proteins are formed in cyanobacteria. The *isiA*-PS I complex has a molecular mass of about 2.000 kDa and increases the number of Chl *a* per P700 to 174. As a consequence the absorbance cross section of PS I is doubled and efficient energy transfer was proven by spectroscopical means [52, 53].

1.4 Aspects of photosynthesis in diatoms

Diatoms (*Bacillariophyceae*) are unicellular, eukaryotic algae that carry out oxygenic photosynthesis and represent one of the most successful taxonomic groups with approximately 100,000 species. It is believed that diatoms contribute close to one quarter of global primary production [54, 55]. The most remarkable feature of diatoms is the highly patterned cell wall composed of amorphous silica $[(\text{SiO}_2)_n(\text{H}_2\text{O})]$. The cell walls can be divided into two halves of equal shape with the smaller hypotheca fitting into the larger epitheca (see figure 3). They inhabit marine and fresh water environments as well as soil and have a strong impact on the biogeochemical cycles of carbon, nitrogen, phosphorus, and silica. Diatoms can be divided into two classes, the centrics (*Mediophyceae*) with a radial symmetry and the pennate (*Bacillariophyceae*) with a bi-lateral symmetry. Fossils of centric diatoms were estimated to be 180 million years old, whereas fossils of the younger pennates were 90 million years old ([56] and references therein). The general features of their photosynthetic apparatus resemble those of higher plants and cyanobacteria, yet

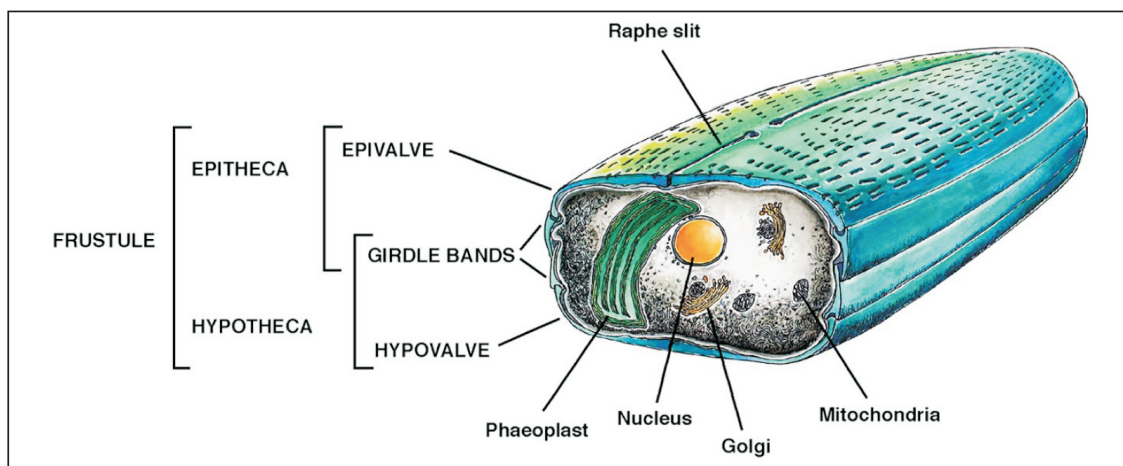


Figure 3: **Scheme of the general structure of a pennate diatom.** Features of the diatom cell wall and several organelles are presented. Note that the chloroplast is referred to as phaeoplast because of its brown colour. The image was taken from [54].

there are some important differences. Diatoms derived from a secondary endosymbiotic event. An as yet unknown eukaryotic host domesticated a phylogenetically related red alga. This endosymbiosis event led to the phenomenon that chloroplasts of diatoms are surrounded by four membranes. Another characteristic of diatom chloroplasts is the even arrangement of thylakoids in bands of three, instead of an organisation into stroma and grana lamellae [57]. Consequently, PS I and PS II are not segregated as in higher plants which has been visualised by immuno-cytochemical experiments [58]. Recently, the genomes of two diatoms, the centric *Thalassiosira pseudonana* and the pennate *Phaeodactylum tricornutum*, were published [56, 59]. Surprisingly, only 57 % of genes are shared between both diatoms although the divergence of centrics and pennates is only 90 million years ago. Furthermore a high number of bacterial genes were found (approximately 5 %), which argues for a strong horizontal gene transfer in diatoms. In case of *T. pseudonana* a progressing gene transfer was observed, i.e. the movement of a chloroplast gene into the nucleus, as copies of the *psb28* were identified on the chloroplast genome and the nuclear genome. The latter possesses a chloroplast transit peptide sequence, which was not found in the chloroplast gene proving the plastidic localisation of the gene product. The same gene in *P. tricornutum* is only found in the chloroplast genome [60].

In the last years the focus laid mainly on biochemical and spectroscopic analyses of the LHCs of diatoms, the fucoxanthin chlorophyll proteins (Fcps) [see e.g. 61–64]. Although Fcps belong to the family of cab proteins (Chl *ab*-binding proteins) like LHC II of the green lineage their pigmentation differs from LHC II of higher plants. Fcps bind fucoxanthin instead of lutein, Chl *c* instead of Chl *b*, and their Chl *a*:carotenoid stoichiometry is 1:1 in contrast to a 2:1 ratio in LHC II [65, 66]. Furthermore, the hydrophilic loop regions connecting the transmembrane spanning helices of Fcps are shortened in comparison to higher plant LHCs. Upon protein binding the absorbance of fucoxanthin

is shifted to the red thus absorbing from 460 nm to 570 nm, a spectral range not used by higher plants and green algae. Furthermore, diatoms exhibit a special xanthophyll cycle during NPQ, converting diadinoxanthin into diatoxanthin in one de-epoxidising step. In contrast to the xanthophyll cycle in higher plants the diatom de-epoxidase can be rapidly activated and possesses a broader pH optimum than its counterpart [67]. As the PsbS protein is not found in the published diatom genomes it is supposed that diatoxanthin is coordinated by the Fcp antennae [56, 59, 68]. The direct participation of diatoxanthin as fluorescence quencher in an isolated FCP complex was recently described [69].

Fcps can be placed into three groups according to sequence homologies. Group I, represented by e.g. the genes *fcp1-3* and 5 of *Cyclotella cryptica* and *fcpA-F* of *Phaeodactylum tricornutum* relate with Fcps of brown algae. The gene *fcp4* of *C. cryptica* and homologues of *P. tricornutum* and *Thalassiosira pseudonana* belong to group II and are related with a PS I associated, intrinsic light harvesting protein lhca-R1/2 of red algae and cryptophytes. The third group shares homologies with LI818r-3 of *Chlamydomonas reinhardtii*, a member of the LHC family, and is represented by the genes *fcp6*, 7, and 12 of *C. cryptica* [56, 57, 59, 70–72]. Despite the knowledge about various gene sequences of Fcps, the knowledge about Fcps on the protein level and their association with the photosystems remains scarce. Since Fcps possess high sequence similarities, small differences in molecular weight, and a strong hydrophobic character, it becomes a challenge to differentiate between polypeptides by immunological methods or sequencing. Nevertheless, in *C. meneghiniana* a FCP trimer and a higher oligomer have been isolated and the associated Fcp polypeptides were identified [61, 62]¹. The FCP trimer, named FCPa, is mainly constituted of 18 kDa subunits encoded by the *fcp2* gene. In smaller amounts also 19 kDa subunits encoded by *fcp6* could be identified. In the higher

¹In the following parts of the thesis, FCP complexes will always be written with capital letters. In case of Fcp polypeptides only the first letter will be capitalised, whereas genes will be emphasised by italic format and small letters, respectively.

oligomer FCPb, probably a hexa- or nonamer, only 19 kDa subunits were detected, encoded most probably by the *fcp5* gene. Recently, trimeric and hexameric FCP complexes were also described in *P. tricornutum* with subunits encoded by the genes *fcpC/D* and *fcpE* [64]. Thus, not only the pigment arrangement but also the assembly into higher oligomeric states seems to distinguish FCP complexes from higher plant LHC II trimers, although for LHC II icosienamers have been described as well [73].

In the 1980s, PS I cores without associated antenna complexes were isolated from diatoms [74, 75]. Later, more gentle solubilisation conditions lead to functional PS I complexes with light harvesting proteins bound [76]. However, with respect to polypeptide composition and pigment content the Fcps associated with PS I were indistinguishable from the main antenna complexes. The authors concluded that only one antenna system exists in diatoms, which serves both photosystems. This is in line with a recent report by Brakemann et al. [77], who demonstrated the occurrence of Fcp2 and Fcp4 polypeptides of *C. cryptica* in both the PS I and the PS II fraction isolated by sucrose gradient centrifugation. Sadly, recent publications from a Japanese group that isolated PS I as well as PS II complexes did not explore the composition of the bound Fcps [78, 79]. Thus, composition and association of Fcps with the two PSs is still unclear.

1.5 Aims of this work

Despite the biological relevance of diatoms and their impact on global primary production our knowledge about the structural architecture of the membrane protein complexes that drive the light reactions of oxygenic photosynthesis is relatively poor. Although the core structures of PS I and PS II are strictly conserved and the light-harvesting antennae of diatoms share their principal motifs with LHCs of higher plants and green algae, the pigment arrangement differs considerably. Chl *b* is replaced by Chl *c*, lutein by fucoxanthin, and the xanthophyll cycle pigments zeaxanthin, antheraxanthin and, violaxanthin

were substituted by diatoxanthin and diadinoxanthin. Furthermore the stoichiometry between chlorophylls and carotenes of the LHCs is dramatically changed. Because of the high content of fucoxanthin the light-harvesting complexes of diatoms are referred to as Fcps (fucoxanthin-chlorophyll binding proteins). Considering the different pool of diatom pigments, the pigment-protein interactions must be different. As an example Chl *c* is mentioned which lacks the phytol chain present in Chl *a* and Chl *b* and thus comprises of an increased polarity. In contrast, the Fcps themselves possess shortened loop regions in comparison to LHCs. As a consequence the ratio of membrane intrinsic regions compared to the whole protein is increased and thus also the hydrophobicity of Fcps. Hence, if the Fcps are structurally different from LHCs of higher plants and green algae, also the Fcp binding motifs of PS I and PS II are certainly affected. Up to now, no structure is available from any of these protein complexes of diatoms. In addition, also the association of Fcp polypeptides with the PSs is unclear. It can be speculated if only one type of antenna exists that serves both PSs or if indeed PS specific Fcp polypeptides exist.

In this work two strategies were followed to study PS I complexes of diatoms. The first strategy involved the development of a purification protocol for a PS I complex of the pennate diatom *Phaeodactylum tricornutum*. Besides the biochemical and spectroscopical analysis of this complex, also the pigment content and functionality were to be determined. Furthermore the isolated complex should be applicable also for electron microscopy studies. As the structural analysis of 2 D or 3 D crystals need a long time until good resolutions are obtained, single particle analysis of electron micrographs provide a good alternative to yield supramolecular structures. Thus a method that lead to the isolation of PS I particles usable for electron microscopy build the basis for revealing the first supramolecular structure of such complexes. The results on this part of the thesis was previously published in [80].

The second strategy took advantage of antibodies directed against specific Fcp polypeptides of the centric diatom *Cyclotella cryptica*. As the antibodies were not functional for *P. tricornutum* but for *Cyclotella meneghiniana* the association of Fcp polypeptides with PS I should be studied in the latter organism. Furthermore, the PS I associated antennae should be compared to the free FCP complexes and PS II. As previous studies indicate that parts of the Fcps are tightly associated with the PS I core [81, 82], re-solubilisation experiments were thought to subsequently remove the respective polypeptides. Thus a consecutive immunological analysis should tell something about the binding and organisation of Fcps with PS I.

2 Materials and methods

All chemicals were purchased in p.a. from Carl Roth, Karlsruhe (Germany), Merck (Darmstadt, Germany), or Serva (Heidelberg, Germany) if not otherwise indicated.

2.1 Biological material

Cyclotella meneghiniana Kützing (SAG 1020-1a)

Phaeodactylum tricornutum Böhlin (SAG 1090-1a)

Synechocystis sp. PCC 6803

Pisum sativum (Kleine Rheinländerin)

2.2 Cell culture

All media mentioned in this section were prepared under sterile conditions under a flow hood (Gelaire, BSB 4A) using autoclaved (121 °C, 20 min) or filtered (Millipore, 2 µm cut-off) solutions.

2.2.1 *Phaeodactylum tricornutum*

Batch cultures of *P. tricornutum* were grown for 10 - 14 days at 18 °C on a shaker (120 rpm) in ASP medium (86 mM NaCl, 4 mM Tris, 21 mM KCl, 8.1 mM MgSO₄, 11.8 mM NaNO₃, 0.58 mM K₂HPO₄, and 0.16 mM H₃BO₃ were adjusted with H₂SO₄ to a pH of 7.7, autoclaved and supplemented with the following trace metals: 2.72 mM CaCl₂, 0.092 mM Na₂-EDTA, 0.012 mM FeCl₃, 0.02 mM MnCl₂, 0.002 mM ZnCl₂, 50 pM CoCl₂, 25 pM Na₂MoO₄, 22.5 pM CuCl₂), a modified version of the protocol published by [83] under a 16 h light (40 µmol m⁻² s⁻¹) to 8 h dark cycle.

2.2.2 *Cyclotella meneghiniana*

Batch cultures of *C. meneghiniana* were grown for 14 days on a shaker (120 rpm) under the same conditions as described for *P. tricornutum* in ASP medium supplemented with 1 mM silica.

2.2.3 *Pisum sativum*

Plants were grown on vermiculit (Klein Dämmstoffe) at room temperature (RT) under room light conditions.

2.2.4 *Synechocystis* sp. PCC 6803

Cells of *Synechocystis* sp. PCC 6803 were a kind gift of G. Sandmann (Frankfurt University). Cells were grown under continuous light ($35 \mu\text{mol m}^{-2} \text{s}^{-1}$) at 28 °C in BG11 medium (1 l of medium contained 1.5 g NaNO₃, 30.5 mg K₂HPO₄, 20 mg Na₂CO₃, 75 mg MgSO₄ × 7 H₂O, 36 mg mM CaCl₂ × 2 H₂O, 6.6 mg NH₃Fe-citrate, 1 mg Na-EDTA, 2.86 mg H₃BO₃, 1.81 mg MnCl₂ × 4 H₂O, 0.222 mg ZnSO₄ × 7 H₂O, 0.39 mg Na₂MoO₄ × 2 H₂O, 0.079 mg CuSO₄ × 5 H₂O, 0.049 mg Co(NO₃)₂ × 6 H₂O published by [84] supplemented with 5 mM TES (pH 8.0) and bubbled with 1.5 CO₂ in air for 4 days. 24 h prior to cell harvesting 100 mg/l penicillin G was added [85].

2.3 Isolation of thylakoids

During the preparation of the membranes, samples, and buffers were kept on ice or at 4 °C. Only pre-cooled equipment was used and the illumination of the samples was strongly avoided.

2.3.1 *P. tricornutum*

Cells were always harvested during a 30 min time period after the onset of the light cycle. The cells were pelleted by a 10 min centrifugation at 5000 rpm and 4 °C (Herolab HiCen 21 C centrifuge, rotor: A6.9, Hermle) and resuspended in less than 20 ml of homogenisation buffer 1 (HB1) containing 10 mM HEPES, 2 mM KCl, 5 mM EDTA (Merck), and 1 M Sorbitol at pH 7.4. Cell breakage was performed by a double frenchpress cycle (Polytec/Thermo) at 20,000 psi cell pressure (1,280 psi gauge pressure). To prevent a contamination with unbroken cells, the homogenate was spun for 2 min at 3,000 *g* (Biofuge primo R, Heraeus) and the supernatant was collected. The pellet was resuspended in HB1 and centrifuged as described above. Both supernatants were combined and the centrifugation step was repeated. The final supernatant was then ultracentrifuged for 20 min at 45,000 rpm (Sorvall Discovery 90 SE ultra centrifuge, rotor: T-865). The pellet was resuspended in washing buffer 1 (WB1 = HB1 without sorbitol) and spun for 20 min at 40,000 rpm (Sorvall Discovery 90 SE ultra centrifuge, rotor: T-865). After resuspending the pellet in WB1 the chlorophyll content was determined. Thylakoids were then used directly for further experiments or frozen by liquid nitrogen and stored in aliquots containing 0.5 mg chlorophyll (Chl) at -20 °C.

2.3.2 *C. meneghiniana*

Preparation of thylakoids was done as described under 2.3.1 with the following variations. The cells were pelleted by a 15 min centrifugation at 5,000 rpm and 4 °C (rotor A6.9, Hermle) and resuspended in homogenisation buffer 2 (HB2) containing 10 mM Mes, 2 mM KCl, 5 mM EDTA (Merck), and 1 M Sorbitol at pH 6.5. The double frenchpress cycle was performed at 8,000 psi cell pressure (520 psi gauge pressure). Cell debris and unbroken cells were removed by 15 min centrifugation at 1,000 rpm (Biofuge primo R, Heraeus). The first ultracentrifugation step was extended to 1 h and sedimented thylakoids were resuspended in washing buffer 2 (WB2 = HB2 without sorbitol).

2.3.3 *P. sativum*

Thylakoids were isolated from 10 – 14 days old plants according to [86] with minor modifications. The upper third of the plants was cut off and approximately 30 g were grinded in cold isolation medium (10 mM Tricin at pH 7.8, 33 mM sorbitol) in a Waring blender with two pulses for 10 s. The homogenate was filtered through a threefolded mesh of Miracloth (Calbiochem) and centrifuged at 5,000 rpm and 4 °C for 3 min (Herolab HiCen 21 C centrifuge, rotor AS 4.13, Hermle). The pellet was resuspended in 200 ml solution A (1 mM Tricin at pH 7.8, 10 mM NaCl) and centrifuged again for 10 min. After repeating the step before in 100 ml solution A, the pellet was resuspended in 100 ml solution B (1 mM Tricin at pH 7.8, 10 mM NaCl, 5 mM EDTA) and left on ice for 30 min. The sample was pelleted at 10,000 rpm for 10 min (Herolab HiCen 21 C centrifuge, rotor: SS 34), resuspended in 40 ml solution C (100 mM sorbitol, 5 mM EDTA), and centrifuged again. The pellet was resuspended in solution D (100 mM sorbitol) and the chlorophyll concentration was determined. For storage the membranes were treated as described under 2.3.1.

2.3.4 *Synechocystis* sp. PCC 6803

Cells were pelleted at 5,000 rpm for 15 min in a Herolab HiCen 21 C centrifuge (rotor A6.9, Hermle) and resuspended in 15 ml buffer A (50 mM Mes, pH 6.0, 10 mM MgCl₂, 5 mM CaCl₂, 25 glycerol) [87]. 200 mg lysozyme (Roth) was added and the cell solution was incubated on a shaker for 30 min at 30 °C. Cells were then broken by five passages through a frenchpress at 20,000 psi. To remove unbroken cells the solution was spun at 3,000 *g* and 4 °C for 2 min. The supernatant was collected and centrifuged again. The resulting supernatant was then ultracentrifuged for 20 min at 40,000 rpm (Sorvall Discovery 90 SE ultra centrifuge, rotor: T-865) and 4 °C. The pelleted membranes were resuspended in 10 mM Mes (pH 6.0) and the ultracentrifugation step was repeated. The final pellet was resuspended again in 10 mM Mes (pH 6.0) and the Chl *a* concentration

was determined. For storage the membranes were treated as described under 2.3.1.

2.4 Purification of pigment-protein complexes

2.4.1 Ion exchange chromatography (IEX)

Thylakoids of *P. tricornutum* were solubilised with 20 mM *n*-dodecyl β -D-malto"-side (DDM, Glycon Biochemicals) at a Chl concentration of 0.25 mg/ml for 20 min on ice. Prior to the solubilisation the samples were adjusted in buffer 1 (B1, 25 mM Tris-HCl, 2 mM KCl at pH 7.4). To remove unsolubilised material, samples were spun for 5 min in a pre-cooled tabletop centrifuge at 13,000 rpm. The supernatant was then loaded onto an XK 16 column (Amersham Biosciences) filled with more than 20 ml of DEAE Toyopearl 650D (TOSOH) connected to an Äkta Purifier P-900 (Amersham Bioscience). The IEX material had to be pre-equilibrated with at least 5 column volumes of buffer B1+ (buffer B1 containing 0.03 % DDM). Up to three thylakoid aliquots, i.e. a total of 1.5 mg of Chl could thereby be separated during one run. To remove free pigments the column was washed with 2 column volumes of B1+. PS I and FCP fractions were then eluted using a NaCl gradient from 86 mM to 90 mM over 5 column volumes. Afterwards a PS II containing fraction could be eluted either by applying a gradient from 90 mM to 200 mM NaCl over three column volumes or by directly starting a washing step with 0.75 M NaCl in B1+. The flow rate was set to 2 ml/min. Elution was spectroscopically controlled at three different wavelengths ($\lambda_1=280$ nm, $\lambda_2=437$ nm, $\lambda_3=530$ nm). Subsequently, the harvested fractions were either used for further analysis or concentrated and stored at -20 °C.

Cleansing of the IEX material included three washing steps using 1 M NaCl, 0.5 N HCl and 0.5 M NaOH. Each step lasted for at least 5 column volumes and was followed by an intermittent step using distilled water to prevent damage of the IEX material. For storage the material was kept at 4 °C in 20 % ethanol.

2.4.2 Discontinuous sucrose gradient centrifugation

Thylakoids of *P. tricornutum* or *C. meneghiniana* were adjusted with buffer B1 to a concentration of 0.25 mg/ml Chl and solubilised with either 15 mM or 20 mM DDM for 20 min on ice. After a 5 min centrifugation in a pre-cooled tabletop centrifuge at 13,000 rpm the supernatant was loaded onto discontinuous sucrose gradients. The gradients consisted of five sucrose layers with concentrations of 40, 30, 25, 20, and 15 % in buffer B1+. Thylakoids were centrifuged for 22 h at 28,000 rpm (Sorvall Discovery 90 SE ultra centrifuge, rotor: Beckmann SW 28) and 4 °C. After the run, pigmented protein bands were removed with a syringe and either concentrated or directly used for further analysis. Samples were stored at -20 °C. For further purification harvested PS I fractions were resolubilised at a Chl *a* concentration of 0.2 mg/ml using a combination of 10 mM nonyl β -D-glucopyranoside (NG, Glycon Biochemicals) and 37.5 mM octyl β -D-glucopyranoside (OG, Glycon Biochemicals) or 3 % Triton X 100 and again fractionated on a sucrose gradient consisting of the same sucrose layers as described above with the exception of the 40 % sucrose layer, which was omitted.

2.4.3 Analytical gel filtration

Solubilised thylakoids of either *P. tricornutum*, *C. meneghiniana*, *P. sativum*, *Synechocystis* sp. or isolated pigment-protein fractions were applied to a Superdex 200 (GE Healthcare) gel filtration column 10/300 GL (Amersham Biosciences) connected to an Äkta Purifier P-900 (Amersham Biosciences). Volumes used varied between 50 μ l and 1 ml. Elution was always carried out with buffer B1+ at a flow rate of 0.5 ml/min. Elution was controlled spectroscopically at three different wavelengths ($\lambda_1=437$ nm, $\lambda_2=530$, $\lambda_3=700$ nm or 280 nm).

2.4.4 Concentration & washing of isolated pigment-protein fractions

Samples were concentrated by centrifugation at 1,000 *g* using Amicon filtration devices with a 30 kDa cut-off. Thereby contaminants as salts, detergents, and sucrose could be reduced by adding fresh B1 or B1+ buffer to the samples in between the centrifugation steps.

2.5 Gel electrophoresis

All organic solvents mentioned in this section were of technical quality.

2.5.1 Sodium dodecyl sulfate-polyacrylamide gel electrophoresis (SDS-PAGE)

Tris Tricine gels were cast according to [88] using the 1 mm Biometra-Minigel set-up (Biometra). The percentage concentration of both monomers, acrylamide and the cross-linker bisacrylamide used is referred to as % T . The concentration of the crosslinker in relation to % T is given as % C . Depending on the purposes, separating gels with concentrations of 8 %, 10 % and 15 % T were used, containing 6 M urea, 1 M Tris-HCl and 0.1 % SDS with pH set to 8.45. In all cases a concentration of 3 % C was used. Polymerisation was started by adding 3 μ l N, N, N', N'-tetra-methylethylenediamine (TEMED) and 30 μ l of a 10 % ammonium persulfate (APS) solution per 10 ml of gel. Stacking gels were cast similarly with 4 % T and 3 % C, without urea. Polymerisation was started by addition of 5 μ l TEMED and 50 μ l of a 10 % APS solution per 5 ml of gel. As cathode buffer a solution containing 0.1 M Tris, 0.1 M Tricine, and 0.1 % SDS was used. Anode buffer contained 0.2 M Tris-HCl, pH 8.9. Depending on their Chl concentration protein samples were either precipitated in acetone before or directly denatured in $1/4$ volume Rotiload (Roth) for 20 min at room temperature (RT). After loading the samples the run was started applying 15 mA until the samples reached the separating gel. Thereafter the current was increased to 30 mA.

As molecular weight (MW) markers either the Roti-Mark Prestained (Roth) or a self-made prestained molecular weight marker (Dr. M. Schmidt, University of Frankfurt) were used. The latter one was prepared according to the protocol by [89]. Proteins used were coupled to several Remazol dyes. Details can be seen in table 1.

2.5.2 Blue native-PAGE (BN-PAGE)

Blue native-PAGE (BN-PAGE) was carried out as described by [90] with slight modifications by [91]. The separating gel was cast using a selfmade gradient mixer connected to a peristaltic pump (Pharmacia LKB pump 1, Pfizer Pharma). Two solutions containing 50 mM Bis-Tris-HCl, 0.5 M 6 -amino-n-caproic acid (pH 7.0) with concentrations of 5 % and 13.5 % T, and 3 % C, as well as 5.6 % and 23.3 % glycerol, respectively, were gradually mixed and filled in between the two glassplates of the electrophoresis unit (Hoefer Mighty Small, 0.75 mm). Prior to the casting, polymerisation was started by adding 2 μ l TEMED and 5 μ l of 10 % APS to both solutions. A similar gel (4 % T, 3 % C) without glycerol was used as stacking gel, polymerised by adding 6 μ l TEMED and 15

Table 1: Molecular weight protein markers Roti-Mark Prestained (Roth) and a self-made prestained protein standard (Dr. M. Schmidt)

Roti-mark Prestained		Self-made protein standard		
Protein	MW (kDa)	Protein	MW (kDa)	Remazol dye
Myosin (beef)	245	Serum albumin (beef)	66	Remazol Turquoise
β -Galactosidase (<i>E. coli</i> , recombinant)	123	Ovalbumin (chicken)	45	Remazol Brilliant Red F3B
Serum albumin (beef, glycosilated)	95	Carbonic anhydrase	29	Remazol Brilliant Orange 3R
Ovalbumin (chicken, glycosilated)	50	Trypsin inhibitor	20	Remazol Brilliant Blue R
Carbonic anhydrase	33	Lysozyme	14	Remazol Golden Yellow RNL/Remazol Brilliant Orange 3R (4:1)
Trypsin inhibitor (soy)	23	Aprotinin	6	Remazol Brilliant Blue R/Remazol Golden Yellow RNL (4:1)
Lysozyme (chicken)	17			

Composition of the used molecular weight protein markers. Information on the Roti-mark Prestained (Roth) is shown on the left, the selfmade protein marker, synthesised according to the protocol of [89], is shown on the right. The molecular weight is given in kDa. Information on the Roti-mark Prestained is taken from the manufacturers data-sheet. Note that the molecular weights of the proteins used for the selfmade protein marker are slightly affected due to the coupling to Remazol dyes given in the last column.

μ l of 10 % APS. A solution of 50 mM Tricine, 15 mM BisTris, and 0.01 % of Coomassie Blue G (Serva) served as cathode buffer. Anode buffer contained 50 mM BisTris-HCl at pH 7.0. Samples of pea thylakoids were adjusted to 2 mg Chl/ml in resuspension buffer (RB, 20 % Glycerol and 25 mM Bis-Tris-HCl at pH 7.0) and solubilised with an equal volume of RB including 2 % DDM for 30 min on ice. After centrifugation at 13,000 rpm in a tabletop centrifuge the supernatant was combined with $1/10$ volume of sample buffer (SB, 100 mM Bis-Tris-HCl, pH 7.0, 0.5 M 6-amino-n-caproic acid, 30 % glycerol) and loaded onto the BN gel. In case of isolated protein fractions, the samples were mixed with SB and loaded directly onto the gel. The pH of all solutions mentioned in this section was adjusted at 4 °C. Electrophoresis was performed at 150 V - 200 V at 4 °C for several hours.

2.5.3 Coomassie staining

Gels were incubated 3 - 12 h in staining solution containing 0.25 % Coomassie Blue G (Serva) in 10 % acetic acid. De-staining was performed in 10 % acetic acid for several hours until a sufficient resolution of the protein band pattern was obtained.

2.5.4 Silver staining

Gels were incubated in 100 ml fixing solution (30 % ethanol, 10 % acetic acid) for 30 min up to several days. The staining procedure was adapted from [92] with the following modifications. The fixing solution was exchanged against 100 ml incubation solution containing 0.5 M Na-acetate \times 3 H₂O, 8 mM Na₂S₂O₃ \times 5 H₂O (Merck), 30 % ethanol, and 500 μ l of glutaraldehyde (25 % w/v). Incubation time was similar to that mentioned before. The gels were then washed thrice for 5 min with distilled water and transferred to 100 ml silvering solution (0.2 % (w/v) AgNO₃) with 20 μ l freshly added formaldehyde (37 % w/v) for 20 min. For the development the gels were incubated in 50 ml 235 mM Na₂CO₃ (pH \geq 11.5) with 5 μ l freshly added formaldehyde (37 % w/v) for 1 min. After

that, the solution was exchanged against 150 ml of the same solution containing 15 μ l freshly added formaldehyde (37 % w/v). Depending on the protein concentration the developing of the bands took 5 min up to 30 min. Reaction was stopped with 100 ml of a 1 % (w/v) glycine solution.

2.6 Protein transfer & immunodetection

All organic solvents mentioned in this section were of technical quality.

2.6.1 Western Blot

Western Blots were carried out according to the method of [93] with minor modifications. Unstained gels were incubated in cathode buffer (25 mM Tris-HCl, 40 mM glycine, 10 % methanol at pH 9.4) for 15 min. Six 3MM Chr Whatman filter papers (Schleicher & Schüll) and a PVDF membrane (Roth) with a similar size as the gel were prepared. Two filter papers were wetted in anode buffer I (0.3 M Tris-HCl, 10 % methanol, pH 10.4) and layered below one filter paper wetted in anode buffer II (25 mM Tris-HCl, 10 % methanol, pH 10.4). The PVDF membrane (Roth) was incubated in methanol for 10 sec, transferred to distilled water for 2 min and then incubated in anode buffer II. The gel was then layered on top of the PVDF membrane and three filter papers wetted in cathode buffer enclosed the sandwich. Transfer was carried out for 1 h at 1.5 mA/cm² in a semi-dry transfer cell (BioRad Trans-blot SD).

2.6.2 Slot Blot

PVDF or nitrocellulose membranes (Roth) were layered on top of three 3MM Chr Whatman filter papers (Schleicher & Schüll), wetted with distilled water, and assembled in the Slot Blot transfer cell (Minifold II, SRC 072/0, Schleicher & Schüll), connected to a water jet pump. 100 μ l of isolated pigment-protein fractions, adjusted by their Chl concentrations, were directly loaded onto the membrane and immobilised by removing

the liquid.

2.6.3 Immunodetection

After proteins were transferred onto PVDF or nitrocellulose (see above), the membranes were incubated for 15 min up to several hours on a shaker (Multi Bio 3D, Biosan) in blocking solution consisting of 5 % milk powder in phosphate buffered saline (PBS, 137 mM NaCl, 2.7 mM KCl, 4.3 mM Na₂HPO₄, 1.4 mM KH₂PO₄). The membrane was then transferred to the first antibody solution (dilution and specification, see below) for 1 h. The membrane was washed thrice for 10 min in PBS and then incubated for at least 30 min in the secondary antibody solution (α -goat anti rabbit IgG with horseradish peroxidase conjugate, Calbiochem, diluted 1:6250 in blocking solution). The washing in PBS was repeated four times for 5 min. Then the membrane was incubated for 1 min in 10 ml ECL (enhanced chemiluminescence) solution containing 100 μ l of 250 mM luminol (in DMSO), 45 μ l of 90 mM p-coumaric acid (Fluka, in DMSO), 1 ml of 1 M Tris-HCl (pH 8.5) and 3 μ l freshly added 30 % H₂O₂ [94]. Afterwards the peroxidase induced luminescence was detected using an x-ray film (Amersham Hyperfilm ECL, GE Healthcare) in a dark chamber. Exposition time varied in between several seconds and 30 min depending on quality of the antibodies and quantity of the protein samples. X-ray films were treated in developing (Roentogen, Tetenal) and fixing solution (Adefofix, Adefo) according to the manufacturers instructions. 2 % acetic acid served as stop bath after the developmental step.

Primary antibodies directed against higher plant reaction centre II PsbD (α -D2) and against Fcp2 (α -Fcp2), Fcp4 (α -Fcp4), Fcp6 (α -Fcp6), and all Fcp polypeptides (α -ccFcp) of *C. cryptica* were kind gifts of Prof. Dr. D. Godde, (University of Bochum) and Prof. Dr. E. Rhiel (University of Oldenburg), respectively. The antibody directed against higher plant reaction center I core subunits PsaA and PsaB (α -CP1) was a kind

gift of Prof. Dr. J. Feierabend (University of Frankfurt). Antibodies were diluted in blocking solution, except for α -Fcp4 which was diluted in PBS. Dilutions used were 1:2000 (α -D2, α -ccFcp), 1:1000 (α -Fcp2, α -Fcp6, α -CP1), and 1:200 (α -Fcp4).

2.7 Spectroscopy

All organic solvents mentioned in this section were of technical quality.

2.7.1 Absorbance spectra

Absorbance spectra between 350 nm and 750 nm were recorded at room temperature with 1 nm band pass and 1 cm optical path length using a Jasco spectrophotometer (V 550).

2.7.2 Determination of P700

Difference spectrum measurements of PS I fractions between 650 nm and 750 nm were performed with 0.025 mM $K_3[Fe(CN)_6]$ (Merck) as oxidant and 0.7 mM Na-ascorbate (Merck) as reductant. A molar extinction coefficient of $64 \text{ mM}^{-1}\text{cm}^{-1}$ for P700 was used for calculating Chl/P700 ratios [95].

2.7.3 Chlorophyll determination

Determination of chlorophylls at single wavelengths were measured with a similar set-up as described above.

2.7.3.1 Chlorophyll *c* containing algae

The chlorophyll content of samples derived from *P. tricornutum* and *C. meneghiniana* was determined according to the method described by [96]. Pigments were extracted using 90 % acetone. Subsequently the samples were spun in a pre-cooled tabletop centrifuge at 13,000 rpm for 5 min and the supernatant was measured against 90 % acetone as

reference. Concentrations of Chl *a* and Chl *c* were calculated with the following equation:

$$\text{Chl } a \text{ [mg/l]} = 11.47 \times (E_{664} - E_{750}) - 0.40 \times (E_{630} - E_{750})$$

$$\text{Chl } c \text{ [mg/l]} = 24.34 \times (E_{630} - E_{750}) - 3.73 \times (E_{664} - E_{750})$$

2.7.3.2 Higher plants

Pigment extraction of pea thylakoids in 80 % acetone was done as described under 2.7.3.1. Chl *a* + *b* concentrations were calculated as described in [97] using the following equation:

$$\text{Chl } a \text{ [mg/ml]} = 0.0127 \times (E_{663} - E_{750}) - 0.00269 \times (E_{645} - E_{750})$$

$$\text{Chl } b \text{ [mg/ml]} = 0.0229 \times (E_{645} - E_{750}) - 0.00468 \times (E_{663} - E_{750})$$

2.7.3.3 Cyanobacteria

Pigment extraction of *Synechocystis* sp. thylakoids in 90 % acetone was done as described under 2.7.3.1. Chl *a* was measured at $\lambda = 664$ nm. To account for effects of light scattering absorbance at $\lambda = 750$ was subtracted. Concentration was calculated using the specific extinction coefficient ($87.67 \text{ g}^{-1}\text{cm}^{-1}$) given by [96].

2.7.4 Fluorescence spectra

Fluorescence spectra were measured with a Jasco fluorometer (FP-6500) at RT and 77 K, respectively. Band passes of 3 nm were used both on emission and excitation side. A rhodamine B spectrum served as a reference for the correction at the excitation side and the photomultiplier was corrected using a calibrated lamp spectrum. Emission spectra were taken upon excitation at $\lambda_{ex}=440$ nm, $\lambda_{ex}=465$ nm, or $\lambda_{ex}=560$ nm and measured from $\lambda_{em}=600$ nm to $\lambda_{em}=800$ nm. For the excitation spectra, emission was recorded at $\lambda_{em}=675$ nm or $\lambda_{em}=717$ nm upon excitation from $\lambda_{ex}=400$ nm to $\lambda_{ex}=600$ nm. In the case of 77 K measurements samples were diluted in B1 containing 60 % glycerol to yield a glass upon freezing. For direct comparison of different fractions, samples were adjusted either to the same Chl *a* concentration (absorbance of 0.03 at the Q_Y band of

Chl *a* in buffer B1/B1 + 60 % glycerol) or the same fucoxanthin absorbance at 560 nm.

2.8 High Performance Liquid Chromatography (HPLC)

All solvents used in this section were of p.a. grade.

Quantification of pigments was performed by analytical HPLC according to [66]. In short, 5 μl of isolated pigment-protein fractions with Chl concentrations of at least 0.2 mg/ml were extracted with 90 % methanol (final concentration). After a 10 min centrifugation at 13,000 rpm in a pre-cooled tabletop centrifuge, 20 μl of the supernatant were loaded onto a reverse phase HPLC column (Lichrosorb RP-18, 5 μm , 250 mm x 4 mm) connected to the Elite LaChrom HPLC system (VWR/Hitachi). Before the run the column was equilibrated with solvent A (80 % methanol) for at least 15 min. Pigments were separated by a two step gradient from solvent A to solvent B (60 % methanol, 40 % acetone). Starting from 100 % solvent A, 90 % were reached after 7 min. Solvent A was then further reduced to 0 % during another 10 min and kept the following 9 min. Within 2 min solvent A was increased to 100 % again. Length of the run was set to 34 min with a flow rate of 1.25 ml/min. Pigment spectra were measured by an diode array detector (Elite LaChrom L-2455). For quantification in pmol/ μl peak areas were multiplied with the following pigment specific calibration factors: 3.1126×10^{-5} (Chl *a*), 1.5084×10^{-5} (Chl *c*), 1.87012×10^{-5} (diadinoxanthin), 2.4696×10^{-5} (diatoxanthin), 2.3933×10^{-5} (fucoxanthin), 2.5102×10^{-5} (β -carotene) [98].

2.9 Electron microscopy

A freshly broken slice of mica (Plano, Wetzlar) was placed on filterpaper in a glas petri dish and set into the vacuum cell of the carbon coater 208 (Cressington). To coat the mica with carbon one pulse of 3.8 V and two pulses of 4 V were applied after the vacuum reached a pressure of $\sim 5 \times 10^{-5}$ mbar. All three pulses lasted 3 sec. The

coated mica could then be stored up to three months or was used directly to apply the carbon film to new copper mesh grids (Agar Scientific 400 square mesh, copper 3.05 mm). To this end the grids were placed onto a flat holder lying below the surface of distilled water in a small selfmade 50 ml tank connected with a syringe. The mica was then carefully pushed under water so that the carbon film floated on the surface. By releasing the water with the syringe the carbon was settled flat on the grids. The plain carbon grids were removed from the holder, dried and stored. In some cases the plain carbon grids were glow discharged (Cressington power unit 208) applying an electric field for 10 sec. with a current of 5 mA for several times using a vacuum with a pressure of approximately 0.02 mbar. 3 μ l of protein sample (PS I, isolated by IEX, approximately 8 ng/ml Chl) was placed on a recently prepared grid. After 30 s incubation, specimens were negatively stained for 45 s with 2 % uranyl acetate (Plano). Images were taken using a Phillips CM12 electron microscope with a LaB₆ filament at 120 kV at a magnification of 60,000 x. Micrographs were scanned with a Super Coolscan 9000 ED (Nikon) with a resolution of 100 pixel/16 nm at specimen level. Alternatively, images at a magnification of 110,000 x were taken with a CCD camera (Gatan Erlangshen ES5W).

2.10 Sequence comparison

Alignment of protein sequences was carried out with ClustalW [99] and Kalign [100]. Search for nucleic acid, and/or protein sequences, as well as computation of molecular weights (MW) was carried out with the database of the National Center for Biotechnology Information (NCBI, link: <http://www.ncbi.nlm.nih.gov/>), the diatom EST databank [101] (link: <http://avesthagen.sznbowler.com/>), the UniProt knowledgebase (UniProtKB, link: <http://www.uniprot.org/>) and the ExPASy proteomics server [102] (link: <http://expasy.org/>).

3 Results

3.1 A monomeric PS I-FCP complex of *P. tricornutum*

3.1.1 Isolation of a PS I complex from *P. tricornutum*

A protocol had to be developed to isolate a functional PS I complex of the diatom *P. tricornutum*. To this end a method that led to the successful isolation of thylakoids from *C. meneghiniana* and the separation of several pigment-protein complexes via ion exchange chromatography was adapted [62]. Preliminary results using a NaCl gradient from 40 mM to 200 mM indicated an incomplete separation between a PS fraction and a FCP fraction (data not shown). However, the isolation procedure had to be optimised since the yield of thylakoids during the preparation was low and it turned out that the isolated thylakoids were still contaminated with unbroken cells. Therefore different methods for cell disruption were tested, including freeze grinding with liquid nitrogen, sonication, disruption in a bead beater, and disruption by frenchpress. The latter led to satisfying results with a low amount of unbroken cells. Beside that also the buffers were modified, and the separation of unbroken cells was optimised to finally gain uncontaminated thylakoid membranes. Also the NaCl gradient had to be adjusted using a flat gradient from 86 mM to 90 mM to separate the PS fraction from the FCP fraction (for the exact protocol see section 2.4.1). This method for the isolation of thylakoids from *P. tricornutum*, the subsequent DDM solubilisation and separation via IEX resulted in the elution of six prominent fractions referred to as fractions I - VI (figure 4). Elution was controlled by measuring at three different wavelengths, 437 nm for Chl *a*, 530 nm for fucoxanthin, and 280 nm mainly for proteins. Fraction I turned out to consist mainly of free pigment (data not shown) and was eluted before the salt gradient step was applied. Fraction II was of yellow colour and represented the smallest fraction, characterised by a significant increase of absorbance at 280 nm and a slight increase

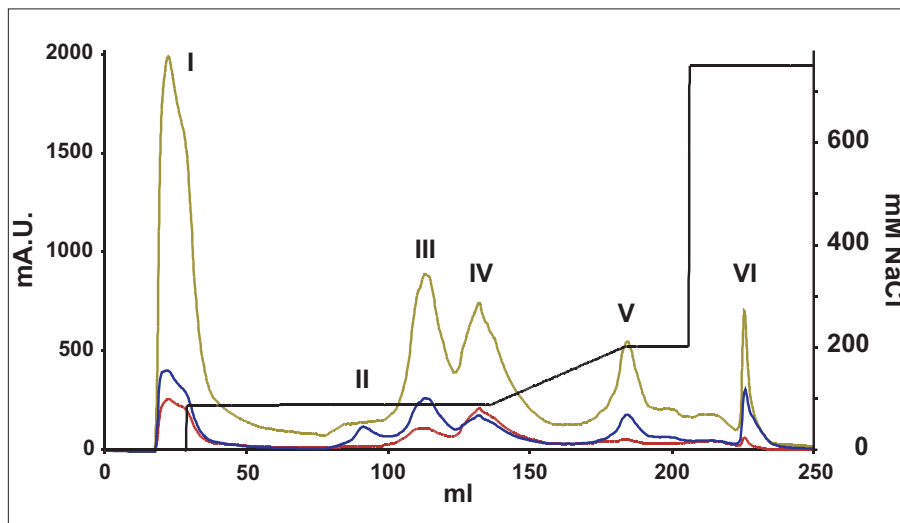


Figure 4: **IEX of solubilised thylakoids of *P. tricornutum***. The absorption at 280 nm is shown in blue, the absorption at 437 nm is shown in green, and the absorption at 530 nm is shown in brown. The black line represents the NaCl gradient used for elution. Eluted fractions I-VI are indicated.

of Chl *a* absorbance. Fractions III and IV resembled the characteristics of the fractions from the preliminary IEX. Fraction III was of green colour and showed approximately the same Chl *a* absorbance as the brown fraction IV, but less absorbance of fucoxanthin. It seemed likely that fraction III contained PS complexes, whereas fraction IV consisted of free Fcps. Fraction V absorbed mainly at 437 nm and resembled fraction III but with reduced fucoxanthin content, e.g. less absorbance at 530 nm. Thus it was suggested that fractions III and V represent the two PS complexes. The sixth fraction was eluted during the wash step (750 mM NaCl) and showed a high ratio between absorbance at 437 nm and 280 nm, e.g. a higher content of un-pigmented proteins. Therefore fraction VI was not analysed any further.

3.1.2 Polypeptide composition of the PS I complex

As the focus lied on the purification of a PS I complex, the respective PS fractions III and V had to be analysed further. Especially considering that it was unclear in the first place if PS I and PS II were eluted separately or if the two fractions contained mixtures of PS I

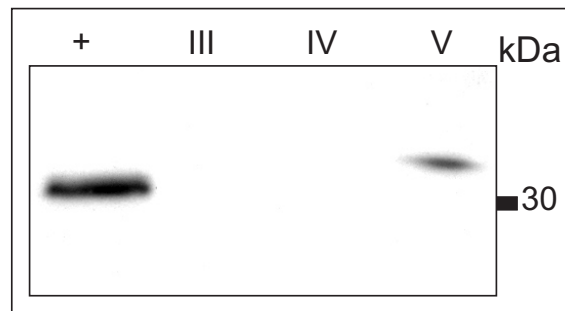


Figure 5: **Western blot using a higher plant α -PsbD antibody.** 4 μ g Chl of Pea thylakoids (+) were loaded as positive control. All IEX fractions loaded contained 2 μ g Chl. Fractions III - V (top) and molecular weights (right) are indicated.

and PS II subunits. Therefore both fractions as well as the Fcp fraction IV were checked for the presence of PS II. A western blot experiment using an antibody against higher plant reaction center II subunit PsbD (D2) revealed the presence of PS II in fraction V (figure 5, compare also with figure 15). In contrast, in fractions III and IV no positive reaction was observed. As it seemed unlikely that fractions I, II, V, and VI contained PS I, further investigations concentrated on fraction III. In parts of the experiments fraction IV was kept as Fcp reference. Analysis of fractions II and V is described under 3.1.6.

Fractions III and IV were separated by high resolution SDS-PAGE (figure 6). A double band around 65 kDa as well as several bands between 10 kDa and 20 kDa were observed in fraction III (lane 1), indicating the presence of PS I core subunits PsaA and PsaB, three bands with molecular weights in the range of Fcp polypeptides around 18 kDa [61] and 4 weaker bands, probably representing smaller PS I subunits. Fraction IV (lane 2) was dominated by a strong band at 18 kDa, the expected molecular mass of Fcp polypeptides. The PS I core subunits PsaA and PsaB were subsequently identified at approximately 65 kDa by Western Blot with an antibody (α -PsaA/B) directed against higher plant PS I core. To check for the presence of Fcp polypeptides, both fractions were immunodecorated using an antibody against all Fcp polypeptides from *C. cryptica* (α -ccFCP). As expected, one strong Fcp signal could be observed in fraction IV. Surprisingly,

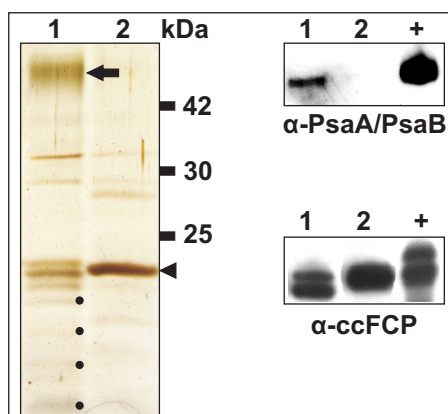


Figure 6: **SDS-PAGE (left panel) and Western Blots (right panels) of the IEX fractions III (lane 1) and IV (lane 2).** SDS-PAGE: The molecular weight marker is indicated on the right side. PS I core subunits PsaA and PsaB are indicated with an arrow, Fcp polypeptides with an arrow head. 4 smaller polypeptides were marked by black circles. Note that three bands were resolved in the Fcp range. 2 μg Chl of both samples were loaded, respectively. Western Blots: In the upper panel a Western Blot using an antibody against higher plant PS I core (α -PsaA/PsaB) is shown. Spinach stroma thylakoids (D. Piano) were used as positive control (+). In the lower panel a Western Blot using an antibody directed against all Fcp polypeptides of *C. meneghiniana* was used. As positive control (+) a FCP preparation of *C. meneghiniana* was used (K. Gundermann). 2 μg Chl of fraction III and 1 μg Chl of fraction IV were loaded, respectively.

two Fcp polypeptides were detected in fraction III with sizes different from the Fcp fraction IV (figure 6). As three bands in the Fcp range were observed in fraction III by SDS-PAGE it is supposed that the third band represents the PS I subunit Psa D with a MW of approximately 18 kDa in *P. tricornutum*. The four lower polypeptides could represent the PS I subunits PsaE, PsaF, PsaI, PsaJ, PsaL, and PsaM (compare with [103, 104]).

3.1.3 Characterisation of the complex

To check for the functionality of the isolated PS I fraction, oxidised minus reduced difference spectra of three independent preparations were recorded. In all cases a maximum peak at 700 nm was observed, thus proving the activity of the reaction centre. Furthermore the Chl/P700 ratio of the three samples was calculated to be 210 (± 6), e.g.

around 200 chlorophylls per PS I. Furthermore, the pigment stoichiometries of fraction III and fraction IV were measured by reverse phase HPLC. In table 2 the pigment ratios (mol/mol) were calculated on the basis of either Chl *a* or fucoxanthin. For better visualisation the ratios are also presented in figure 7. Whereas fraction IV had similar values compared to FCPs from *C. meneghiniana* [14], fraction III differed significantly from that. The fucoxanthin/Chl *a* ratio was reduced to 1:2 and the Chl *c*/Chl *a* ratio was approximately 1:10. Nonetheless, the ratio between Chl *c* and fucoxanthin remained the same in both fractions (1:5). These data indicated that Fcp polypeptides with a similar Chl *c* to fucoxanthin ratio were present in fraction III as well. However, the amount of diadinoxanthin and diatoxanthin (pigments that play a role in a photoprotection mechanism named NPQ, see section 1.3) measured in both fractions differed significantly. In relation to the amount of Chl *a*, twice as much was bound in fraction III compared to fraction IV. If compared to the amount of fucoxanthin, i.e. referring to the Fcps in fraction III, the ratio of the xanthophylls was even five times higher than in fraction IV (see figure 7 b). This discrepancy is also reflected in the de-epoxidation rates (mol diatoxanthin/(mol diadinoxanthin + diatoxanthin)) of both complexes as can be seen in figure 7 a. The ratio of diatoxanthin per xanthophyll cycle pigments was significantly increased in fraction III compared to fraction IV.

Table 2: Pigment determination of IEX fractions III and IV by analytical HPLC

	fucoxanthin	Chl <i>c</i>	diadinoxanthin	diatoxanthin	β -carotene
<i>pigment per Chl a [mol/mol]</i>					
Fraction III	0.505 \pm 0.055	0.080 \pm 0.017	0.024 \pm 0.008	0.014 \pm 0.008	0.093 \pm 0.035
Fraction IV	1.054 \pm 0.088	0.233 \pm 0.053	0.013 \pm 0.003	0.004 \pm 0.001	0.054 \pm 0.008
<i>pigment per fucoxanthin [mol/mol]</i>					
Fraction III	1	0.158 \pm 0.026	0.048 \pm 0.011	0.033 \pm 0.017	0.182 \pm 0.060
Fraction IV	1	0.220 \pm 0.033	0.012 \pm 0.002	0.003 \pm 0.001	0.052 \pm 0.011

Values were calculated on the basis of Chl *a* (upper part of the table) or fucoxanthin (lower half of the table) content. Ratios are given as mean \pm standard deviation of 6 measurements on 4 independent preparations (fraction III) and of 4 measurements on 2 preparations (fraction IV), respectively.

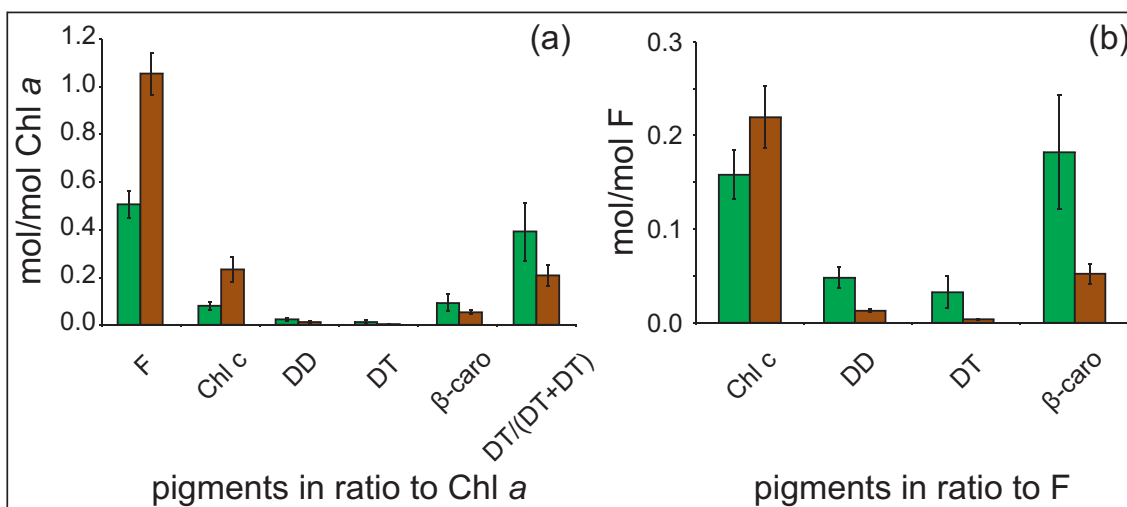


Figure 7: **Analytical HPLC of IEX fractions III and IV.** Pigments analysed were fucoxanthin (F), Chl c, diadinoxanthin (DD), diatoxanthin (DT), and β -carotene (β -caro). Pigment ratios were calculated on the basis of Chl a (a) or fucoxanthin (b) content [mol/mol]. Apart from that also the de-epoxidation rate (mol diatoxanthin/(mol diadinoxanthin + diatoxanthin)) of both fractions was calculated. The \pm standard deviation is indicated (compare with table 2). IEX fraction III is shown in green, fraction IV in brown colour.

From the PS I crystal structures of cyanobacteria and higher plants it is known that 96 and 101 chlorophyll *a* are bound per PS I core, respectively, as well as 22 carotenoids [17, 26, 29]. The stoichiometry between the two pigments is therefore approx. 1:5. In fraction III the ratio of β -carotene/Chl *a* was 1:10, which means that twice as much Chl *a* is bound. The P700 difference spectra measurements mentioned above revealed a coordination of approximately 200 Chl *a* molecules in fraction III, which is in good accordance to the β -carotene/Chl *a* ratio (22:200 \simeq 1:10). The measured fucoxanthin and Chl *c* values indicate that fraction III indeed contains Fcps beside PS I and thus support the Western Blot results. Also the Chl *c*/fucoxanthin ratio of Fcps in the PS I fraction III is similar to the Fcp fraction IV (see figure 7 b) and matches pigment data published for *C. meneghiniana* [66]. Furthermore, from *C. meneghiniana* a fucoxanthin/Chl *a* ratio of approximately 1:1 is reported for FCP complexes which coincides with the value of

fraction IV. Interestingly, in fraction III this ratio adds up to 1:2. To summarise, the PS I complex in fraction III coordinates approximately 100 Chl *a* molecules more than reported for PS I cores and comprises of a doubled β -carotene/Chl *a* ratio (relating to PS I cores) and a doubled fucoxanthin/Chl *a* ratio (relating to Fcps). These data lead to the assumption that 50 % of the measured Chl *a* (100 molecules) are associated with the Fcps in fraction III and accord to 100 fucoxanthin molecules. Thus a fucoxanthin/Chl *a* ratio of 1:1 is achieved if only the Fcps of fraction III are regarded. The remaining 100 Chl *a* molecules are coordinated by the PS I core of *P. tricornutum*. This model is consistent with PS I cores of cyanobacteria and higher plants and demonstrates the strong conservation of PS I cores among photosynthetic organisms [31].

However, it had to be proven whether the co-purified Fcps in fraction III were functionally associated with the PS I complex. Therefore, fractions III and IV were analysed spectroscopically (figure 8). In fraction III mainly Chl *a* absorbance was detected with a broad Chl *a* Q_y band with a maximum at 676 nm, thus resembling a PS I spectrum

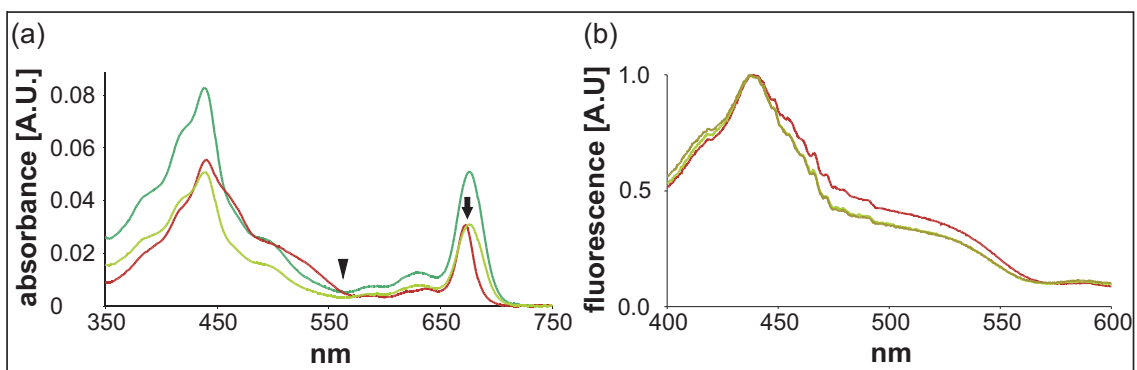


Figure 8: **Room temperature absorbance and fluorescence excitation spectra.** In panel (a) absorbance spectra of fraction III (light green) and fraction IV (brown) adjusted to an identical absorption at the Q_y band of Chl *a* (marked with an arrow) are depicted. Fraction III adjusted to an identical fucoxanthin absorption as fraction IV at a wavelength of 560 nm (marked with an arrowhead) is shown in dark green. Excitation spectra (b) of the same samples were recorded at 675 nm and normalised at 440 nm.

(figure 8 a) [105, 106]. Furthermore a minor Chl *c* shoulder at 465 nm and fucoxanthin were detected as well. As expected, fraction IV resembled a typical FCP spectrum showing strong Chl *c* and fucoxanthin absorbance beside the Chl *a* maxima, and the Chl *a* Q_y peak at 672 nm [61–64]. Fluorescence excitation spectra of fraction III and IV normalised at 440 nm demonstrated an energy transfer from the pigments Chl *a*, Chl *c* and fucoxanthin to a final Chl *a* emitter in both samples, although energy transfer of the pigments Chl *c* and fucoxanthin was more pronounced in fraction IV. Thus, a decoupling of these pigments was ruled out (see figure 8 b). To distinguish between Fcps co-eluted with PS I and Fcps specifically bound to PS I, RT fluorescence emission of both fractions were measured (data not shown). Both fractions revealed similar maxima at approx. 677 nm. Thus no differentiation depending on the emission wavelength of both fractions was possible. Advantage was taken regarding the different fluorescence yields of the complexes. Whereas Fcps show a strong fluorescence, PS I complexes are known for their poor fluorescence yield, also in diatoms [76, 107]. If Chl *c* and/or fucoxanthin of functionally bound Fcps transfer energy to PS I, the emission should be lower compared to the emission of free Fcps with the same pigment concentration. Furthermore, the measurements were performed at 77 K to identify possible far red fluorescing Chls of PS

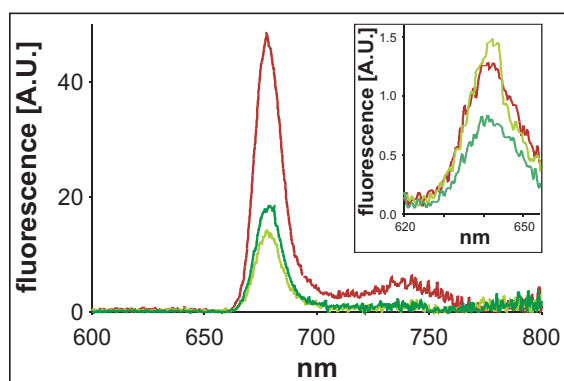


Figure 9: **77 K fluorescence emission spectra of fractions III (green) and fraction IV (brown)**. Fraction III was either adjusted to a similar Chl *a* (light green) or a similar fucoxanthin absorbance (dark green) as fraction IV (for comparison see figure 8 a). Excitation wavelength was set to 560 nm. A similar measurement with excitation wavelength set to 465 nm can be seen in the inset.

I, that cannot be resolved under RT conditions [108]. When the fucoxanthin concentrations of both samples were adjusted (compare with figure 8 a), i.e. similar absorbance of Fcps in both samples but with a higher emitter (Chl *a*) concentration in fraction III, the emission peak of fraction III showed a significant quench of ~63 % in comparison to fraction IV when fucoxanthin was excited (figure 9). This value was even increased to ~71 % when the emitter concentration was similar in both fractions, i.e. if both samples were adjusted to the same Chl *a* concentration. Similar results were obtained when the samples were excited at 465 nm (Chl *c*). However, besides the Chl *a* emission also a small Chl *c* peak around 640 nm arose, indicating a partial loss of function during the isolation process (see inset of figure 9). In comparison to RT emission fluorescence the spectra measured at 77 K were red shifted (Chl *a* maxima of all samples at 678.5 nm) and fluorescence bands got more sharpened. No increase of far red emitting Chls were identified in fraction III in comparison to RT spectra.

Although it could be proven that the Fcps transfer light energy to the PS I core in fraction III, the similar fluorescence peaks and the discrepancy of pigments Chl *c* and fucoxanthin between the absorbance and the excitation spectra indicated a co-purification of decoupled Fcps in that fraction. Indeed, when fraction III was loaded onto an analytical gel filtration column, elution resulted in a major peak absorbing at 437 nm, 530 nm and 700 nm², whereas the fractions of the following shoulder absorbed only at 437 nm and 530 nm. However, the main peak fraction was similar to fraction III (see figure 10 a) regarding its absorbance (not shown) and its fluorescence excitation characteristics (figure 10 b). However, the main fraction of the shoulder resembled a damaged Fcp with a reduced Chl *c* content and blue-shifted Chl *a* Q_y peak in the absorbance spectrum and a decoupling of Chl *c* in the fluorescence spectra (emission and excitation, data not

²PS I RC pigments absorb at 700 nm, a wavelength not used by other photosynthetic complexes (with the exception of LHC I associated with PS I of higher plants).

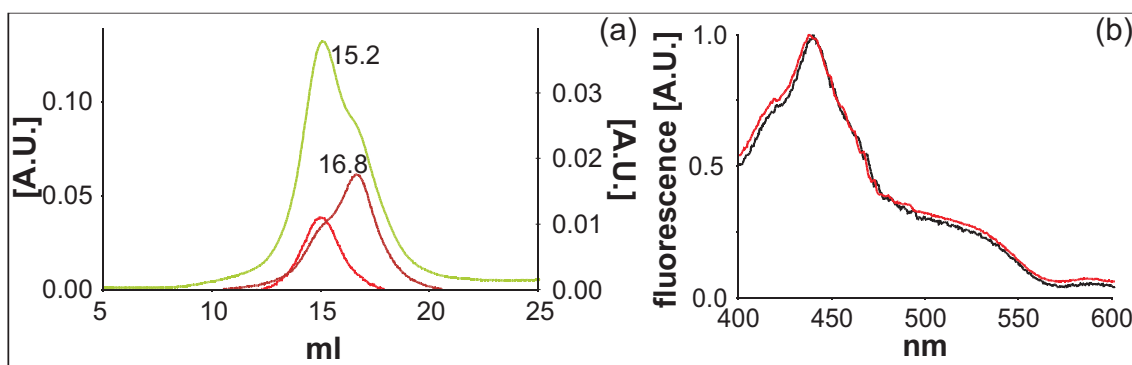


Figure 10: **Gel filtration and fluorescence excitation of the IEX fraction III.**(a) Gel filtration of fraction III from the IEX. Elution was controlled at 437 nm (green), 530 nm (brown), and 700 nm (red). Peak maxima are indicated in ml. For better visualisation the absorbance at 437 nm is depicted on the left y-axis, whereas the two other wavelengths were plotted according to the right y-axis. (b) Fluorescence excitation spectra of fraction III (red) in comparison with fraction III purified via gel filtration (i.e. the main peak). Spectra were normalised at 440 nm.

shown). Therefore the relative strong energy transfer of Chl *c* in fraction III (before and after gel filtration) must be due to Fcps that are energetically coupled to the PS I core.

It was concluded that the isolated PS I complex in fraction III is indeed functionally coupled with Fcps which actively transfer light energy to the PS I core. This transfer resulted in the significant fluorescence quench observed in the PS I sample. Furthermore, fucoxanthin seems to transfer its energy directly to Chl *a* and not via Chl *c*. Otherwise the Chl *c* emission should have been detected also when the samples were excited at 560 nm. This has been previously reported also for isolated FCP complexes from *C. meneghiniana* [66]. Astonishingly, no far red fluorescing Chls were detected under 77 K conditions. From higher plants, green algae, and cyanobacteria the occurrence of such LWCs are reported [32]. LWCs are usually not detected at RT due to an efficient uphill energy transfer towards P700 but at low temperatures excitation energy migrates predominantly towards LWCs, characterised by a fluorescence increase of PS I samples in the far red of the spectrum. Therefore the LWCs are either not existent in *P. tricornutum*,

were lost due to the purification method, or the energy coupling towards the LWCs is decoupled in this preparation. The first assumption can be excluded since a 715 nm emitter was reported by Berkaloﬀ and co-workers for a PS I fraction purified by sucrose density centrifugation [76]. To exclude a preparation artefact another more gentle method for purifying a PS I complex was chosen, which is presented in section 3.1.7.

3.1.4 Higher organisation of the PS I-FCP complex

Although the genome of *P. tricornutum* has been published recently [56] the knowledge about nuclear encoded proteins that play a role in diatom photosynthesis beside Fcps is still little. Up to now, no nuclear PS I subunit has been identified in diatoms. As diatoms derive from a secondary endosymbiosis event of the red algal line we cannot exclude the existence of PS I subunits that share little or no similarity with PS I subunits described for other photosynthetic organisms. Especially considering that only recently a novel extrinsic PS II subunit, encoded in the nucleus, has been described for the diatom *Chaetoceros gracilis* [78]. However, at least 10 PS I subunits, namely Psa -A, -B, -C, -D, -E, -F, -I, -J, -L, and -M can be found on the plastome of diatoms (e.g. *P. tricornutum*, *Odonotella sinensis*) [60, 109]. To get an impression of the higher organisation of the isolated PS I-FCP complex, several subunits were compared with the corresponding sequences of higher plants and cyanobacteria where genomes as well as structural information are available. On protein level, the trimeric state of PS I in cyanobacteria is the most obvious difference compared to the monomeric PS I from higher plants surrounded by its LHC I belt. To decide whether the PS I from diatoms is of higher plant or cyanobacterial type, subunits that are either involved in trimerisation of PS I, or prevent trimerisation, or are otherwise typical for one of the two systems were chosen for sequence comparison. In contrast to higher plants, the *P. tricornutum* plastome contains subunit PsaM which is settled between two PS I monomers in cyanobacteria (figure 11). The *P. tricornutum*

protein sequence shares 50 % identity with the sequence from *Thermosynechococcus elongatus*, thus maybe enabling trimerisation. Furthermore, PsaG, the anchoring point of the LHC I belt is missing in the plastome of *P. tricornutum*. A special serin residue in subunit PsaI of higher plants is responsible for the binding of PsaH, which is probably

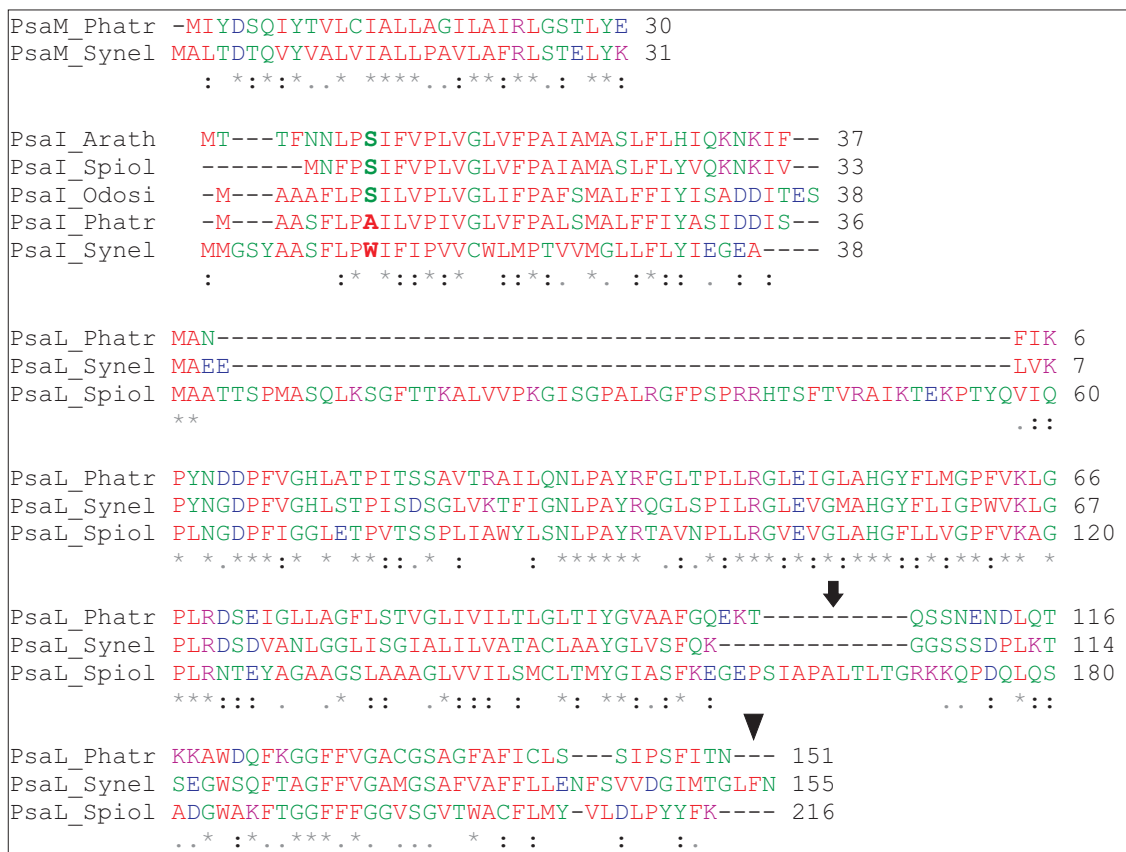


Figure 11: **A comparison of protein sequences of PS I subunits from different organisms.** Aminoacids were coloured depending on their physico-chemical properties. The protein sequences of subunit PsaM of *P. tricornutum* (Phatr) and *Thermosynechococcus elongatus* (Synel) are shown in the upper panel. Comparison of PsaI sequences of *Arabidopsis* (Arath), spinach (Spiol), *Odontella sinensis* (Odos), *P. tricornutum*, and *Thermosynechococcus elongatus* can be seen in the second panel. A special serin residue of *Arabidopsis* and its aligned counterparts are emphasised for better visualisation. In the third panel the PsaL subunits of *P. tricornutum*, spinach, and *Thermosynechococcus* are compared. A loop region in the sequence of *P. tricornutum* and *Thermosynechococcus* are indicated by an arrow. The C-terminus in the *Thermosynechococcus* sequence is indicated by an arrowhead.

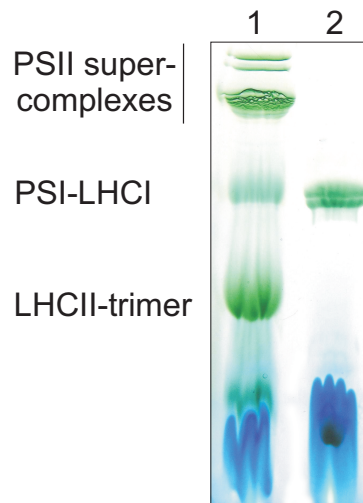


Figure 12: **A BN-PAGE of pea thylakoids and the PS I-FCP complex isolated by IEX from *P. tricornutum*.** Solubilised thylakoids of pea (lane 1) were loaded as molecular weight marker for 5 μg of Chl of the PS I-FCP complex (lane 2). The bands found in pea thylakoids are labelled according to [110, 111].

hindering trimerisation [31]. In cyanobacteria this serin is replaced by a tryptophane and the PsaH subunit does not exist. In the diatom *O. sinensis* we find the serin, in *P. tricornutum* it is replaced by an alanin. The corresponding nuclear gene for the PsaH subunit has not been identified in diatoms. PsaL, a subunit at the interface of all three monomers in cyanobacteria, contains a loop region in higher plants which might interact with PsaH and LHC II. This region is missing in the *P. tricornutum* sequence as well as the cyanobacterial C-terminus involved in trimerisation. To summarise these data, we can say that there are more cyanobacterial features than features of higher plants exhibited by PS I genes of diatoms. Still, due to lacking sequences, it is impossible to predict any structural features of this complex.

Since the comparison of several sequences was insufficient to define the organisation of the PS I complex of diatoms, the isolated PS I-FCP complex was analysed by BN-PAGE (figure 12). As a reference isolated thylakoids of pea were also loaded. The major band of the isolated complex was of similar molecular weight as the corresponding

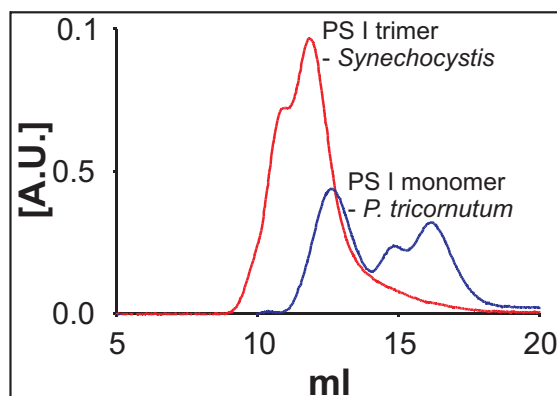


Figure 13: **Gel filtration of DDM solubilised thylakoids of *P. tricornutum* (blue line) and *Synechocystis* sp. (red line) directly applied to the column.** Elution was controlled at 700 nm. The largest maxima represent the eluted PS I complexes of both organisms, which was proven spectroscopically. The cyanobacterial trimer and the diatom monomer are indicated.

PS I-LHC I complex of pea indicating a molecular weight of more than 500 kDa. The less pronounced second band of the PS I-FCP complex was located below the respective LHC II trimer, most probably composed of the same Fcp monomers that were washed off in the gel filtration experiment (see figure 10 a).

To exclude a monomerisation of the PS I-FCP complex due to the isolation by IEX or during the BN-PAGE, solubilised thylakoids of *P. tricornutum* and of the cyanobacterium *Synechocystis* were separated on a gel filtration column (figure 13). To identify PS I containing fractions elution had to be followed by a wavelength typical for PS I complexes. Therefore the elution was controlled at 700 nm and absorbance spectra of the respective fractions were recorded (not shown). As the cyanobacterial complex was significantly larger (elution at approx. 12 ml) than the complex of *P. tricornutum* (elution at approx. 13 ml) it was concluded that the PS I-FCP complex is indeed a monomer³. This assumption was supported by electron microscopy studies with negatively stained

³The different elution volume compared to the pure PS I-FCP fraction in section 3.1.3 is mainly due to the use of a shorter column for gel filtration here.

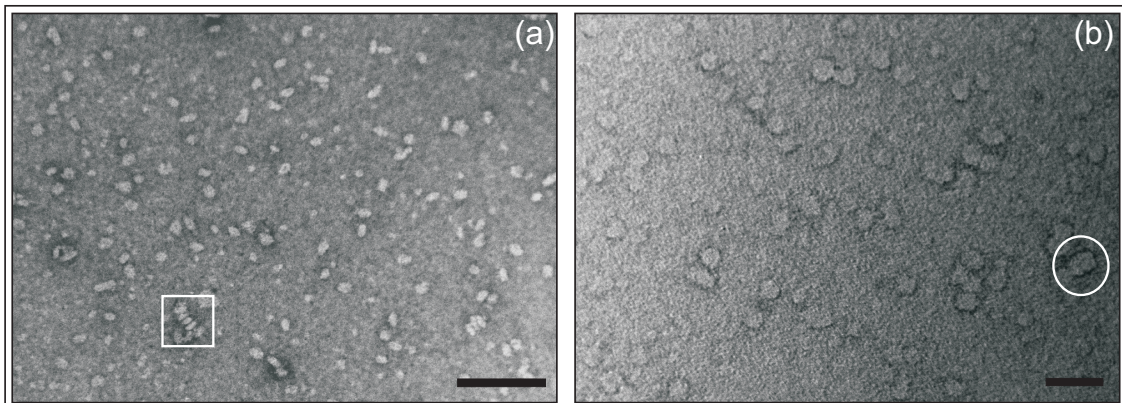


Figure 14: **Electron micrographs of the PS I-FCP complex.** In panel (a) a micrograph recorded with a magnification of 53,000 \times is shown. Scale bar represents 100 nm. Note the stacked particles from side view at the lower left representing a typical artefact of PS I particles (white box). Panel (b) shows a micrograph from glow discharged particles recorded at a magnification of 110,000 \times . Scale bar represents 50 nm. Note that particles are mainly top views (white circle).

particles of the same complex (figure 14). Two different kinds of particles were observed. The dominant version was flat and elongated and the minor version was nearly circular. Furthermore, the elongated particles had the tendency to attach to each other at their elongated sites and build stacks (panel a). These artefacts of PS I specimen have been described previously [112, 113]. Similar distances for both particles were observed when the length of the elongated particles was compared with the diameter of the circular particles. When using freshly prepared or glow discharged grids the number of the circular particles was increased (panel b). Therefore both kinds represent a different projection, i.e. orientation of the same particles which is influenced by the preparation of the grids. The flat elongated projections represent the side-view (membrane plane), whereas the circular ones are top-views. The observed particles (top view) had a diameter of 21.1 ± 3.2 nm ($n=32$) and resembled the size and shape of monomeric PS I particles isolated from green algae [18, 114] and thus exceeded the size of the single PS I cores of cyanobacteria [113], i.e. referring to the monomers. As no additional diatom specific

PS I subunits are known it is supposed that the associated Fcps are responsible for the increased size. No trimers or higher oligomeric states were observed. Therefore it is concluded that diatoms comprise of monomeric PS I complexes associated with Fcps as additional light-harvesting antenna.

3.1.5 Preparation yield

Taken together, the presented protocol provides the possibility to isolate a functional PS I-FCP complex from a diatom starting from the cell harvest up to the preparation of specimen for electron microscopy during one day. Concerning the yield, the concentration of total Chl of 12 d old cells was estimated to be 14 ± 1.95 mg/l ($n=17$). From that around 8 mg Chl of thylakoids were isolated that lead to the purification of approximately 0.5 mg Chl of the PS I-FCP complex.

3.1.6 Analysis of the IEX fractions II and V

Fractions II and V of the IEX were separated by SDS-PAGE (figure 15). Concentration of fraction II was so low that only upon silverstaining of the gel two polypeptides became visible. However, one stronger band at approximately 16 kDa and a weak band at approximately 17 kDa could be resolved. In fraction V a band at 47 kDa, two bands around 35 kDa, one band at 25 kDa and a strong band at 18 kDa were detected. As has been shown by Western Blot (figure 5), fraction V contained the PsbD reaction centre II protein. If compared to another PS II preparation from diatoms [78] the mentioned bands could resemble CP47, CP43, PsbO, D1 and D2. Furthermore, the 18 kDa band indicates the presence of a Fcp polypeptide. Therefore both fractions were immunodecorated with the α -ccFCP antibody (figure 16). As controls the PS I-FCP complex (fraction III) and the FCP (fraction IV) were loaded. Interestingly, fraction V showed a positive reaction, but the signal had a higher molecular weight as the signals in the fractions III and IV. Fraction II however, gave no signal at all. If

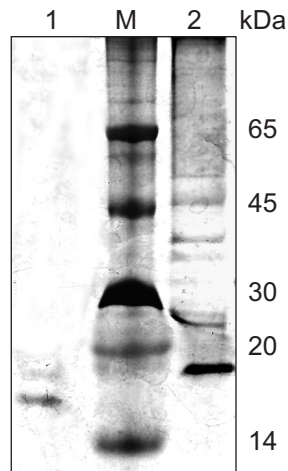


Figure 15: **SDS-PAGE of the IEX fractions II and V.** 300 μ l of fraction II (lane 1) were directly precipitated with 80 % acetone and loaded onto the gel. 2 μ g Chl of fraction V (lane 2) were loaded. Molecular weight marker proteins (lane M) are indicated on the right.

analysed spectroscopically, fraction II showed a typical carotenoid absorbance spectrum, with three maxima at approximately 430, 455, and 482 nm (figure 17). By HPLC analysis solely two pigments, fucoxanthin and diadinoxanthin, were identified in fraction II. The stoichiometry was approx. 2 fucoxanthin per 1 diadinoxanthin (mol/mol, data not shown). In contrast, the absorbance of fraction V was mainly dominated by Chl *a*, with a Q_y peak at 674 nm and only traces of Chl *c* and fucoxanthin, resembling a PS spectrum. Thus it was concluded that fraction V indeed represents a PS II fraction.

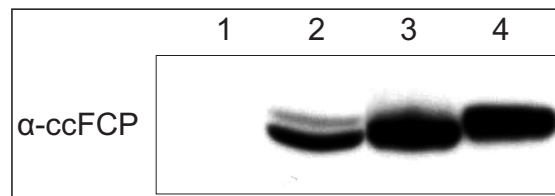


Figure 16: **Western Blot of IEX fractions II - V (lanes 1 – 4).** 10 μ l of concentrated fraction II were loaded directly on the gel. Fractions III - V were adjusted by their Chl concentration. 1 μ g Chl of fractions III and V, and 0.1 μ g Chl of fraction IV were loaded, respectively. The antibody directed against all Fcp polypeptides is indicated on the left.

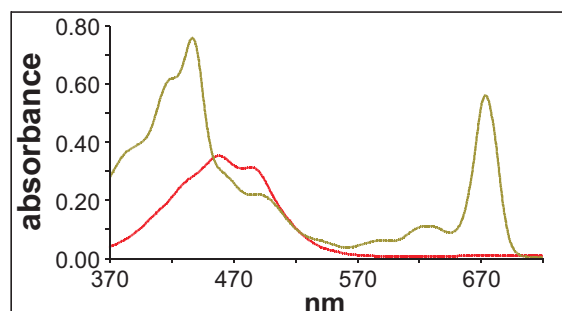


Figure 17: **Absorbance spectra of IEX fractions II (red line) and V (green line).** Spectra were measured at room temperature between 370 nm and 750 nm.

3.1.7 Purification of a PS I complex by discontinuous sucrose gradient centrifugation

As already mentioned, PS I complexes show a low fluorescence yield. Due to limitations of the photomultipliers usually concentrated PS I samples are used for fluorescence measurements. Nevertheless, upon increasing concentrations of samples the optical density (OD) rises as well. As an effect, re-absorption processes can be induced, the original fluorescence spectra get changed, and longer wavelengths become overestimated. To circumvent these artefacts, only diluted samples were used for the spectroscopic measurements (Chl *a* absorbance of $0.03 \simeq 0.3 \mu\text{g Chl } a/\text{ml}$, see figure 8). Since no LWCs were identified in the PS I-FCP sample (fraction III) by 77 K fluorescence spectroscopy (section 3.1.3) it had to be tested if the respective Chls were lost due to the isolation procedure by IEX. RT fluorescence emission measurements of *P. tricornutum* cell solutions starting from an $\text{OD}_{700\text{nm}} \simeq 10$ and subsequent dilutions lead to the identification of peaks at 735 nm and 705 nm. A similar experiment with the PS I-FCP complexes yielded similar emission maxima when the concentration of the sample was increased by a factor of approximately 10 (data not shown). These maxima were independent of the wavelength chosen for excitation ($\lambda_{Ex} = 440 \text{ nm}, 465 \text{ nm}, 560 \text{ nm}$). However, the far red fluorescence emission only increased under conditions allowing for re-absorption. Thus either the concentration of the respective chlorophylls is very low or they are not

energetically coupled. Otherwise the same wavelengths should have been detected at 77 K.

To check whether these data were due to the IEX purification, solubilised thylakoids were fractionated by another, more gentle separation method. Thus they were applied to a discontinuous sucrose gradient and ultra-centrifuged. After the run two pigment-protein bands were harvested (figure 18 a). The lower band 1 was of green colour and the upper band 2 was of brown colour, thus representing a photosystem and a Fcp fraction. To exclude that band 1 consisted of a PS I/PS II mixture, both bands were screened for the PS II core subunit PsbD via Slot Blot. As can be seen in figure 18 b the antibody only detected the positive control. Separation of bands 1 and 2 by SDS-PAGE resulted in a band pattern that mainly resembled the PS I-FCP and the FCP complexes of the IEX purification. Band 1 was mainly characterised by the PS I core polypeptides PsaA/B around 65 kDa and a strong band in the FCP range, whereas in band 2 a FCP

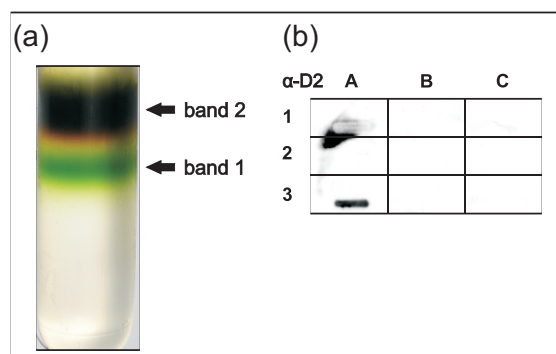


Figure 18: **Discontinuous sucrose gradient and Slot Blot.** (a) Thylakoids of *P. tricornutum* were solubilised and separated on a discontinuous sucrose gradient. The bands harvested are indicated on the right. (b) Approx. 0.25 μg Chl of the bands 1 and 2 from two independent sucrose gradients were loaded on a Slot Blot and analysed with an antibody directed against higher plant PS II core subunit PsbD. Samples of band 1 were loaded in the slots A1 and A2, samples of band 2 were loaded in the slots B1 and B2. 25 ng Chl of fraction V from the IEX (see section 3.1.1) was taken as positive control (A3). Slots C1 - 3 were loaded with buffers B1+, B1, and water respectively as negative control.

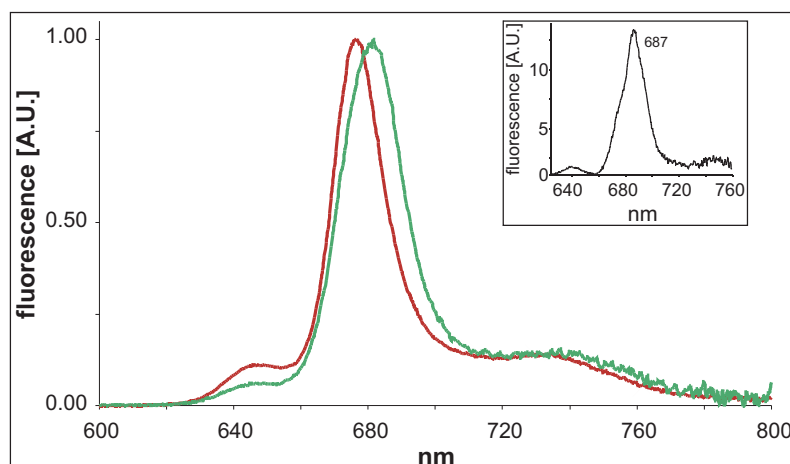


Figure 19: **Fluorescence emission of bands 1 (green line) and 2 (brown line) isolated by discontinuous sucrose gradient centrifugation.** Fluorescence emission was measured at RT with the excitation wavelength set to 465 nm. Spectra were normalised at their emission maxima, respectively. The inset displays the fluorescence emission of band 2 at 77 K with excitation wavelength set to 440 nm.

band around 18 kDa was observed (data not shown). Bands 1 and 2 were analysed spectroscopically. After adjustment of the Chl *a* concentration the fluorescence emission was recorded. Exemplary shown are the spectra with excitation wavelength set to 465 nm. Single maxima at 681 nm (band 1) and 677 nm (band 2) (figure 19) were detected. Thus the emission maximum of band 1 is shifted to the red in comparison to the PS I-FCP complex isolated by IEX (for comparison see figure 8). Also a minor Chl *c* emission fluorescence was detected, thus a partial impairment in energy transfer from Chl *c* to Chl *a* occurred. However, when the fluorescence emission of band 1 was measured at 77 K the emission maximum was shifted to 687 nm and two shoulders around 677 nm and 705 nm became visible (see inset figure 19). Thus an energy transfer to one emitter (at 705 nm), previously detected under re-absorption conditions only, could be proven. However, an energy transfer to the second emitter at 735 nm could not be resolved. These data indicate that the purification by IEX decoupled a Chl pool that fluoresces at 705 nm. Whether this pool is associated with the PS I core or with associated proteins that were affected upon IEX but not by sucrose gradient centrifugation could not be

clarified. Independent of the isolation procedure used no active energy transfer to the 735 nm emitter could be proven.

3.2 Association of Fcp polypeptides with PS I in the diatom *C. meneghiniana*

3.2.1 Isolation of pigment-protein complexes

In chapter 3.1.2 it was shown that the composition of Fcp polypeptides in the PS I-FCP complex differed from the free Fcp. To identify specific Fcp polypeptides associated with PS I, pigment-protein complexes of *C. meneghiniana* were isolated by discontinuous sucrose gradient centrifugation based upon the work of Z. Girmatsion and J. Brauns [81, 82]. The method of choice provided several advantages in comparison to the PS I-FCP preparation from *P. tricornutum*. First of all it was possible to use antibodies specific for Fcp polypeptides from *C. cryptica* whose functionality for preparations from *C. meneghiniana* were already demonstrated [62]. Furthermore, the purification of FCP complexes via sucrose gradient was already established and indicated a good chance to separate the two photosystems since two distinct green bands were obtained after the ultra-centrifugation [69]. Thylakoids of *C. meneghiniana* were solubilised with 15 mM DDM and subsequently loaded onto the sucrose gradient. In figure 20 the resulting separation into 5 pigmented protein bands is shown. Fraction A consisted mainly of free pigment and was not considered further. The second fraction represented the free FCP pool consisting of an upper phase of FCPa trimers and a lower phase consisting of FCPa trimers and FCPb higher oligomers [61, 69]. Both phases were pooled and considered as fraction B. Fractions C and D were of green colour and represented the 2 photosystems. To discriminate between the photosystems, fractions B, C, and D were analysed by a Western Blot, revealing a strong reaction of fraction C with an antibody directed against the PS II core subunit PsbD (see inset figure 20). No reaction was

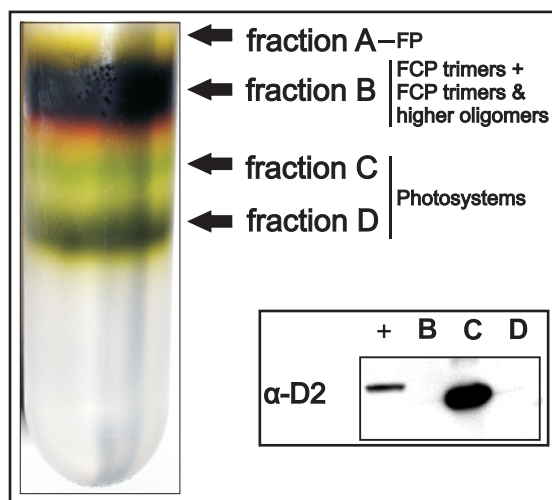


Figure 20: **A sucrose gradient after fractionation of thylakoids solubilised with DDM.** Pigmented bands are indicated. The inset depicts a Western Blot of the sucrose gradient fractions B, C, and D and thylakoids of pea (+) as positive control. The antibody used was directed against the PS II subunit PsbD. 4 μg Chl of all samples were loaded, except for fraction B (0.5 μg Chl).

observed in the other fractions B and D. Thus, PS II was solely located in fraction C and fraction D was devoid of PS II. Absorbance spectra supported these results (figure 21a). Whereas fraction B represented a typical FCP (for comparison see figure 8), fraction C showed a red shifted Chl *a* Q_y peak at 673 nm. Absorbance of Chl *c* and fucoxanthin were hardly visible in the spectrum. Fraction D showed similar features as fraction C but with a broadened Q_y band of Chl *a* with a maximum at 679.5 nm, thus resembling a PS I spectrum. Furthermore fraction D exhibited a red shifted fluorescence emission that was quenched by 95 % in comparison to fraction B (figure 21 b), when the emitter concentration was adjusted similarly (Chl *a* absorbance set to 0.03, compare with panel (a)). Fraction C however fluoresced at the similar wavelength as fraction D (680 nm) but was only quenched by 68 % in comparison to fraction B. In the 77 K fluorescence excitation spectra measured at 675 nm fraction B showed transfer from the pigments Chl *a*, Chl *c*, and fucoxanthin towards Chl *a* (figure 22 a). Although the absorbance spectra of fraction C showed little fucoxanthin, energy transfer from this pigment to Chl *a* was

still visible, whereas this was almost not the case for fraction D. Similar results were obtained when the excitation fluorescence was measured at room temperature (data not shown).

As already mentioned in chapter 3.1.3 the fluorescence yield of PS I complexes at RT is known to be very low [76]. Therefore the fluorescence emission of all fractions was measured again but at 77 K (figure (22 b)). Upon excitation at 440 nm, fraction B showed a strong Chl *a* peak at 676 nm. Fraction C revealed a typical 77 K PS II signal with a splitted Chl *a* maximum, peaking at 676 nm and 687.5 nm, the latter being more pronounced [115]. Fraction D showed two maxima at 676 nm and at 717 nm, as well as a shoulder at 688 nm. It should be mentioned that all three fractions exhibited also a slight Chl *c* emission, indicating a partial decoupling of pigments inside the Fcp antenna. To identify the pigments inducing the several fluorescence emission peaks of fraction D, the fluorescence excitation measurements were repeated with emission measured at 688 nm and 717 nm. Interestingly, a transfer of a carotenoid, probably fucoxanthin, was detected in both cases (exemplary shown in figure 22 a, black line, emission wavelength

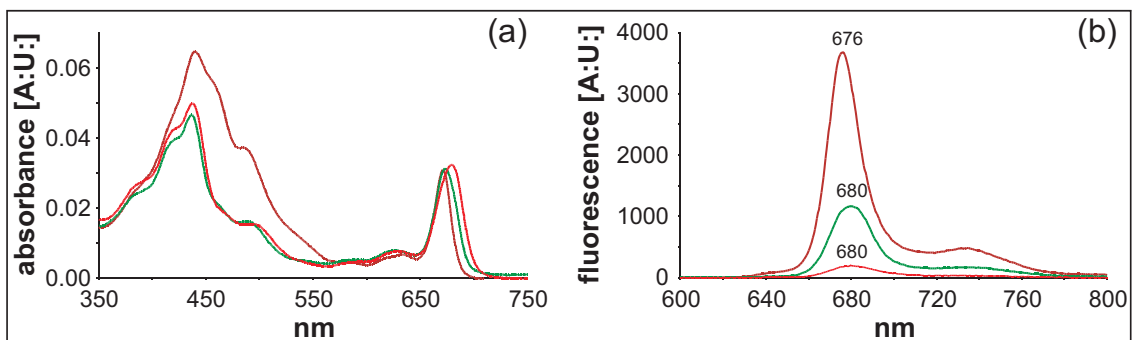


Figure 21: **Absorbance and fluorescence emission spectra of the sucrose gradient fractions B, C, and D.** In panel (a) the absorbance spectra of fractions B (brown line), C (green line), and D (red line) are shown. All samples were adjusted to a Chl *a* Q_y absorbance of about 0.03. In panel (b) the same samples were used for fluorescence emission measurements. Excitation wavelength was set to 440 nm. Emission maxima are indicated.

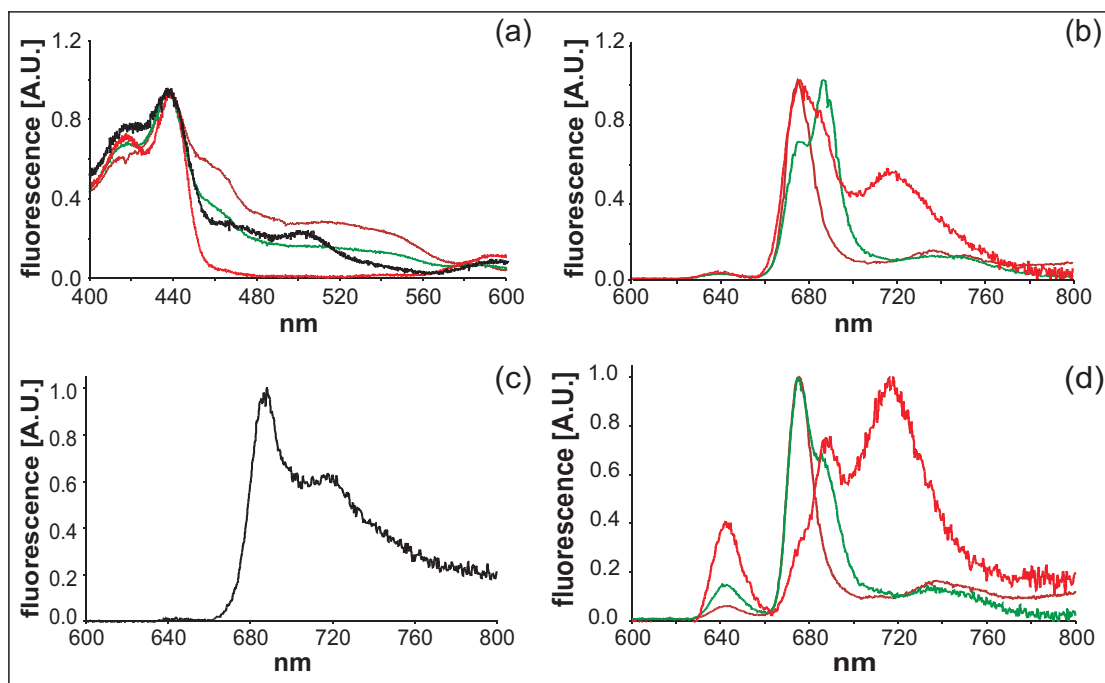


Figure 22: **77 K fluorescence emission and excitation spectra of the sucrose gradient fractions B, C, and D.** In panel (a) the fluorescence excitation spectra of fractions B (brown line), C (green line), and D (red line) measured at 675 nm are shown. All samples were adjusted to a Chl *a* Q_y absorbance of 0.03. Furthermore, fluorescence excitation of fraction D (black line) with emission wavelength set to 717 nm is included. In panel (b) the same samples were used for fluorescence emission measurements with excitation wavelength set to 440 nm. For comparison, the emission fluorescence of fraction D further purified by gel filtration (D_A) is given in panel (c). Excitation wavelength was set to 440 nm. Emission fluorescence of the fractions B, C, and D with the excitation wavelength set to 465 nm is shown in panel (d).

measured at 717 nm). Therefore both pigments belong to an Fcp antenna, whose contribution to fluorescence in fraction D could not be distinguished from the fluorescence of PS I under room temperature conditions. To exclude that no free Fcp not properly bound to the PS I complex in fraction D contaminated the spectra an analytical gel filtration chromatography was performed (figure 23). In this way it would be possible also to find out which of the detected emission peaks were caused by Fcps. Due to the gel filtration fraction D was separated into two peaks, named thereafter D_A and D_B , the first representing the main peak. D_A absorbed at all detection wavelengths,

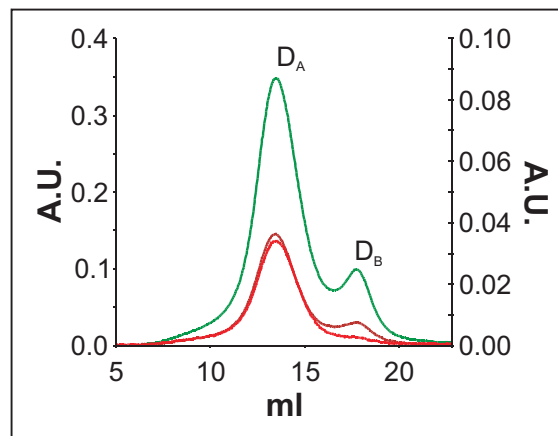


Figure 23: **Gel filtration of the sucrose gradient fraction D.** The separated peaks D_A and D_B are indicated. Elution was controlled at 437 nm (green), 530 nm (brown), and 700 nm (red). For better visualisation the absorbance at 437 nm is depicted on the left y-axis, whereas the two other wavelengths were plotted according to the right y-axis.

437 nm, 530 nm, and 700 nm, whereas D_B absorbed only at 437 nm and 530 nm. Thus D_A represented PS I and D_B represented washed off polypeptides, probably Fcps. The absorbance spectrum of D_A resembled fraction D (data not shown). D_B showed a Chl *a* Q_y absorbance at approximately 670 nm. However, due to its low concentration D_B could not be analysed properly, thus no further analysis of this sample was performed.

77 K fluorescence emission of D_A with the excitation wavelength set to 440 nm resulted in Chl *a* maxima at 688 nm and 717 nm (figure 22 c). The Chl *c* emission and the Chl *a* peak at 676 nm detected in fraction D were not visible. Thus both signals originated from the fluorescence of Fcp polypeptides that were removed by the gel filtration. This interpretation was supported by measuring the fluorescence emission of fraction D again with the excitation wavelength set to 465 nm, i.e. into the Chl *c* absorption band. Thereby an obvious Chl *c* emission was caused and revealed the presence of uncoupled and most probably unfunctional Fcp polypeptides within this sample. Nevertheless, also functional Fcps properly bound were present in fraction D, since the maxima at 718 nm and 688 nm were increased and the 676 nm signal became

a shoulder which was hardly visible (figure 22 d). This means that upon excitation of the bound Fcp antenna in fraction D, energy is transferred towards PS I and subsequently emitted at 688 nm or 717 nm. Furthermore, the 717 nm emission maximum indicates that the Fcps bound to PS I have different properties as the main FCP complexes (fraction B). The emission maximum of fraction B was independent from the excitation wavelengths chosen and remained at 676 nm. Fraction C however, showed an inversion of the fluorescence maxima. Upon excitation of Chl *c* (465 nm) the former maximum peak at 687.5 nm decreased, while the peak at 676 nm became the maximum.

3.2.2 Polypeptide analysis

To find out if the different spectroscopic characteristics of the sucrose gradient fractions B, C, and D are related with a different composition of Fcp polypeptides they were separated by SDS-PAGE and analysed immunologically (figure 24). Fraction B showed the typical pattern of Fcp polypeptides described for *C. meneghiniana*, with two dominant bands at 18 and 19 kDa (panel a). One band at approximately the same size was found in fraction C together with several bands between 40 and 25 kDa which probably resemble the core subunits of PS II. Fraction D seemed to contain a PS I complex showing the typical PS I core polypeptides (PsaA/B) at 65 kDa and several bands below 20 kDa which could be Fcps as well as smaller PS I subunits (for comparison see section 3.1.1). The same samples were immunodecorated with an antibody against all Fcp polypeptides of *C. cryptica* (α -ccFcp) (figure 24, panel b). As already seen in the SDS-PAGE, two signals at 18 kDa and 19 kDa were detected in fraction B. A similar reaction was observed in fraction C. However, in fraction D three bands were detected. Two signals at 19 kDa and 18 kDa signals resembled the results of fractions B and C. The third signal was located approximately at 17 kDa. The same experiment was repeated using the specific antibodies α -Fcp2, α -Fcp4, and α -Fcp6 of *C. cryptica*. Fcp2 belongs to class I Fcps with a predicted molecular weight of 18.4 kDa [116]. In fractions B and C the

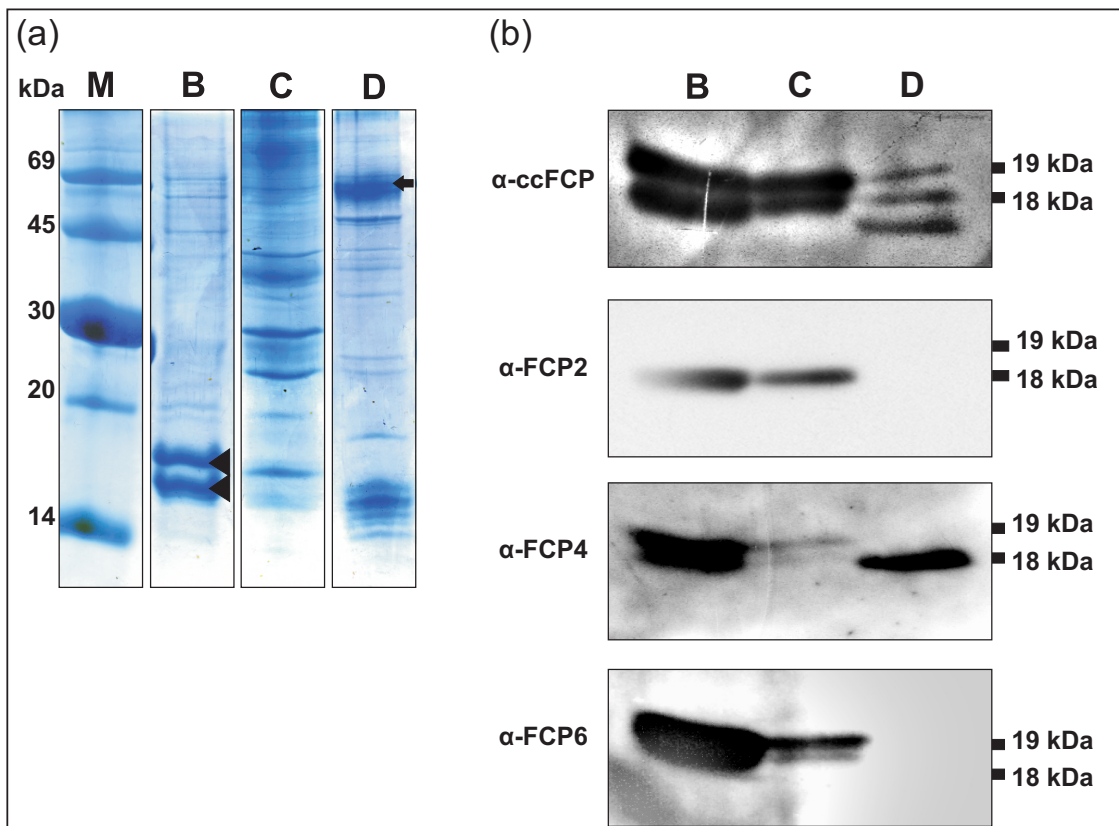


Figure 24: **SDS-PAGE (a) and Western Blot (b) of pigment-protein fractions B, C, and D.** Lanes are named according to the loaded samples. All samples contained 4 μg Chl each, besides fraction B (0.5 μg Chl). In panel (a) the marker proteins (M), 18 kDa and 19 kDa Fcp polypeptides (arrowheads), and PS I core subunits PsaA/B (arrow) are indicated. In panel (b) the antibodies used (α -ccFcp, α -Fcp2, α -Fcp4, and α -Fcp6) are shown on the right of the respective Western Blots, molecular weights are given on the right.

antibody detected a single 18 kDa band, whereas fraction D showed no signal at all. Thus fraction B and C resemble the results published for the trimeric FCPa complex of *C. meneghiniana*. Again the typical 18/19 kDa signal of fraction B was detected, when the samples were incubated with the α -Fcp4 antibody. In this case a cross reaction of the antibody is supposed because the predicted molecular weight of Fcp4 (18.1 kDa) is less than the predicted molecular weights of Fcp2 or Fcp6. Thus this effect might have occurred due to the high concentration of Fcp polypeptides in this fraction. Faint, but

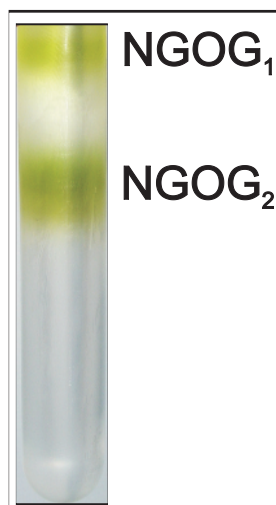


Figure 25: **Discontinuous sucrose gradient centrifugation of re-solubilised fraction D.** Exemplary shown is the result of a NGOG re-solubilisation and following separation by ultracentrifugation. Pigment-protein fractions NGOG₁ (upper band) and NGOG₂ (lower band) are indicated.

similar signals were also detected in fraction C. In contrast, only one band at 18 kDa was detected in fraction D. In case of the α -Fcp6 antibody mainly 19 kDa polypeptides of the fractions B and C were detected, again with minor unspecific signals at 18 kDa. In fraction D no reaction was observed and it should be mentioned that none of the antibodies used, beside the α -ccFcp antibody, detected the 17 kDa band in fraction D.

3.2.3 Further purification of PS I

To study the binding of the Fcp polypeptides bound to the PS I complex in fraction D they had to be sequentially removed. Therefore fraction D was re-solubilised with either a mixture of NG and OG or TX 100 and then again ultracentrifuged on a discontinuous sucrose gradient. In both cases the ultracentrifugation resulted in the splitting of fraction D into two green bands (exemplary shown for a NGOG re-solubilisation in figure 25). Fractions were named after the detergent used and ₁ for the upper band and ₂ for the lower band. None of the chosen treatments resulted in a complete removal of Fcp polypeptides from the PS I core (detected immunologically). The two fractions were

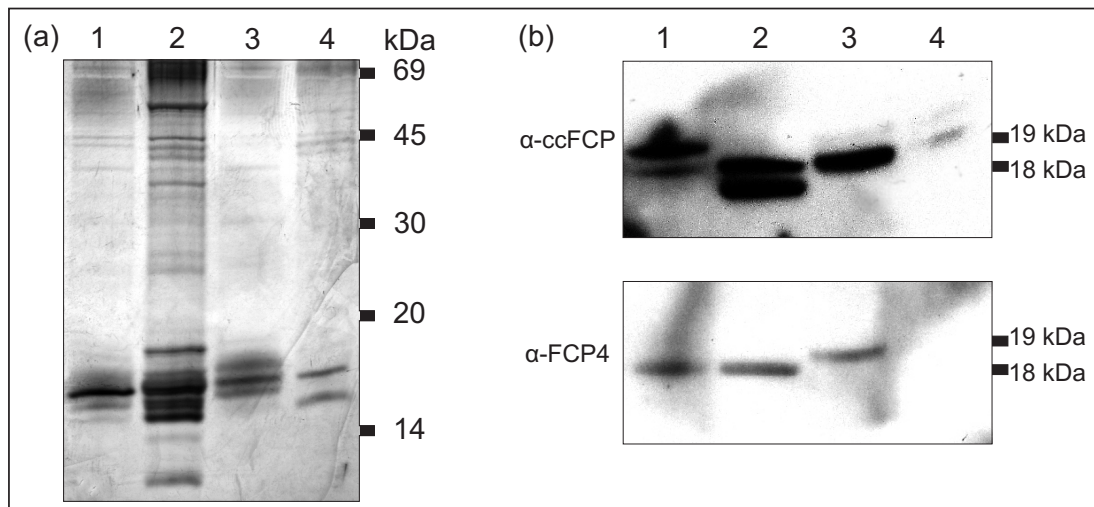


Figure 26: **SDS-PAGE (a) and Western Blot (b) of purified fractions derived from re-solubilisation of fraction D and further separation by sucrose density centrifugation.** All loaded samples contained 4 μ g Chl each. In (a) the fractions NGOG₁ and NGOG₂ (lanes 1 and 2) and TX₁ and TX₂ (lanes 3 and 4) are presented. Molecular weight marker proteins are given on the right. In (b) the respective Western Blots are displayed. Antibodies used were α -ccFcp, and α -Fcp4. Molecular weights are indicated on the right.

harvested and separated by SDS-PAGE (figure 26 a). In the upper fraction NGOG₁ (lane 1) the PsaA/B core subunits of PS I disappeared, whereas several bands below 20 kDa were preserved. In contrast, the lower fraction NGOG₂ (lane 2) nearly reflected the band pattern of fraction D (for comparison see 24, lane D) albeit with different strength of the various bands. The upper fraction TX₁ was comparable to NGOG₁ (lane 3), fraction TX₂ however was mainly characterised by two bands between 16 and 18 kDa (lane 4). The PsaA/B subunits were hardly visible. The samples were again immunodecorated with the α -ccFcp and the α -Fcp4 antibodies (figure 26 b). No analysis was performed with the α -Fcp2 or α -Fcp6 antibodies since both failed to detect any Fcp polypeptides in fraction D. The incubation with the α -ccFcp antibody resulted in the detection of the Fcp 18/19 kDa signal in fraction NGOG₁ (lane 1). However, the reaction of the 19 kDa signal was more pronounced. In contrast, an 18 kDa and a 17 kDa signal were detected

in fraction NGOG₂ (lane 2). Fraction TX₁ (lane 3) somehow resembled NGOG₁ but with different strengths of the detected bands. A strong 18 kDa band and an extremely faint 19 kDa band were observed. In fraction TX₂ nearly the detection limit was reached and signals at 18 kDa and 19 kDa were hard to detect at all (lane 4).

To complete the analysis of these sucrose gradient fractions, the pigment contents of fractions B, C, D, and the re-solubilised fractions were estimated by HPLC. The resulting pigment stoichiometries (mol pigment per mol Chl *a*) are presented in table 3. The data for fraction B resembled the results published in [66, 69] although with a slightly reduced amount of Chl *c*, which might be due to the varied isolation procedure. Lower amounts of Chl *c*, fucoxanthin, diadinoxanthin and diatoxanthin with respect to Chl *a* were found in fractions C and D. It should be mentioned that during the concentration procedure of fraction C a protein precipitation occurred. Thus the measured pigment values are hardly representative. Especially the concentration of the xanthophyll cycle pigments was so low, that in some of the measurements they were not detectable at all. Nevertheless, for completion of the presented data the pigment values of fraction C were included. The only pigments of fraction C with a decent amount were Chl *a*

Table 3: Analytical HPLC of sucrose gradient fractions B, D, NGOG₁, NGOG₂, TX₁, and TX₂

	fucoxanthin	Chl <i>c</i>	diadinoxanthin	diatoxanthin	β -carotene
<i>pigment per Chl a [mol/mol]</i>					
Fraction B	0.935 ± 0.081	0.181 ± 0.019	0.189 ± 0.013	0.237 ± 0.023	0.012 ± 0.008
Fraction C	0.033 ± 0.010	0.016 ± 0.008	0.015 ± 0.005	0.0015 ± \	0.050 ± 0.018
Fraction D	0.137 ± 0.019	0.015 ± 0.001	0.068 ± 0.008	0.096 ± 0.019	0.122 ± 0.010
Fraction NGOG ₁	0.068 ± 0.006	0.008 ± 0.002	0.043 ± 0.004	0.035 ± 0.008	0.006 ± 0.001
Fraction NGOG ₂	0.067 ± 0.003	0.005 ± 0.000	0.034 ± 0.002	0.033 ± 0.001	0.060 ± 0.003
Fraction TX ₁	0.100 ± 0.006	0.010 ± 0.001	0.042 ± 0.002	0.053 ± 0.005	0.019 ± 0.001
Fraction TX ₂	0.007 ± 0.004	0.001 ± 0.001	0.016 ± 0.007	0.005 ± 0.002	0.078 ± 0.011

Values were calculated on the basis of Chl *a* content. Ratios are given as mean ± standard deviation of 6 measurements on 2 independent preparations (B), 5 measurements on 1 preparation (C), 10 measurements on 3 independent preparations (D), 3 measurements on 1 preparation (NGOG_{1/2}, TX₁), and 6 measurements on 2 independent preparations (TX₂), respectively. For completion, parts of the pigment data were taken from [82]

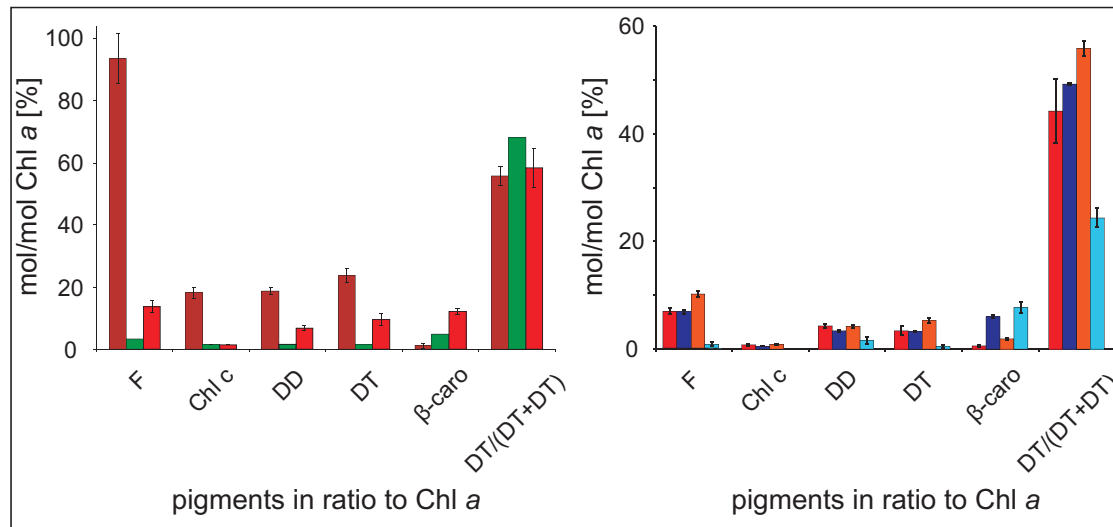


Figure 27: **Analytical HPLC of the sucrose gradient fractions B, C, D, (panel a) and the re-solubilised fractions NGOG₁, NGOG₂, TX₁, and TX₂ (panel b).** Pigments analysed were fucoxanthin (F), Chl c, diadinoxanthin (DD), diatoxanthin (DT), and β -carotene (β -caro). Pigment ratios were calculated on the basis of Chl a content [mol/mol]. Apart from that also the de-epoxidation rate (mol diatoxanthin/(mol diadinoxanthin + diatoxanthin)) of all fractions was calculated. The \pm standard deviation is indicated (compare with table 3). Fraction B is shown in brown, fraction C in green, and fraction D in red (panel a). In panel b NGOG₁ is given in red, NGOG₂ in dark blue, TX₁ in orange, and TX₂ in light blue.

and β -carotene. The latter being even increased by a factor of ~ 4 in comparison to fraction B. In the case of fraction D fucoxanthin was decreased by a factor of ~ 7 , whereas diadinoxanthin (DD) and diatoxanthin (DT) decreased only by a factor of ~ 2.5 in comparison to fraction B. Still, the de-epoxidation rate in both samples was nearly the same (~ 0.6) (see figure 27). As expected for a PS I fraction, the β -carotene ratio in D was increased by a factor of ten. In the resolubilised fractions NGOG₁ and NGOG₂, all the pigments were reduced further. In both fractions the Chl c:Chl a ratio was below 1 % and fucoxanthin was reduced to approximately 7 %. However, fraction NGOG₂ still contained ten times more β -carotene than NGOG₁. In contrast, fraction TX₁ nearly contained ten times more Chl c, fucoxanthin, and diatoxanthin as fraction TX₂. Still, the ratio of β -carotene in fraction TX₂ was approx. 4 times higher than in fraction TX₁.

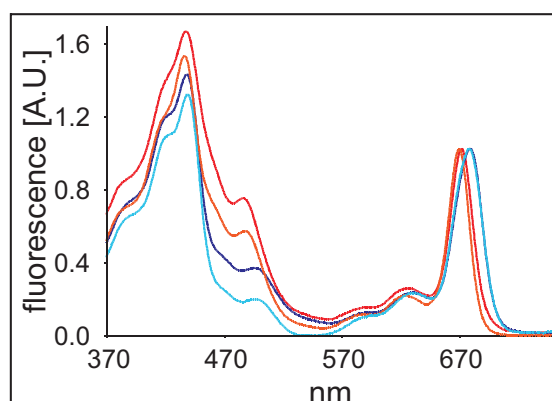


Figure 28: **Absorbance spectra of the re-solubilised fractions NGOG_{1/2} and TX_{1/2}.** Absorbance spectra were recorded at room temperature between 370 nm and 750 nm. The spectra of NGOG₁ (red line), NGOG₂ (dark blue line), TX₁ (orange line), and TX₂ (light blue line) were normalised to 1 at their respective Chl *a* Q_y peaks.

Absorbance spectra of the re-solubilised fractions led to comparable characteristics of NGOG₂ and TX₂ if compared to fraction D (figure 28). NGOG₁ and TX₁ rather resembled a spectrum of a Fcp albeit with strongly reduced concentrations of Chl *c* and fucoxanthin (for comparison see absorbance spectrum of fraction D in figure 21). The Chl *a* Q_y maximum were shifted to 672 nm and 670 nm, respectively and upon excitation at 465 nm a noticeable Chl *c* emission around 645 nm became visible (data not shown). Taken together with the results from SDS-PAGE and HPLC it was concluded that NGOG₂ represents a further purified PS I complex, although not completely devoid of Fcps. The same was in principle true for TX₂ regarding the spectroscopic properties, although the harsh re-solubilisation seemed to have affected the polypeptide composition. NGOG₁ and TX₁ contained mainly the washed off Fcp polypeptides and a higher amount of the Fcp specific pigments fucoxanthin and Chl *c* but lost their abilities of intact excitation energy transfer. Since Fcp6 was only found in fraction C, i.e. the only PS II containing fraction, and the 17 kDa Fcp polypeptide and Fcp4 were visible in fraction D and the re-solubilised fractions, i.e. PS I, we had to conclude that the distribution of these polypeptides differs between the photosystems.

4 Discussion

During the last years detailed structural as well as spectroscopic information about PS I supercomplexes has accumulated. The PS I crystal structures of *T. elongatus* [26] and *P. sativum* [17, 28], as well as supramolecular structures derived from electron microscopy of green algae [18, 114] and prochlorophytes [112] demonstrated the differences in the organisation of the light harvesting complexes but also showed the similarity of the core complexes. Based on the 2.5 Å and 4.4 Å crystal structures of cyanobacteria and higher plants it was possible to build a theoretical model of plant PS I [17, 26, 31] revealing that the core structure of a protein complex as complicated as PS I has been conserved over more than a billion years. Diatoms, another group of photosynthetic organisms that evolved very quickly during the last 250 million years [57], possess the same PS I subunits as cyanobacteria or higher plants, but differ considerably in the accessory pigment composition of their LHCs (FCPs), with Chl *c* and fucoxanthin bound. Since there is no structure of photosynthetic protein complexes from diatoms available a method was developed to isolate a PS I-FCP complex from thylakoids of the pennate diatom *P. tricornutum*. The protocol using IEX to purify the complex allowed for a complete isolation of the PS I-FCP complex within one day, starting from the cell harvest. The obtained PS I-FCP particles were then ready to be used for electron microscopy studies. Besides, also the isolation of a Fcp, a PS II containing fraction, and a so far not identified candidate of a xanthophyll-binding protein was possible using the same procedure. To further investigate in the organisation of Fcps bound by PS I of diatoms another method was chosen. The purification of pigment-protein complexes by discontinuous sucrose density centrifugation, previously described by [69], led to the isolation of PS I samples from *C. meneghiniana*. Re-solubilisation experiments with the isolated PS I fraction allowed for a partial separation of Fcp polypeptides from the PS I core. Taking use of specific antibodies single Fcp polypeptides associated with PS I and PS

II of *C. meneghiniana* were identified. Thus it was possible to identify Fcp polypeptides more tightly associated with PS I of diatoms.

In the following section the results on the isolation of the PS I-FCP complex of *P. tricornutum* will be discussed. For better comprehension the second section is focussed on the association of Fcp polypeptides with PS I of *C. meneghiniana*. Finally, some concluding remarks will be made.

4.1 The monomeric PS I-FCP complex of *P. tricornutum*

SDS-PAGE and Western Blot analysis revealed that the PS I-FCP fraction contained two Fcp polypeptides of different molecular weight compared to the main Fcp fraction. The band pattern obtained resembles mainly the data from Berkaloff et al. [76] but these authors did not elucidate the polypeptide composition any further. Herein, Fcp polypeptides of *P. tricornutum* were identified for the first time, which differ from the main Fcp pool and are associated with PS I (published in [80]). Some unbound and functionally impaired Fcp polypeptides co-purified in the PS I-FCP fraction were removed by analytical gel filtration but the spectroscopic properties of the PS I-FCP complex remained unaffected (see figure 10). Furthermore the polypeptide pattern obtained for the PS I-FCP complex indicated the presence of several smaller PS I subunits. At least five bands could be observed that are different in size compared to the Fcps detected by Western Blot. As several of the smaller PS I subunits as PsaL or E and Psa C, I and J can hardly be separated by SDS-PAGE as shown by Amunts as well as Chitnis and co-workers [103, 104] it is supposed that all of the 10 PS I subunits found in the genome are preserved in the PS I-FCP sample. Nevertheless, to be sure about the identity of these polypeptides they have to be analysed by immunological means or sequencing.

From the *T. pseudonana* genome [59] and studies on genes encoding Fcp of *C. cryptica* [70, 71, 116] three different groups were found on gene level. They were defined by homologies towards either *fcps* of brown algae (group 1), PS I related *lhcs* of red algae (group 2), or light-inducible *lhcs* of green algae (group 3) (for details see section 1.4). Until very recently, only 6 group 1 genes were described for *P. tricornutum* (*fcpA-F*) [72]. The sequences derived from cDNAs, i.e. from highly expressed genes. Two of them (FcpC or D and E) were identified to be located in the free Fcp pool by MALDI-TOF/TOF-MS [64]. Taking into account the different composition of Fcp polypeptides in the PS I-FCP complex and the free Fcp isolated during this work, it seems likely that the PS I associated Fcp polypeptides do not belong to group 1 Fcps. However, with the publication of the whole *P. tricornutum* genome by Bowler and co-workers [56] and the previously published EST data [101] also group 2 and 3 genes were identified and annotated in *P. tricornutum*, represented by e.g. *lhcr3* (Gene ID: 7197307) and *lhcx1* (GeneID: 7200476). The predicted molecular masses of translated *lhcr3* and *lhcx1* including the transit peptide are 21.11 kDa and 21.95 kDa and differ from FcpsA-F (between 21.21 kDa and 21.36 kDa)⁴. So far, only the supposed transit peptides of FcpsA-F are known to be 31 aminoacids (approximately 3 kDa). It is suggested that the transit peptides of *lhcx1* and *lhcr3* are of similar size. Therefore the molecular weights of *lhcr3* and *lhcx1* should still differ from FcpsA-F after the cleavage of the transit peptides. Referring to the observed Fcp band pattern in the PS I-FCP complex an association of group 1 or 2 Fcp polypeptides (*lhcr3* and *lhcx1*) with PS I can be assumed. However, until no specific antibodies are available or protein sequencing of the PS I associated Fcps has been performed these assumptions remain speculative.

⁴The transit peptide of diatoms is a bipartite sequence containing an ER-like signal peptide and the following chloroplast transit peptide. Note that 4 plastid membranes have to be crossed if proteins are targeted to the stroma. The outermost envelope membrane is studded with ribosomes and continuous with the ER itself [117]

Apart from the analysis of Fcp polypeptides the specific activity of the PS I reaction centre P700 was proven by difference spectra measurements. The calculated chlorophyll/PS I ratio of approximately 200 is comparable to data from [76] and [79] and became hardened by the analytical HPLC data. The measured chlorophyll/ β -carotene ratio of the PS I-FCP complex of 10 argues for around 100 chlorophyll molecules more than the cyanobacterial PS I core, which coordinates 96 chlorophylls and 22 β -carotenes [26]. Furthermore, these calculations are in good agreement with PS I-LHC I preparations from green algae [18]. Beside that, the HPLC measurements also indicate that the Fcps bound by PS I and the free FCP complex isolated retain a comparable Chl *c*/fucoxanthin ratio (1:5) as reported for FCP complexes from *C. meneghiniana* [62, 66]. Still, concerning the amount of the xanthophylls diadinoxanthin and diatoxanthin in relation to fucoxanthin of the PS I-FCP complex, an increase was denoted compared to the free Fcps. This holds true also for the already mentioned FCP complexes from *C. meneghiniana*. Thus the NPQ involved xanthophylls, coordinated by PS I specific Fcp polypeptides, might serve as photoprotectants of PS I.

After the detection of Fcp polypeptides associated with the PS I complex via SDS-PAGE, Western Blot, gel filtration and HPLC it had to be proven that both complexes are also energetically coupled. In the beginning of the experiments it was expected that the fluorescence characteristics of a PS I complex would differ from a light-harvesting complex such as the free Fcp. The isolated PS I-FCP complex showed a reduced amount of accessory pigments Chl *c* and fucoxanthin (in comparison to the free Fcp) as well as a broadened and red-shifted Chl *a* Q_y absorbance peak, the latter being a characteristic of PS I complexes [105, 106, 118]. It was supposed that in a fluorescence experiment the emitting wavelengths would be red-shifted in comparison to the free Fcp. This was not the case. Emission fluorescence peaks of both complexes were located at an identical wavelength (677 nm). However, another characteristic of PS I complexes is the

high quantum efficiency of PS I at RT, which is close to 1 [13, 119], i.e. nearly every photon absorbed leads to charge separation at the RC. As an effect the fluorescence yield of PS I is extremely low [107, 120] which is even enhanced by the capability of the oxidised P700* to efficiently quench excitation energy [32, 121, 122]. As an example the work of Croce and co-workers should be mentioned who reported a fluorescence yield of PS I-LHC I complexes of *Chlamydomonas reinhardtii* of 0.5 % [123]. Advantage of the high fluorescence yield of Fcps in comparison to PS I complexes was taken, which has been shown to be the case also in diatoms [76], to prove that an energetical coupling existed between Fcps and PS I. A significant decrease in fluorescence of the PS I-FCP fraction compared to the free Fcp was observed when either the same Chl *a* or fucoxanthin concentrations were used, i.e. similar emitter or Fcp concentrations in both samples. Without an energetic coupling the fluorescence emission should have been similar at least in case of the same Fcp concentration in both samples. Instead, the fluorescence decreased and energy transfer occurred which was quenched by the PS I core.

As already mentioned the PS I-FCP complex and the free Fcp showed a fluorescence emission at similar wavelengths at RT. Surprisingly, also fluorescence emission measurements at low temperature (e.g. 77 K), a method chosen to identify long wavelength chlorophylls (LWCs) of PS I that cannot be resolved under RT conditions, yielded no differences between the two samples. In cyanobacteria as well as higher plants and green algae, the presence of LWCs are reported, located either in the PS I core complex or distributed between the PS I core and the LHCs [124–128]. LWCs are defined by an absorbance with a maximum longer than 700 nm (i.e. less excited state energy than P700). The fluorescence yield of LWCs strongly increases at low temperatures because excitation energy not utilized by the RC migrates predominantly to LWC (see [32] and references therein). These LWCs were absent in the PS I-FCP fraction of *P. tricornutum* purified by IEX which is contrast to results published by Berkaloff and co-workers [76]. In

their work digitonin solubilised thylakoids of *P. tricornutum* applied to a sucrose gradient yielded a PS I fraction with a maximum fluorescence emission peak at 715 nm measured at 77 K. Upon re-solubilisation with DDM this peak was lost and subsequent fractions, again purified by sucrose density centrifugation, did not exhibit any LWC fluorescence. However, it is unclear whether the 715 nm emission of the first purification step was due to the solubilisation with digitonin or because of a high concentration of sample used during the prior fluorescence measurements. Because of the limitations of the photomultipliers and the low fluorescence yield of PS I complexes increased concentrations are often used. As an effect re-absorption processes can occur which result in an overestimation of fluorescence of the pigments with the lowest excited state energy. Therefore a real energy transfer from pigments with high excited state energy to pigments with low excited state energy cannot be proven. At such conditions, allowing for re-absorption of the participating pigments, LWCs were detected also in the IEX isolated PS I-FCP complex at RT. Beside the already mentioned 677 nm fluorescence maximum, a peak at 735 nm and a shoulder at 705 nm were identified, whereas it has to be thought of whether the latter can be declared as a LWC. LWCs usually undergo a Stokes' shift (distance between absorbance and fluorescence maximum) of at least 9 nm [129]. Since the absorbance Chl *a* Q_y peak of the PS I-FCP complex at RT was very broad, the origin of that emitter could not be clarified. It is assumed that the absorbance of the 705 nm emitter is located at a wavelength shorter than 700 nm. Nevertheless, a 77 K fluorescence emission shoulder at about 705 nm was identified also in a PS I complex of *P. tricornutum* when prepared under less harsh conditions by sucrose density centrifugation. In this case the fluorescence was measured preventing re-absorption to occur (i.e. diluted sample). Therefore the energy transfer towards the 705 nm emitter in that sample is of real nature and indicates a pigment coupling non-existent in the PS I-FCP sample purified by IEX. However, it is impossible to locate the origin of the 705 nm emitter. Probably the 705 nm emitter did not derive from the PS I core but from Fcps that were not remo-

ved due to the different preparation method. Spectroscopic studies on LHC I of higher plants and green algae led to the identification of Chl *a* pools with absorbance maxima between 690 and 695 nm and fluorescence peaks between 702 nm and 705 nm [129, 130].

The 735 nm emitter only occurred due to re-absorption events. Independent from the isolation method chosen no direct energy transfer to this LWC could be proven. This result allows for three interpretations: both isolation procedures, probably due to a similar solubilisation of thylakoids, lead to a decoupling of the 735 nm emitter. Therefore no energy transfer can be observed. This could be due to the usage of DDM, as the PS I preparation using digitonin reported by Berkaloff et al. led to a 715 nm emission fluorescence. Nevertheless, the PS I complex prepared from *C. meneghiniana* (discussed below) was isolated using a nearly identical method (referring to DDM solubilisation and the isolation by sucrose gradients) and LWCs were preserved. Thus it seems unlikely, that the usage of DDM as detergent is the reason for the loss of the LWCs. Another possibility would be a structural change of the pigment arrangement in the complexes which led to a decoupling, induced by the measurements at low temperatures (77 K). Under RT conditions the LWC pool cannot be resolved due to the consumption of excitation energy by the RC, besides one allows for re-absorption processes to occur. It would be interesting to know how the complex behaves under conditions of 5 K. The energy transfer and subsequent fluorescence would be at their maximum and an even weak fluorescing Chl *a* pool could be identified. The third possibility would be a complete oxidation of the samples. As mentioned above the oxidised P700* functions as an efficient quencher also under low temperature conditions [32, 121, 122]. However, this would mean that under both isolation procedures an unknown oxidation event of P700 occurred, which was not the case in the *C. meneghiniana* preparation. However, the absence of LWCs have been described also for the cyanobacterium *Gloeobacter violaceus* [131]. A species dependent characteristic cannot be excluded.

Apart from these results, the spectroscopic analysis of the PS I-FCP complex and the free Fcp revealed an direct excitation energy transfer (EET) from fucoxanthin to Chl *a*. A transfer from fucoxanthin via Chl *c* to Chl *a* can be excluded as the Chl *c* emission at 630 nm only occurred upon direct excitation of Chl *c* at 465 nm. Exciting fucoxanthin at 560 nm resulted in the disappearance of the 630 nm emission and thus supports the EET model previously published by [66].

The sequence comparison of several PS I subunits from diatoms, cyanobacteria, and higher plants points to more cyanobacterial than higher plant features in the PS I of diatoms. However, up to now no structural data of photosynthetic complexes is available from diatoms. The data obtained by BN-PAGE, gel filtration and electron microscopy show that the PS I-FCP complex is a monomeric complex. Unfortunately only the pigment stoichiometries of FCPs are known and not the exact number of pigments per monomer. Still, if we take into account the similarity of Fcps with LHC II [116] a total of 8 Chl *a* molecules could be assumed also for Fcp monomers [65]. Therefore the PS I-FCP complex possesses more light-harvesting subunits compared to the PS I-LHC I complex with Lhc la-d bound [17]. Germano et al. estimated a number of 14 LHC I monomers to be bound to PS I of *Chlamydomonas* by single particle analysis [18]. Thus an increased number of light-harvesting subunits seems to be more realistic also for the PS I-FCP complex from *P. tricornutum*, even if one takes into account the contamination by some functionally impaired Fcps in the preparation. The recent supramolecular structures of PS I complexes of the red alga *Cyanidium caldarium* and of the cryptophyte *Rhodomonas* CS24 also point in this direction, since the determined size for the PS I-FCP complex exceeds the size of these samples [132, 133]. However, as long as no real structural information is available, no estimation can be given.

Beside the analysis of the PS I-FCP complex and the free Fcp, also a PS II containing fraction was isolated by IEX as has been shown by Western Blot and spectroscopy. Due to the increased salt concentration at the elution point of this fraction it seems unlikely that this fraction still retains the ability to produce oxygen. Experiments with *C. meneghiniana* in a similar buffer (though low salt concentration) indicate the necessity of e.g. MgCl_2 and betaine during the whole purification to protect the extrinsic PS II subunits responsible for oxygen production [134]. However, Western Blots show that another Fcp polypeptide is co-eluted. The MW of this Fcp is increased in comparison to the free Fcp and the Fcp polypeptides in the PS I-FCP complex. Thus the association of different Fcps with the two PSs is assumed and will be discussed in more detail in the next section 4.2.

Furthermore a so far unidentified protein was eluted by the IEX. SDS-PAGE indicated two polypeptides with apparent MWs of approximately 16 kDa and 17 kDa. By Western Blot it was shown that these polypeptides are not Fcp polypeptides. Absorbance measurements indicated the presence of only carotenoids. No chlorophyll absorbance was detected, explaining the yellow colour of that fraction. As the colour remained also after the concentration of the sample by size-exclusion centrifugation an association of the pigments with the protein is supposed. Analytical HPLC showed that this fraction contains the xanthophylls fucoxanthin and diadinoxanthin. Still, it cannot be excluded that the pigments were just co-purified and preserved in that fraction due to an association with the DDM micelle. Protein sequencing of the polypeptides will be necessary to identify and characterise this fraction. So far, possible functions like pigment delivery can only be suggested.

4.2 Association of Fcp polypeptides with PS I of *C. meneghiniana*

Discontinuous sucrose density centrifugation of solubilised thylakoids of *C. meneghiniana* led to the separation of five pigmented fractions. In earlier publications the first three bands, a fraction consisting mainly of free pigment (fraction A) and two FCP fractions (herein considered as fraction B, consisting of trimers and higher oligomers) have been analysed thoroughly [62, 69]. In this work the photosystems and their associated Fcps laid in the focus of interest. First of all, it had to be clarified if the latter two green bands (fractions C and D) were mixtures of PS II and PS I or if the photosystems were separated. A Western Blot experiment proved that the PS II core subunit PsbD was entirely located in fraction C. Absorbance spectra confirmed this result. Both fractions showed a decreased content of fucoxanthin in comparison to the FCPs and a red shift of the Chl Q_y band. This red shift was most prominent in fraction D (band 4) and the whole peak was broadened in comparison to all other fractions. Furthermore, fraction D exhibited a strong quench in fluorescence, a unique feature of PS I at RT (demonstrated in e.g. [120]).

Upon analysis at 77 K, fraction D also showed an increased far red fluorescence at 717 nm when excited at 440 nm. Such a fluorescence maximum was attributed to PS I complexes in cyanobacteria, green algae and higher plants (see section 4.1) but also in the spectra of whole diatom cells and PS I samples from diatoms [76, 77, 135]. This effect was only observed in fraction D, since fractions B and C exhibited only Chl *a* maxima at wavelengths shorter than 700 nm. In addition, peaks at 676 nm and 688 nm were observed, as already reported for *C. cryptica* by Brakemann and co-workers [77]. When Chl *c* was excited the 688 nm peak became even stronger together with the 717 nm peak, whereas the 676 nm emission was strongly reduced. After removing

loosely bound Fcps by gel filtration the latter signal got lost completely. This led to the interpretation that the 676 nm emission in fraction D is due to those Fcp polypeptides. However, since Chl *c* excitation led to an enhancement of both the 688 nm and the 717 nm emission bands, some Fcps were properly bound to PS I in fraction D. Thus, regarding spectroscopical characteristics, the PS I complex of *C. meneghiniana* differs from the PS I-FCP complex of *P. tricornutum*. In the latter only under conditions of reabsorbance an LWC peak at 735 nm was detected, together with a shoulder at approximately 705 nm. Even the preparation of a PS I complex of *P. tricornutum* by sucrose density centrifugation, i.e. similar preparation as for the PS I complex of *C. meneghiniana*, only an energy transfer to the 705 nm shoulder was observed. Although it cannot be completely ruled out that the absence of LWCs in the *P. tricornutum* was caused during the isolation procedures (IEX or sucrose density centrifugation) the data points to differences of the pigment arrangements of the PS I complexes of the two diatom species.

None of the experiments of re-solubilisation of fraction D led to PS I cores completely devoid of Fcp polypeptides. Fcps isolated by these methods from PS I complexes were all impaired in excitation energy transfer. This includes not only the detergents TX and the NGOG combination presented in this work but also DDM, HG, NG and OG used in previous experiments [82]. Thus it is impossible to directly identify the origin of the long wavelength emissions at 688 nm and 717 nm, which could arise from the Fcps specifically bound to PS I or the core itself. However, in a recent publication decay-associated spectra (DAS) of a PS I-FCP complex of the diatom *C. gracilis* led to the conclusion that only the longer wavelength components are located within the PS I core [79]. Only the DAS component with the shortest wavelength at 685 nm could be attributed to derive from Fcps by comparison with DAS measured with FCP complexes. However, if both the 688 nm and the 717 nm emission maximum would belong to core chlorophylls, we would have to assume a 100 % energy transfer from the Fcps into the cores at 77

K, because no other emission maxima are found. Therefore, it is suggested that at least the 688 nm emission is due to Fcp polypeptides closely bound to the PS I cores.

Analysis by HPLC revealed that the known pigment values of FCPs have been preserved in fraction B despite smaller changes due to the changed isolation procedures [62, 69]. Concerning the data of the PS I fraction D, quite large differences can be seen in comparison to other PS I preparations of diatoms, especially considering the proportion of the Fcp antenna associated with the PS I core, represented by the pigments fucoxanthin and Chl *c*. From *C. meneghiniana* a fucoxanthin/Chl *a* ratio of 1 has been published for the free FCP complexes [62, 66], which is supported by the data from *P. tricornutum* obtained in this study. For better comprehension the fucoxanthin/Chl *a* stoichiometry will be regarded as a general measure of the antenna size of the complexes. The stoichiometries of fucoxanthin per Chl *a* measured herein for the PS I-FCP complex of *P. tricornutum* (IEX purification) were 50 % [80]. 31 % and 5 % fucoxanthin were reported for another PS I and a PS I enriched *P. tricornutum* preparation [64, 68]. For *C. gracilis* 24 % fucoxanthin were observed [79]. Thus, with one exception, the proportions of the Fcp antennas compared to the whole isolated complexes, varied between one quarter and a half of the total Chl *a*. However, in fraction D the ratio was only 14 % fucoxanthin per Chl *a* pointing to a reduced antenna size. An even stronger indication is obtained if Chl *c* is chosen as an indicator of the Fcp antenna sizes. In FCP complexes of *C. meneghiniana* a Chl *c*/fucoxanthin ratio between 1:4 to 1:5 was determined (and subsequently the same Chl *c*/Chl *a* ratio, respectively) [62, 66]. This ratio held true for the free Fcp and the isolated PS I-FCP complex of *P. tricornutum*. Moreover, for most of the above mentioned studies, independent of the organisms the 1:4, 1:5 Chl *c*/fucoxanthin ratio was also preserved. In contrast, the Chl *c*/fucoxanthin ratio of fraction D was about 1:9. Additionally, the added ratios of the diatom specific xanthophyll cycle pigments, diadinoxanthin (DD) and diatoxanthin (DT) per Chl *a*, were

approximately 17 %, whereas 13 % were reported for *C. gracilis* and 6.5 % for *P. tricornutum* [64, 68]. The ratio of the PS I-FCP complex of *P. tricornutum* presented herein was 4 %. Beside species related differences, these changes in pigment stoichiometries are certainly due to the fact that *P. tricornutum* and *C. gracilis* were grown under less strong light regimes. In this study *C. meneghiniana* was illuminated with $140 \mu\text{E m}^{-2} \text{s}^{-1}$, *C. gracilis* was illuminated with only $13 \mu\text{E m}^{-2} \text{s}^{-1}$, and *P. tricornutum* with $40 \mu\text{E m}^{-2} \text{s}^{-1}$. Therefore, a rearrangement in size and pigmentation of the light harvesting antennae of PS I has to be expected. This assumption became hardened by the fact that the de-epoxidation rate ($\text{DT}/\text{DD}+\text{DT}$, a measurement that correlates with NPQ) in fraction D as well as in fraction B were 3 to 4 times higher than those reported for FCPs isolated under low light regimes, but comparable to high light FCPs [62, 69]. Regarding the fractions derived from re-solubilisation of the PS I fraction D, it occurs that the lower fractions contained an increased amount of β -carotene in comparison to the upper fractions. Thus it seems likely that the PS I cores, though not devoid of Fcp polypeptides, are located in the fractions NGOG_2 and TX_2 . This assumption is supported by the polypeptide pattern in the SDS-PAGE and the red shifted Chl *a* Q_y peaks in comparison to the upper fractions NGOG_1 and TX_1 .

There has been an ongoing discussion whether the two photosystems of diatoms share one antenna system, or if two separate light harvesting systems exist, as in higher plants and green algae [61, 70, 74, 77]. The first theory might be supported by the fact that there is no segregation of thylakoids into grana and stroma regions, and therefore no separation of the two photosystems [58]. However, this distribution of the two photosystems in diatom thylakoids appears to be problematic. Since PS I absorbs at longer wavelengths and exhibits a shortened trapping time until a charge separation occurs in comparison to PS II most of the absorbed light would be transferred to PS I (spill-over). Concomitantly the capacity of PS II to utilise light for photochemistry would decrease

to a high extent. To circumvent this, the two photosystems are either separated as in higher plants and green algae or only PS II is coupled with the major light-harvesting antenna as in cyanobacteria (phycobilisomes) [13]. So far, in diatoms such regulations are unknown. Solely, higher PS II/PS I ratios are reported for diatoms in comparison to higher plants and cyanobacteria [13, 136]. Therefore it can be speculated that such regulations are obtained by PS-specific Fcp antennae. Sequence homologies relate Fcp4 of *C. cryptica* to the PS I associated lhca protein of red algae [70]. Therefore, one could interpret Fcp4 to be part of a PS I specific light harvesting antenna. In several publications, mainly concerning the light harvesting properties of diatoms, the isolation of PS I or PS II enriched fractions was reported [63, 64, 76]. However, specific analyses of Fcp polypeptides in photosystem fractions were not performed. Also the recent isolation of PS I and PS II complexes from *C. gracilis* only proved a coupling of Fcp polypeptides to both photosystems, but did not provide any information about differences or similarities of these Fcps [78, 79]. Merely, Brakemann et al. [77] studied the association of Fcp polypeptides towards PS I and PS II isolated by sucrose density centrifugation and Deriphate-PAGE in *C. cryptica*. In their work, two Fcp polypeptides were identified in both photosystems and in a FCP fraction using an antibody directed against all Fcp polypeptides of *C. cryptica* with a molecular weight of 18 kDa and 22 kDa. Furthermore, Fcp2 and Fcp4 at 18 kDa were identified in both photosystems via specific antibodies. Thus it was suggested that both photosystems indeed share the same antenna system.

This is in contrast to the results presented herein. Two Fcp polypeptides were found in the FCP and the PS II fraction with apparent molecular weights at 18 kDa and 19 kDa. The difference in molecular weight (19 kDa instead of 22 kDa as reported in [77]) might be due to the behaviour of membrane proteins separated by different gel electrophoresis systems as has been supposed already [137]. However, in the PS I fraction three Fcp polypeptides were detected. Two bands with similar molecular weights (18

kDa and 19 kDa) and a third slightly below the 18 kDa signal. Fcp2 was detected only in the FCP and the PS II fraction at 18 kDa. The α -Fcp4 antibody reacted strongly with 18 kDa and 19 kDa polypeptides in the FCP and only with 18 kDa polypeptides in the PS I fraction. In case of the PS II fraction only weak signals were obtained of which the 19 kDa signal was more pronounced. As the predicted molecular weight of Fcp4 is 18.1 kDa the obtained 19 kDa signals in the FCP and PS II fractions are probably due to unspecific cross-reactions of the antibody [70]. The α -Fcp6 antibody, which was not tested by Brakemann and co-workers [77], reacted exclusively in the FCP and the PS II fractions at 19 kDa.

The inner PS I antenna consisted of at least three different Fcp polypeptides with molecular weights of 19 kDa, 18 kDa, and approximately 17 kDa. The 18 kDa polypeptide is represented by Fcp4 but not by Fcp2. Also the re-solubilisation with NG plus OG could not remove the Fcp4 polypeptide entirely from PS I, although it was also detected in the virtually photosystem free NGOG₁ fraction. Furthermore, the immunoreaction of the α -Fcp4 antibody in the PS I fraction was as strong as the reaction of the α -ccFcp antibody. This was not true for the FCP and the PS II fractions. Also the harsher re-solubilisation with TX could not remove the 18 kDa (Fcp4) polypeptide completely as the α -ccFcp antibody still detected a weak signal in TX₂. However, the α -Fcp4 antibody failed to detect any signal, which might be due to the marginal Fcp concentration (see figure 26). Thus, the Fcp4 polypeptide seems to constitute the major fraction of the 18 kDa Fcp proteins in the PS I fraction and is strongly bound to the complex.

The 17 kDa Fcp signal was only visible in fractions D and NGOG₂, but in every preparation done. Therefore it seems unlikely that it is a degradation artefact, especially since it is still bound to a protein complex after the second separation step. Since no gene encoding a Fcp of this size was found so far in *C. meneghiniana* the shorter size

could be due to post-translational modifications. The 17 kDa Fcp polypeptide can still belong to the Fcp4 group albeit it was not detected by the respective antibody. A minimum copy number of four related genes has been determined by southern blotting [70] but no investigations on possible transcripts were carried out. Thus only one polypeptide is described on protein level (Fcp4).

The 19 kDa Fcp polypeptide found in the PS I fraction could not be detected by any of the specific antibodies. In contrast to the FCP and PS II fractions, we can exclude Fcp6. The only other FCP described for *C. cryptica* with a similar molecular weight is Fcp5. From its sequence, Fcp5 can be placed into the same group as Fcp 1, 2, and 3, and it is the only constituent of the oligomeric FCPb complex. Since the 19 kDa polypeptide was completely removed from the PS I core fractions NGOG₂ and TX₂, it is less tightly bound to PS I than Fcp4 and an interaction between PS I and Fcp5, i.e. FCPb complexes can be proposed.

The results concerning the PS II fraction resembled the ones published for the trimeric FCPa complex of *C. meneghiniana*, grown under similar light and nutrient conditions [62], except that FCPa does not contain the Fcp4 polypeptide. However, the Fcp4 signal in the PS II fraction might be due to cross reactions of the antibody (see above). It was mentioned before that the FCP fraction B inhabited not only the FCPa complex, but was a pooled fraction together with the oligomeric FCPb complex. However, FCPb consists of only Fcp5 polypeptides, which could not be identified due to the lack of a specific antibody. Therefore, FCPb should not have influenced the quality of the results obtained using the antibodies α -Fcp2 or α -Fcp6 in the FCP fraction B. It has to be considered that FCPa has been shown to undergo structural and pigmentational changes under stronger light regimes [62]. The Fcp6 to Fcp2 stoichiometry is increased and the FCPa complex exhibits a fluorescence quench when isolated under high light conditions [69].

Fcp6 is a homologue of LI818r-3 of *C. reinhardtii* and it is known that the mRNA levels of both increase abruptly upon illumination [138, 139]. Currently, a photoprotective mechanism of LI818r-3 is discussed [140]. As the detected Fcp polypeptides in the FCP fraction and the PS II fraction were similar, it is supposed that parts of the FCPa complexes are closely associated with PS II. Furthermore, the obtained HPLC data indicate another possible photoprotective mechanism of PS II. Though obtaining a low amount of NPQ xanthophylls in relation to Chl *a* a high de-epoxidation rate was calculated. The role of diatoxanthin correlating with fluorescence quenching is a matter of debate [68, 69, 141] and could thus display another possibility to dissipate excess light energy. Nevertheless, in the case of the PS II fraction C it has to be considered that the used buffer system seems to be inadequate for the isolation of an oxygen evolving PS II (as already mentioned in the previous section 4.1). The precipitation of the sample during the concentration for the HPLC analysis and a general poor yield made it hard to obtain any (trustworthy) HPLC data. Still, besides the mentioned xanthophylls, chlorophyll *a* and β -carotene were detected as expected from a PS. The 77 K spectra of fraction C resembled those described for higher plant PS II, where the 687.5 nm emission is attributed to the core complex, thus pointing to the similarity of PS II among all organisms [142, 143, 144].

From the data above, it is concluded that *C. meneghiniana* possesses two different light harvesting antenna systems for photosystem I and II. This seems to be species independent, since high resolution SDS PAGE and Western Blots of PS I, FCP and PS II fractions isolated from *P. tricornutum* also showed that Fcp polypeptides of different molecular weights were associated with the two PS fractions. In *C. meneghiniana* the PS II light harvesting antenna resembles the polypeptide composition of the trimeric FCPa complex, whereas PS I binds an unknown 17 kDa Fcp polypeptide, Fcp4, and the less tightly bound 19 kDa Fcp5, representing a possible linker to the FCPb oligomer. These

data are supported by spectroscopy showing similarity between the maximum fluorescence peak of the isolated FCP complexes and the short fluorescence peak of the PS II fraction, independent of the excitation wavelength chosen. In the case of PS I it was shown that the associated Fcps are capable in transferring energy from Chl *c* towards two emitting Chl *a* pools. In FCP complexes, some of the Fcp polypeptides seem to be interchangeable upon changes in illumination [62]. A similar adaptation concerning the polypeptides more closely associated with the PSs might also explain the differences to what is described for *C. cryptica* [77].

4.3 Concluding remarks

During this work it was possible to isolate PS I complexes from two diatom species, the pennate *P. tricornutum* and the centric *C. meneghiniana*. In both cases the (energetic) coupling of Fcps was proven by biochemical and spectroscopical means. Electron microscopy, gel filtration, and BN-PAGE revealed that the PS I complex of diatoms is a monomer and therefore differs from the cyanobacterial structure, although some features of cyanobacterial subunits have been preserved. Biochemical evidence shows that the PS I of diatoms more likely resembles the PS I structures of e.g. green algae. Furthermore it could be shown that the associated Fcps differ from the free Fcp pools as well as from PS II enriched fractions in both organisms despite different preparation methods were chosen. Thus it seems likely that diatoms, as higher plants and green algae, possess two different light-harvesting systems, either associated with PS I or PS II. Still, it cannot be excluded that parts of the antenna system are interchangeable between the two PSs, depending on e.g. light quality etc. As the exchange of antenna systems occurs in higher plants under state 1/state 2 transitions (LHC II delocalises from PS II and associates with PS I [45]) such an event might be even more common in organisms with equally dispersed PSs and an even arrangement of the thylakoid membrane. However, beside the

similarities of the two complexes it has to be mentioned that there are also differences. Whereas in *C. meneghiniana* far red fluorescing Chls were easily identified, no such Chls have been found in *P. tricornutum*. Only under conditions allowing for re-absorption a maximum at 735 nm was detected in the *P. tricornutum* sample. But no real energy transfer to the 735 nm pool was detected. Whether this is a species artefact or due to preparation methods remains unclear. The comparison of the plastid genomes of *P. tricornutum*, *O. sinensis*, and *T. pseudonana* (the two latter belonging to centric diatoms) revealed no differences concerning PS I encoding subunits, i.e. all encoded subunits are present in all three organisms [60]. Nevertheless, this does not mean that differences in the absorbance and fluorescence characteristics of PS I of diatoms do not occur. In cyanobacteria several LWCs of PS I were reported to differ, even when the samples were isolated from the same genera (see [120, 126] and references therein). Concerning the association of Fcp polypeptides with the PS I core at least three polypeptides were found in *C. meneghiniana* whereas two were found in *P. tricornutum*. Still, it cannot be excluded that several different Fcp polypeptides share the same apparent MWs. Due to the lack of specific antibodies for *P. tricornutum* the number of detected Fcps might be under-represented.

Attempts have to be made to characterise those Fcp polypeptides that could not be identified in both organisms. Identifying their sequences on genetic and on protein level will be necessary to complete our understanding of the organisation of the light harvesting systems in different species of diatoms. In this way the PS I-FCP preparation provides a good basis to start a single particle analysis to yield a first supramolecular structure of PS I of diatoms.

5 Summary

Photosystem (PS) I is a huge membrane protein complex which coordinates around 200 co-factors. Upon light excitation a charge separation at the PS I reaction centre is induced which leads to an electron transport across the thylakoid membrane and the generation of redox equivalents needed for several biochemical reactions, e.g. the synthesis of sugars. For higher plants and cyanobacteria the crystal structure of PS I complexes were resolved to resolutions of 4.4 Å and 2.5 Å. Furthermore, supramolecular structures of PS I of eukaryotic algae, mainly of the green line, were obtained recently. However, up to now, no structure of diatoms is available yet. Diatoms are key players in global primary production and derived from a secondary endosymbiosis event. Their chloroplasts are surrounded by four envelope membranes and their thylakoids are evenly arranged in bands of three, i.e. no separation in grana and stroma regions is apparent. In this thesis a protocol was developed to isolate a functional PS I complex of diatoms which can be used for structural analysis by transmissional electron microscopy (TEM). A photosystem I-fucoanthin chlorophyll protein (PS I-FCP) complex was isolated from the pennate diatom *Phaeodactylum tricornutum* by ion exchange chromatography. Spectroscopic analysis proved that bound Fcp polypeptides function as a light-harvesting complex. An active light energy transfer from Fcp associated pigments, Chl *c* and fucoxanthin, towards the PS I core was proven by fluorescence spectroscopy. Oxidised minus reduced difference spectroscopy evidenced the activity of the PS I reaction centre P700 and yielded a chlorophyll *a*/P700 ratio of approximately 200:1. These data indicate that the isolated PS I-FCP complex exceeds the PS I cores from cyanobacteria and higher plants in the numbers of chlorophyll *a* molecules. Because of the strict conservation of PS I cores among organisms the additional 100 chlorophyll *a* molecules must either be coordinated by Fcps or function as linker molecules between the Fcp antenna and the PS I core as shown for the PS I-LHC I complex of higher plants. The chlorophyll *a*/P700 ra-

tio was indirectly verified by analytical HPLC analysis. The PS I-FCP complex comprises of a doubled chlorophyll *a*/ β -carotene ratio in comparison to PS I cores which can be explained by the 100 additional chlorophyll *a* molecules. Furthermore, the estimated ratios of Fcp specific pigments point into the same direction. The chlorophyll *a*/fucoxanthin ratio of FCP complexes is 1:1. In the PS I-FCP complex the ratio adds up to 2:1. In case of chlorophyll *a*/chlorophyll *c* ratios FCP complexes exhibit a 5:1 stoichiometry, the PS I-FCP complex 10:1. Therefore it can be assumed that the PS I-FCP complex really coordinates around 200 chlorophyll *a* molecules whereby one half is associated with Fcps. To tell something about the structural organisation, the PS I-FCP complex was compared with its cyanobacterial and higher plant counterparts. Whereas cyanobacterial PS I cores aggregate to trimers, usually without associated antennae, higher plant PS I is a monomer and binds additionally two LHC I heterodimers. BN-PAGE and gel filtration experiments showed that also diatoms contain PS I monomers associated with Fcps as light-harvesting antenna. First TEM studies evidenced these observations. Negatively stained PS I-FCP particles had an increased size compared to PS I cores of other organisms. No PS I trimers or higher oligomers have been found. The calculated diameter and shape of the particles correspond to PS I-LHC I particles obtained from green algae, which also comprise of a higher number of LHC I polypeptides compared to the higher plant x-ray structure. Additionally, the analysis of polypeptides indicates that the PS I associated Fcps differ from the free Fcp pool and also from Fcps of a PS II enriched fraction. The assumption that diatoms harbour just one Fcp antenna that serve both Photosystems equally seems to be wrong. To further study the association of Fcps with the two Photosystems, both complexes plus the free FCP complexes were isolated from the centric diatom *Cyclotella meneghiniana*. Because of the availability of antibodies directed against specific Fcp polypeptides of *Cyclotella* the PS I-FCP complex of *Phaeodactylum* could not be used. A trimeric FCP complex, FCPa, and a higher FCP oligomer, FCPb, have already been described for *C. meneghiniana*. The latter is assumed

to be composed of only Fcp5, whereas the FCPa contains Fcp2 and Fcp6. Biochemical and spectroscopical evidences revealed a different subset of associated Fcp polypeptides within the isolated photosystem complexes. Whereas the PS II associated Fcp antenna resembles FCPa, at least three different Fcp polypeptides are associated with PS I. By re-solubilisation of the PS I complex and a further purification step Fcp polypeptides were partially removed from PS I and both fractions were analysed again by biochemical and spectroscopical means, as well as by HPLC. Thereby Fcp4 and a so far undescribed 17 kDa Fcp were found to be strongly coupled to PS I, whereas another Fcp, presumably Fcp5, is only loosely bound to the PS I core. Thus an association of FCPb and PS I is assumed.

6 Zusammenfassung

Bei Photosystem (PS) I handelt es sich um einen großen Membranproteinkomplex, welcher ca. 200 Cofaktoren koordiniert. Durch die Anregung mit Licht wird eine Ladungstrennung am Reaktionszentrum von PS I verursacht, die zu einem Elektronentransport über die Thylakoidmembran führt und letztendlich Redoxäquivalente generiert, welche für verschiedene biochemische Prozesse, wie z.B. für die Zuckersynthese, benötigt werden. Die Struktur von PS I Komplexen höherer Pflanzen sowie Cyanobakterien wurden mit Auflösungen von 4.4 Å bzw. 2.5 Å durch Röntgenstrukturanalyse bestimmt. Desweiteren existieren mittlerweile mehrere supramolekulare Strukturen von PS I aus eukaryotischen Algen, wobei deren Mehrzahl auf Strukturen aus Grünalgen beruht. Bis heute liegen keinerlei Strukturen von photosynthetischen Membranproteinkomplexen aus Diatomeen vor.

Aufgrund ihrer Form, pennat bzw. zentrisch, unterscheidet man verschiedene Klassen von Diatomeen. Sie nehmen eine Schlüsselrolle in der globalen Primärproduktion ein und entstanden durch sekundäre Endosymbiose. Dabei wurden Verwandte der heutigen Rotalgen von einem unbekanntem eukaryotischen Einzeller aufgenommen. Die Chloroplasten der Diatomeen sind infolgedessen von vier Membranen umschlossen. Ihre Thylakoide sind gleichmäßig in Form von Dreierbändern organisiert, d.h. es werden keine Grana- und Stromaregionen ausgebildet.

Ziel dieser Arbeit war es, ein Protokoll zu entwickeln, welches die Isolierung eines funktionsfähigen PS I Komplexes aus Diatomeen ermöglicht und der für die Strukturanalyse mittels Transmissionselektronenmikroskopie (TEM) geeignet ist. Mittels Ionenaustauschchromatographie wurde ein Komplex aus PS I und Fucoxanthin-Chlorophyll bindenden Proteinen (PS I-FCP Komplex) aus der pennaten Diatomee *Phaeodactylum tricorutum* gereinigt. Spektroskopische Analysen wiesen auf die Funktion der Fcps

als funktioneller Lichtsammelkomplex für PS I hin. Aktiver Energietransfer von Fcp assoziierten Pigmenten, wie Fucoxanthin und Chlorophyll *c*, zum PS I Reaktionszentrum konnte durch Fluoreszenzspektroskopie nachgewiesen werden. Weiterhin bestätigten differenzspektroskopische Messungen von oxidierten minus reduzierten Proben die Aktivität des P700 Reaktionszentrums. Zudem konnte ein Verhältnis von 200 Chlorophyll *a* Molekülen pro Reaktionszentrum ermittelt werden. Im Vergleich zu monomeren PS I-Core Komplexen aus Cyanobakterien oder höheren Pflanzen (etwa 100:1) deutet dieses Verhältnis auf eine höhere Anzahl von Chlorophyll *a* im PS I-FCP Komplex von Diatomeen hin. Da die Grundstruktur von PS I stark konserviert ist, werden die ca. 100 zusätzlichen Chlorophylle entweder von den gebundenen Fcps koordiniert oder sie fungieren als Verbindungschlorophylle zwischen der Fcp Antenne und dem PS I Core, ähnlich den Verbindungschlorophyllen zwischen dem LHC I und dem PS I-Core höherer Pflanzen. Indirekt konnten die 100 zusätzlichen Chlorophyll *a* Moleküle auch per analytischer HPLC nachgewiesen werden. Das Verhältnis von Chlorophyll *a* zu β -Carotin des PS I-FCP Komplexes war doppelt so hoch wie in den erwähnten PS I-Cores, was sich durch 100 zusätzliche Chlorophyll *a* Moleküle leicht erklären läßt. Außerdem wiesen die ermittelten Stöchiometrien der Fcp spezifischen Pigmente auf das gleiche Ergebnis hin. Die Chlorophyll *a*/Fucoxanthin Ratio aus FCP Komplexen beträgt nachweislich 1:1. Im PS I-FCP Komplex hingegen wurde eine Ratio von 2:1 bestimmt. Auch das Chlorophyll *a*/Chlorophyll *c* Verhältnis von FCP Komplexen, ca. 5:1, betrug 10:1 im PS I-FCP Komplex. Aus diesem Grund kann man davon ausgehen, daß ca. 200 Chlorophyll *a* Moleküle vom gesamten PS I-FCP Komplex koordiniert werden. Um etwas über den strukturellen Aufbau des PS I-FCP Komplexes zu erfahren, fand ein Vergleich mit den entsprechenden Komplexen aus Cyanobakterien und höheren Pflanzen statt. Die Methoden der Wahl waren hierbei BN-PAGE sowie Gelfiltrationsexperimente. Während PS I in Cyanobakterien Trimere ausbildet, welche üblicherweise keine weiteren Lichtsammelkomplexe binden, liegt in höheren Pflanzen ein PS I Monomer assoziiert mit zwei Heterodimeren

LHC I Komplexen vor. Die Vergleiche zeigten, dass PS I in Diatomeen ebenfalls als Monomer vorliegt und mit Fcp Lichtsammelkomplexen assoziiert ist. Erste TEM Studien bestätigten diese Beobachtungen. Negativ kontrastierte PS I-FCP Partikel deuteten darauf hin, daß PS I-Cores anderer Organismen eine geringere Größe aufweisen. Keine PS I Trimere oder gar höhere Oligomere wurden beobachtet. Der berechnete Durchmesser und die Form der PS I-FCP Partikel ähnelten PS I-LHC I Partikel aus Grünalgen. Letztere weisen im Vergleich zu der PS I-LHC I Struktur höherer Pflanzen ebenfalls eine höhere Anzahl an gebundenen LHC I Proteinen auf. Zusätzlich deutete die Untersuchung der Polypeptide darauf hin, daß sich die PS I assoziierten Fcps von ungebundenen Fcps sowie Fcps einer PS II angereicherten Fraktion unterscheiden. Aus diesem Grund erscheint die Annahme falsch, dass Diatomeen über eine einzige Fcp Antenne verfügen, die sowohl für PS I und PS II gleichermaßen die Funktion als Lichtsammelkomplex übernimmt. Um die Assoziation von Fcps mit den zwei Photosystemen zu untersuchen, wurden PS I- und PS II-Komplexe sowie ungebundene FCP Komplexe aus der zentralen Diatomee *Cyclotella meneghiniana* isoliert. Aufgrund der Tatsache, daß spezifische *Cyclotella* Fcp Antikörper zur Verfügung standen, konnte der PS I-FCP Komplex aus *P. tricornutum* nicht verwendet werden. Trimere, sogenannte FCPa Komplexe sowie höhere FCPb Oligomere wurden für *C. meneghiniana* bereits beschrieben. Während der letztere vermutlich ausschließlich aus Fcp5 zusammengesetzt ist, besteht der FCPa Komplex zumindest aus Fcp2 und Fcp6 Untereinheiten. Spektroskopische und biochemische Nachweismethoden zeigten, daß unterschiedliche Fcp Polypeptide mit den zwei Photosystemen assoziiert sind. Die PS II assoziierten Fcps entsprechen den Eigenschaften und dem Aufbau des FCPa Komplexes, während PS I mindestens drei unterschiedliche Fcp Polypeptide bindet. Mittels Resolubilisierungsexperimenten und einem weiteren Reinigungsschritt konnten Fcp Polypeptide teilweise vom PS I Komplex entfernt werden und beide Fraktionen wurden erneut biochemisch, spektroskopisch und mittels HPLC-Analyse untersucht. Demnach scheinen Fcp4 sowie ein bislang unbekanntes 17 kDa Fcp Polypeptid relativ stark mit

PS I gekoppelt zu sein. Das FCPb-bildende Fcp5 hingegen zeigte nur eine schwache Assoziation mit PS I. Aus diesem Grund läßt sich eine Bindung des FCPb Komplexes mit PS I lediglich vermuten.

References

- [1] J. M. Olson, R. E. Blankenship, Thinking about the evolution of photosynthesis, in: Govindjee, J. T. Beatty, H. Gest, J. F. Allen (Eds.), *Discoveries in Photosynthesis*, Vol. 20 of *Advances in Photosynthesis and Respiration*, Springer Netherlands, 2005, Ch. 14, pp. 1073–1086.
- [2] R. Emerson, R. Chalmers, C. Cederstrand, Some factors influencing the long-wave limit of photosynthesis, *Proc. Natl. Acad. Sci. U. S. A.* 43 (1957) 133–143.
- [3] R. Hill, Oxygen produced by isolated chloroplasts, *Proc. R. Soc. Lond.* 127 (847) (1939) 192 – 210.
- [4] R. Hill, F. Bendall, Function of the two cytochrome components in chloroplasts: A working hypothesis, *Nature* 186 (4719) (1960) 136 – 137.
- [5] Govindjee, D. Krogmann, *Discoveries in oxygenic photosynthesis (1727–2003): a perspective*, *Photos. Res.* 80 (1–3) (2004) 15 – 57.
- [6] M. Calvin, J. Bassham, A. Benson, Chemical transformations of carbon in photosynthesis, *Fed. Proc.* 9 (2) (1950) 524–534.
- [7] G. I. McFadden, Primary and secondary endosymbiosis and the origin of plastids, *J. Phycol.* 37 (2001) 951–959.
- [8] N. Sato, Origin and evolution of plastids: Genomic view on the unification and diversity of plastids, in: R. R. Wise, J. K. Hooper (Eds.), *Advances in Photosynthesis and Respiration: The Structure and Function of Plastids*, Vol. 23, Springer Netherlands, 2006, Ch. 4, pp. 75–102.
- [9] J. K. Hooper, Chloroplast development: Whence and whither, in: R. R. Wise,

- J. K. Hooper (Eds.), *Advances in Photosynthesis and Respiration: The Structure and Function of Plastids*, Vol. 23, Springer Netherlands, 2006, Ch. 2, pp. 27–51.
- [10] R. R. Wise, The diversity of plastid form and function, in: R. R. Wise, J. K. Hooper (Eds.), *Advances in Photosynthesis and Respiration: The Structure and Function of Plastids*, Vol. 23, Springer Netherlands, 2006, Ch. 1, pp. 3–26.
- [11] N. Nelson, A. Ben-Shem, The complex architecture of oxygenic photosynthesis, *Nat. Rev. Mol. Cell Biol.* 5 (2004) 971–982.
- [12] P. Fromme, H. Yu, Y. S. DeRuyter, C. Jolley, D. K. Chauhan, A. Melkozernov, I. Grotjohann, Structure of photosystems I and II, *C. R. Chimie* 9 (2) (2006) 188 – 200, conversion photochimique et stockage de l'énergie solaire - Volume 1.
- [13] H.-W. Trissl, C. Wilhelm, Why do thylakoid membranes from higher plants form grana stacks?, *Trends Biochem. Sci.* 18 (11) (1993) 415 – 419.
- [14] R. E. Blankenship, *Molecular Mechanisms of Photosynthesis*, Blackwell Science Ltd, 2002, chapter 6.
- [15] P. Fromme, I. Grotjohann, Overview of photosynthesis, in: P. Fromme (Ed.), *Photosynthetic Protein Complexes*, WILEY-VCH Verlag GmbH & Co. KGaA, Weinheim, Germany, 2008, Ch. 1, pp. 1–22.
- [16] J. Deisenhofer, O. Epp, K. Miki, R. Huber, H. Michel, X-ray structure analysis of a membrane protein complex electron density map at 3 Å resolution and a model of the chromophores of the photosynthetic reaction center from *Rhodospseudomonas viridis*, *J. Mol. Biol.* 180 (2) (1984) 385–398.
- [17] A. Ben-Shem, F. Frolow, N. Nelson, Crystal structure of plant photosystem I, *Nature* 426 (6967) (2003) 630–635.

- [18] M. Germano, A. E. Yakushevskaya, W. Keegstra, H. J. van Gorkom, J. P. Dekker, E. J. Boekema, Supramolecular organization of photosystem I and light-harvesting complex I in *Chlamydomonas reinhardtii*, *FEBS Lett.* 525 (1-3) (2002) 121–125.
- [19] R. Bassi, S. Y. Soen, G. Frank, H. Zuber, J. D. Rochaix, Characterization of chlorophyll a/b proteins of photosystem I from *Chlamydomonas reinhardtii*, *J. Biol. Chem.* 267 (36) (1992) 25714–25721.
- [20] S. Jansson, The light-harvesting chlorophyll a/b-binding proteins, *Biochim. Biophys. Acta* 1184 (1) (1994) 1–19.
- [21] E. J. Boekema, H. van Roon, F. Calkoen, R. Bassi, J. P. Dekker, Multiple types of association of photosystem II and its light-harvesting antenna in partially solubilized photosystem II membranes, *Biochemistry* 38 (8) (1999) 2233–2239.
- [22] B. Hankamer, E. Morris, J. Nield, A. Carne, J. Barber, Subunit positioning and transmembrane helix organisation in the core dimer of photosystem II, *FEBS Lett.* 504 (3) (2001) 142–151.
- [23] Z. Liu, W. Chang, Structure of the light - harvesting complex ii, in: P. Fromme (Ed.), *Photosynthetic Protein Complexes*, WILEY-VCH Verlag GmbH & Co. KGaA, Weinheim, Germany, 2008, Ch. 10, pp. 217–242.
- [24] T. Förster, Zwischenmolekulare Energiewanderung und Fluoreszenz, *Annalen der Physik* 437 (1-2) (1948) 55–75.
- [25] G. D. Scholes, Long-range resonance energy transfer in molecular systems, *Annu. Rev. Phys. Chem.* 54 (2003) 57–87.
- [26] P. Jordan, P. Fromme, H. T. Witt, O. Klukas, W. Saenger, N. Krauss, Three-dimensional structure of cyanobacterial photosystem I at 2.5 Å resolution, *Nature* 411 (6840) (2001) 909–917.

- [27] P. E. Jensen, R. Bassi, E. J. Boekema, J. P. Dekker, S. Jansson, D. Leister, C. Robinson, H. V. Scheller, Structure, function and regulation of plant photosystem I, *Biochim. Biophys. Acta* 1767 (5) (2007) 335–352.
- [28] A. Amunts, O. Drory, N. Nelson, The structure of a plant photosystem I supercomplex at 3.4 Å resolution, *Nature* 447 (7140) (2007) 58–63.
- [29] N. Nelson, A. Ben-Shem, Structure, function, and regulation of plant photosystem I, in: J. H. Golbeck (Ed.), *Photosystem I The Light-Driven Plastocyanin:Ferredoxin Oxidoreductase*, Vol. 24, Springer Netherlands, 2006, Ch. 7, pp. 71–77.
- [30] P. Fromme, I. Grotjohann, Structural analysis of cyanobacterial photosystem I, in: J. H. Golbeck (Ed.), *Photosystem I The Light-Driven Plastocyanin:Ferredoxin Oxidoreductase*, Vol. 24, Springer Netherlands, 2006, Ch. 6, pp. 47–69.
- [31] C. Jolley, A. Ben-Shem, N. Nelson, P. Fromme, Structure of plant photosystem I revealed by theoretical modeling, *J. Biol. Chem.* 280 (39) (2005) 33627–33636.
- [32] N. V. Karapetyan, E. Schlodder, R. van Grondelle, J. P. Dekker, The long wavelength chlorophylls of photosystem I, in: J. H. Golbeck (Ed.), *Photosystem I The Light-Driven Plastocyanin:Ferredoxin Oxidoreductase*, Vol. 24, Springer Netherlands, 2006, Ch. 13, pp. 177–192.
- [33] T. Watanabe, M. Kobayashi, A. Hongut, M. Nakazato, T. Hiyama, N. Murata, Evidence that a chlorophyll a' dimer constitutes the photochemical reaction centre 1 (P700) in photosynthetic apparatus, *FEBS Lett.* 191 (2) (1985) 252–256.
- [34] M. G. Müller, J. Niklas, W. Lubitz, A. R. Holzwarth, Ultrafast transient absorption studies on photosystem I reaction centers from *Chlamydomonas reinhardtii*. 1. a new interpretation of the energy trapping and early electron transfer steps in photosystem I, *Biophys. J.* 85 (6) (2003) 3899–3922.

- [35] N. Krauß, Structure and function of cyanobacterial photosystem I, in: P. Fromme (Ed.), *Photosynthetic Protein Complexes*, WILEY-VCH Verlag GmbH & Co. KGaA, Weinheim, Germany, 2008, Ch. 2, pp. 23–64.
- [36] A. D. Quintana, M. Hervas, J. A. Navarro, , M. A. D. la Rosa, Plastocyanin and cytochrome c 6: the soluble electron carriers between the cytochrome b 6 f complex and photosystem I, in: P. Fromme (Ed.), *Photosynthetic Protein Complexes*, WILEY-VCH Verlag GmbH & Co. KGaA, Weinheim, Germany, 2008, Ch. 8, pp. 181–200.
- [37] M. Hippler, J. Reichert, M. Sutter, E. Zak, L. Altschmied, U. Schröer, R. G. Herrmann, W. Haehnel, The plastocyanin binding domain of photosystem I, *EMBO J.* 15 (23) (1996) 6374–6384.
- [38] A. Amunts, N. Nelson, Functional organization of a plant photosystem I: evolution of a highly efficient photochemical machine, *Plant Physiol. Biochem.* 46 (3) (2008) 228–237.
- [39] G. Kurisu, M. Kusunoki, E. Katoh, T. Yamazaki, K. Teshima, Y. Onda, Y. Kimata-Arigo, T. Hase, Structure of the electron transfer complex between ferredoxin and ferredoxin-NADP(+) reductase, *Nat. Struct. Biol.* 8 (2) (2001) 117–121.
- [40] P. Setif, Electron transfer from the bound iron-sulfur clusters to ferredoxin/ferredoxin: Kinetic and structural properties of ferredoxin/ferredoxin reduction by photosystem I, in: J. H. Golbeck (Ed.), *Photosystem I The Light-Driven Plastocyanin:Ferredoxin Oxidoreductase*, Vol. 24, Springer Netherlands, 2006, Ch. 26, pp. 439–454.
- [41] R. M. L. McKay, R. J. Geider, J. LaRoche, Physiological and biochemical response of the photosynthetic apparatus of two marine diatoms to Fe stress, *Plant Physiol.* 114 (2) (1997) 615–622.

- [42] J. Forsberg, J. F. Allen, Protein tyrosine phosphorylation in the transition to light state 2 of chloroplast thylakoids, *Photosynth. Res.* 68 (1) (2001) 71–79.
- [43] J. Barber, Influence of surface charges on thylakoid structure and function, *Annu. Rev. Plant Physiol.* 33 (1982) 261–295.
- [44] L. Mustárdy, G. Garab, Granum revisited. A three-dimensional model - where things fall into place, *Trends Plant Sci.* 8 (3) (2003) 117 – 122.
- [45] E. J. Boekema, R. Kouril, J. P. Dekker, P. E. Jensen, Association of photosystem I and light-harvesting complex II during state transitions, in: J. H. Golbeck (Ed.), *Photosystem I The Light-Driven Plastocyanin:Ferredoxin Oxidoreductase*, Vol. 24, Springer Netherlands, 2006, Ch. 5, pp. 41–46.
- [46] J. P. Dekker, E. J. Boekema, Supramolecular organization of thylakoid membrane proteins in green plants, *Biochim. Biophys. Acta* 1706 (1-2) (2005) 12–39.
- [47] P. Joliot, A. Joliot, Cyclic electron transfer around photosystem I, in: J. H. Golbeck (Ed.), *Photosystem I The Light-Driven Plastocyanin:Ferredoxin Oxidoreductase*, Vol. 24, Springer Netherlands, 2006, Ch. 37, pp. 639–656.
- [48] E. Teardo, P. P. de Laureto, E. Bergantino, F. D. Vecchia, F. Rigoni, I. Szabò, G. M. Giacometti, Evidences for interaction of psbs with photosynthetic complexes in maize thylakoids, *Biochim. Biophys. Acta* 1767 (6) (2007) 703–711.
- [49] P. Müller, X. P. Li, K. K. Niyogi, Non-photochemical quenching. A response to excess light energy, *Plant Physiol.* 125 (4) (2001) 1558–1566.
- [50] E. J. Boekema, A. Hifney, A. E. Yakushevskaya, M. Piotrowski, W. Keegstra, S. Berry, K. P. Michel, E. K. Pistorius, J. Kruip, A giant chlorophyll-protein complex induced by iron deficiency in cyanobacteria, *Nature* 412 (6848) (2001) 745–748.

- [51] T. S. Bibby, J. Nield, J. Barber, Three-dimensional model and characterization of the iron stress-induced cp43'-photosystem I supercomplex isolated from the cyanobacterium *Synechocystis* PCC 6803, *J. Biol. Chem.* 276 (46) (2001) 43246–43252.
- [52] J. Barber, J. Nield, J. Duncan, T. S. Bibby, Accessory chlorophyll proteins in cyanobacterial photosystem I, in: J. H. Golbeck (Ed.), *Photosystem I The Light-Driven Plastocyanin:Ferredoxin Oxidoreductase*, Vol. 24, Springer Netherlands, 2006, Ch. 9, pp. 99–117.
- [53] A. N. Melkozernov, T. S. Bibby, S. Lin, J. Barber, R. E. Blankenship, Time-resolved absorption and emission show that the cp43' antenna ring of iron-stressed *Synechocystis* sp. PCC 6803 is efficiently coupled to the photosystem I reaction center core, *Biochemistry* 42 (13) (2003) 3893–3903.
- [54] A. Falciatore, C. Bowler, Revealing the molecular secrets of marine diatoms, *Annu. Rev. Plant Biol.* 53 (2002) 109–130.
- [55] P. G. Falkowski, M. E. Katz, A. H. Knoll, A. Quigg, J. A. Raven, O. Schofield, F. J. R. Taylor, The evolution of modern eukaryotic phytoplankton, *Science* 305 (5682) (2004) 354–360.
- [56] C. Bowler, A. E. Allen, J. H. Badger, J. Grimwood, K. Jabbari, A. Kuo, U. Maheswari, C. Martens, F. Maumus, R. P. Otiillar, E. Rayko, A. Salamov, K. Vandepoele, B. Beszteri, A. Gruber, M. Heijde, M. Katinka, T. Mock, K. Valentin, F. Verret, J. A. Berges, C. Brownlee, J.-P. Cadoret, A. Chiovitti, C. J. Choi, S. Coesel, A. D. Martino, J. C. Detter, C. Durkin, A. Falciatore, J. Fournet, M. Haruta, M. J. J. Huysman, B. D. Jenkins, K. Jiroutova, R. E. Jorgensen, Y. Joubert, A. Kaplan, N. Kröger, P. G. Kroth, J. L. Roche, E. Lindquist, M. Lommer, V. Martin-Jézéquel, P. J. Lopez, S. Lucas, M. Mangogna, K. McGinnis, L. K. Medlin, A. Montsant,

- M.-P. O.-L. Secq, C. Napoli, M. Obornik, M. S. Parker, J.-L. Petit, B. M. Porcel, N. Poulsen, M. Robison, L. Rychlewski, T. A. Ryneerson, J. Schmutz, H. Shapiro, M. Siaut, M. Stanley, M. R. Sussman, A. R. Taylor, A. Vardi, P. von Dassow, W. Vyverman, A. Willis, L. S. Wyrwicz, D. S. Rokhsar, J. Weissenbach, E. V. Armbrust, B. R. Green, Y. V. de Peer, I. V. Grigoriev, The Phaeodactylum genome reveals the evolutionary history of diatom genomes, *Nature* 456 (7219) (2008) 239–244.
- [57] C. Wilhelm, C. Büchel, J. Fisahn, R. Goss, T. Jakob, J. Laroche, J. Lavaud, M. Lohr, U. Riebesell, K. Stehfest, K. Valentin, P. G. Kroth, The regulation of carbon and nutrient assimilation in diatoms is significantly different from green algae, *Protist* 157 (2) (2006) 91–124.
- [58] M. Pyszniak, S. Gibbs, Immunocytochemical localization of photosystem I and the fucoxanthin-chlorophyll a/c light-harvesting complex in the diatom *Phaeodactylum tricornutum*, *Protoplasma* 166 (1992) 208–217.
- [59] E. V. Armbrust, J. A. Berges, C. Bowler, B. R. Green, D. Martinez, N. H. Putnam, S. Zhou, A. E. Allen, K. E. Apt, M. Bechner, M. A. Brzezinski, B. K. Chaal, A. Chiovitti, A. K. Davis, M. S. Demarest, J. C. Detter, T. Glavina, D. Goodstein, M. Z. Hadi, U. Hellsten, M. Hildebrand, B. D. Jenkins, J. Jurka, V. V. Kapitonov, N. Kröger, W. W. Y. Lau, T. W. Lane, F. W. Larimer, J. C. Lippmeier, S. Lucas, M. Medina, A. Montsant, M. Obornik, M. S. Parker, B. Palenik, G. J. Pazour, P. M. Richardson, T. A. Ryneerson, M. A. Saito, D. C. Schwartz, K. Thamatrakoln, K. Valentin, A. Vardi, F. P. Wilkerson, D. S. Rokhsar, The genome of the diatom *Thalassiosira pseudonana*: ecology, evolution, and metabolism, *Science* 306 (5693) (2004) 79–86.
- [60] M.-P. O.-L. Secq, J. Grimwood, H. Shapiro, E. V. Armbrust, C. Bowler, B. R. Green, Chloroplast genomes of the diatoms *Phaeodactylum tricornutum* and *Tha-*

- lassiosira pseudonana: comparison with other plastid genomes of the red lineage, *Mol. Genet. Genomics* 277 (4) (2007) 427–439.
- [61] C. Büchel, Fucoxanthin-chlorophyll proteins in diatoms: 18 and 19 kDa subunits assemble into different oligomeric states, *Biochemistry* 42 (44) (2003) 13027–13034.
- [62] A. Beer, K. Gundermann, J. Beckmann, C. Büchel, Subunit composition and pigmentation of fucoxanthin-chlorophyll proteins in diatoms: evidence for a subunit involved in diadinoxanthin and diatoxanthin binding, *Biochemistry* 45 (43) (2006) 13046–13053.
- [63] G. Guglielmi, J. Lavaud, B. Rousseau, A.-L. Etienne, J. Houmard, A. V. Ruban, The light-harvesting antenna of the diatom *Phaeodactylum tricornutum*. Evidence for a diadinoxanthin-binding subcomplex, *FEBS J.* 272 (17) (2005) 4339–4348.
- [64] B. Lepetit, D. Volke, M. Szabó, R. Hoffmann, G. Garab, C. Wilhelm, R. Goss, Spectroscopic and molecular characterization of the oligomeric antenna of the diatom *Phaeodactylum tricornutum*, *Biochemistry* 46 (34) (2007) 9813–9822.
- [65] J. Standfuss, A. C. T. van Scheltinga, M. Lamborghini, W. Kühlbrandt, Mechanisms of photoprotection and nonphotochemical quenching in pea light-harvesting complex at 2.5 Å resolution, *EMBO J.* 24 (5) (2005) 919–928.
- [66] E. Papagiannakis, I. H. M. van Stokkum, H. Fey, C. Büchel, R. van Grondelle, Spectroscopic characterization of the excitation energy transfer in the fucoxanthin-chlorophyll protein of diatoms, *Photosynth. Res.* 86 (1-2) (2005) 241–250.
- [67] T. Jakob, R. Goss, C. Wilhelm, Unusual pH-dependence of diadinoxanthin de-epoxidase activation causes chlororespiratory induced accumulation of diatoxanthin in the diatom *Phaeodactylum tricornutum*, *J. Plant Physiol.* 158 (2001) 383–390.

- [68] J. Lavaud, B. Rousseau, A.-L. Etienne, Enrichment of the light-harvesting complex in diadinoxanthin and implications for the nonphotochemical fluorescence quenching in diatoms, *Biochemistry* 42 (19) (2003) 5802–5808.
- [69] K. Gundermann, C. Büchel, The fluorescence yield of the trimeric fucoxanthin-chlorophyll-protein FCPa in the diatom *Cyclotella meneghiniana* is dependent on the amount of bound diatoxanthin, *Photos. Res.* 95 (2-3) (2008) 229–235.
- [70] M. Eppard, E. Rhiel, Investigations on gene copy number, introns and chromosomal arrangement of genes encoding the fucoxanthin chlorophyll a/c-binding proteins of the centric diatom *Cyclotella cryptica*, *Protist* 151 (1) (2000) 27–39.
- [71] M. Eppard, W. E. Krumbein, A. Haeseler, E. Rhiel, Characterization of fcp4 and fcp12, two additional genes encoding light harvesting proteins of *Cyclotella cryptica* (Bacillariophyceae) and phylogenetic analysis of this complex gene family, *Plant Biol.* 2 (3) (2000) 283–289.
- [72] D. Bhaya, A. R. Grossman, Characterization of gene clusters encoding the fucoxanthin chlorophyll proteins of the diatom *Phaeodactylum tricornutum*, *Nucleic Acids Res.* 21 (19) (1993) 4458–4466.
- [73] J. P. Dekker, H. van Roon, E. J. Boekem, Heptameric association of light-harvesting complex II trimers in partially solubilized photosystem II membranes, *FEBS Lett.* 449 (2-3) (1999) 211–214.
- [74] T. G. Owens, E. R. Wold, Light-harvesting function in the diatom *Phaeodactylum tricornutum*: I. Isolation and characterization of pigment-protein complexes, *Plant Physiol.* 80 (3) (1986) 732–738.
- [75] L. Caron, J. Brown, Chlorophyll-carotenoid protein complexes from the diatom, *Phaeodactylum tricornutum*: spectrophotometric, pigment and polypeptide analysis, *Plant Cell Physiol.* 28 (1987) 775–785.

- [76] C. Berkaloff, L. Caron, B. Rousseau, Subunit organization of PSI particles from brown algae and diatoms: polypeptide and pigment analysis, *Photosynth. Res.* 23 (2) (1990) 181–193.
- [77] T. Brakemann, W. Schlörmann, J. Marquardt, M. Nolte, E. Rhiel, Association of fucoxanthin chlorophyll a/c-binding polypeptides with photosystems and phosphorylation in the centric diatom *Cyclotella cryptica*, *Protist* 157 (4) (2006) 463–475.
- [78] R. Nagao, A. Ishii, O. Tada, T. Suzuki, N. Dohmae, A. Okumura, M. Iwai, T. Takahashi, Y. Kashino, I. Enami, Isolation and characterization of oxygen-evolving thylakoid membranes and photosystem II particles from a marine diatom *Chaetoceros gracilis*, *Biochim. Biophys. Acta* 1767 (12) (2007) 1353–1362.
- [79] Y. Ikeda, M. Komura, M. Watanabe, C. Minami, H. Koike, S. Itoh, Y. Kashino, K. Satoh, Photosystem I complexes associated with fucoxanthin-chlorophyll-binding proteins from a marine centric diatom, *Chaetoceros gracilis*, *Biochim. Biophys. Acta* 1777 (4) (2008) 351–361.
- [80] T. Veith, C. Büchel, The monomeric photosystem I-complex of the diatom *Phaeodactylum tricornutum* binds specific fucoxanthin chlorophyll proteins (FCPs) as light-harvesting complexes, *Biochim. Biophys. Acta* 1767 (12) (2007) 1428–1435.
- [81] Z. Girmatsion, Untersuchungen zur Interaktion des Photosystem I mit Fucoxanthin-Chlorophyll-Proteinen bei der Diatomee *Cyclotella meneghiniana*, Diploma Thesis, University of Frankfurt (2005).
- [82] J. J. Brauns, Aufbau der Photosystem I–Fucoxanthin-Chlorophyllkomplexe bei der Diatomee *Cyclotella meneghiniana*, Diploma Thesis, University of Frankfurt (2007).
- [83] L. Provasoli, J. McLaughlin, M. Droop, The development of artificial media for marine algae, *Arch. Mikrobiol.* 25 (1957) 392–428.

- [84] R. Rippka, J. Deruelles, J. B. Waterbury, M. Herdman, R. Y. Stanier, Generic assignments, strain histories and properties of pure cultures of cyanobacteria, *J. Gen. Microbiol.* 111 (1979) 1–61.
- [85] J. A. Navarro, M. Hervás, M. A. Rosa, Purification of plastocyanin and cytochrome *c* 6 from plants, green algae, and cyanobacteria, in: R. Carpentier (Ed.), *Photosynthesis Research Protocols*, Vol. 274 of *Methods in Molecular Biology*, Humana Press Inc., Totowa, USA, 2004, Ch. 10, pp. 79–92.
- [86] W. Kühlbrandt, T. Thaler, E. Wehrli, The structure of membrane crystals of the light-harvesting chlorophyll *a/b* protein complex, *J. Cell Biol.* 96 (5) (1983) 1414–1424.
- [87] D. V. Vavilin, Isolation of functional photosystem II core particles from the cyanobacterium *Synechocystis* sp. PCC 6803, in: R. Carpentier (Ed.), *Photosynthesis Research Protocols*, Vol. 274 of *Methods in Molecular Biology*, Humana Press Inc., Totowa, USA, 2004, Ch. 5, pp. 37–47.
- [88] H. Schägger, G. von Jagow, Tricine-sodium dodecyl sulfate-polyacrylamide gel electrophoresis for the separation of proteins in the range from 1 to 100 kDa, *Anal. Biochem.* 166 (2) (1987) 368–379.
- [89] M. M. Compton, S. A. Lapp, R. Pedemonte, Generation of multicolored, prestained molecular weight markers for gel electrophoresis, *Electrophoresis* 23 (19) (2002) 3262–3265.
- [90] H. Schägger, G. von Jagow, Blue native electrophoresis for isolation of membrane protein complexes in enzymatically active form, *Anal. Biochem.* 199 (2) (1991) 223–231.
- [91] K. Cline, H. Mori, Thylakoid Δ pH-dependent precursor proteins bind to a cpTatC-

- Hcf106 complex before Tha4-dependent transport, *J. Cell Biol.* 154 (4) (2001) 719–729.
- [92] J. Heukeshoven, R. Dernick, Improved silver staining procedure for fast staining in PhastSystem Development Unit. I. Staining of sodium dodecyl sulfate gels, *Electrophoresis* 9 (1) (1988) 28–32.
- [93] H. Towbin, T. Staehelin, J. Gordon, Electrophoretic transfer of proteins from polyacrylamide gels to nitrocellulose sheets: procedure and some applications, *Proc. Natl. Acad. Sci. U. S. A.* 76 (9) (1979) 4350–4354.
- [94] H. Rehm, *Der Experimentator: Proteinbiochemie/Proteomics*, Spektrum Akad. Verlag, Heidelberg, 2002.
- [95] T. Hiyama, B. Ke, Difference spectra and extinction coefficients of P700, *Biochim. Biophys. Acta* 267 (1) (1972) 160–171.
- [96] S. Jeffrey, G. Humphrey, New spectrometric equations for determining chlorophyll a, b, c1 and c2 in higher plants, algae and natural phytoplankton, *Biochem. Physiol. Pflanzen* 167 (1975) 191–194.
- [97] D. I. Arnon, Copper enzymes in isolated chloroplasts. polyphenoloxidase in *Beta vulgaris*, *Plant Physiol.* 24 (1) (1949) 1–15.
- [98] K. Gundermann, Die Änderungen in den Pigment- und Polypeptidzusammensetzungen sowie Fluoreszenzquantenausbeuten der Fucoxanthin/ Chlorophyll a/c-Proteine von *Cyclotella meneghiniana* unter verschiedenen Lichtbedingungen, Diploma Thesis, University of Frankfurt (2007).
- [99] J. D. Thompson, T. J. Gibson, D. G. Higgins, Multiple sequence alignment using clustalW and clustalX, *Curr. Protoc. Bioinformatics* Chapter 2 (2002) Unit 2.3.

- [100] T. Lassmann, E. L. L. Sonnhammer, Kalign—an accurate and fast multiple sequence alignment algorithm, *BMC Bioinformatics* 6 (2005) 298.
- [101] U. Maheswari, A. Montsant, J. Goll, S. Krishnasamy, K. R. Rajyashri, V. M. Patell, C. Bowler, The diatom est database, *Nucleic Acids Res.* 33 (Database issue) (2005) D344–D347.
- [102] E. Gasteiger, A. Gattiker, C. Hoogland, I. Ivanyi, R. D. Appel, A. Bairoch, ExPASy: The proteomics server for in-depth protein knowledge and analysis, *Nucleic Acids Res.* 31 (13) (2003) 3784–3788.
- [103] P. R. Chitnis, Q. Xu, V. P. Chitnis, R. Nechushtai, Function and organization of photosystem I polypeptides, *Photos. Res.* 44 (1) (1995) 23–40.
- [104] A. Amunts, A. Ben-Shem, N. Nelson, Solving the structure of plant photosystem I—biochemistry is vital, *Photochem. Photobiol. Sci.* 4 (12) (2005) 1011–1015.
- [105] I. Ikegami, S. Kato, Enrichment of photosystem I reaction center chlorophyll from spinach chloroplasts, *Biochim. Biophys. Acta* 376 (3) (1975) 588–592.
- [106] I. Ikegami, S. Itoh, Chlorophyll organization in P-700-enriched particles isolated from spinach chloroplasts. CD and absorption spectroscopy, *Biochim. Biophys. Acta* 851 (1) (1986) 75–85.
- [107] G. H. Krause, E. Weis, Chlorophyll fluorescence and photosynthesis: The basics, *Ann. Rev. Plant Physiol. Plant Mol. Biol.* 42 (1991) 313–349.
- [108] E. Weis, Chlorophyll fluorescence at 77 K in intact leaves: Characterization of a technique to eliminate artifacts related to self-absorption, *Photosynth. Res.* 6 (1) (1985) 73–86.
- [109] P. G. Pancic, H. Strotmann, K. V. Kowallik, The delta subunit of the chloroplast

- ATPase is plastid-encoded in the diatom *Odontella sinensis*, *FEBS Lett.* 280 (2) (1991) 387–392.
- [110] M. Kügler, L. Jansch, V. Kruff, U. K. Schmitz, H.-P. Braun, Analysis of the chloroplast protein complexes by blue-native polyacrylamide gel electrophoresis (BN-PAGE), *Photosynth. Res.* Volume 53 (1) (1997) 35–44.
- [111] R. Danielsson, M. Suorsa, V. Paakkarinen, P.-A. Albertsson, S. Styring, E.-M. Aro, F. Mamedov, Dimeric and monomeric organization of photosystem II. distribution of five distinct complexes in the different domains of the thylakoid membrane, *J. Biol. Chem.* 281 (20) (2006) 14241–14249.
- [112] L. Garczarek, G. W. M. van der Staay, J. C. Thomas, F. Partensky, Isolation and characterization of photosystem I from two strains of the marine oxychlorobacterium *Prochlorococcus*, *Photosynth. Res.* 56 (2) (2004) 131–141.
- [113] E. Boekema, J. Dekker, M. Roegner, I. Witt, H. Witt, M. van Heel, Refined analysis of the trimeric structure of the isolated photosystem I complex from the thermophilic cyanobacterium *Synechococcus* sp., *Biochim. Biophys. Acta* 974 (81) (1989) 81–87.
- [114] J. Kargul, J. Nield, J. Barber, Three-dimensional reconstruction of a light-harvesting complex I–photosystem I (LHCI–PSI) supercomplex from the green alga *Chlamydomonas reinhardtii*. Insights into light harvesting for PSI, *J. Biol. Chem.* 278 (2003) 16135–16141.
- [115] M. Seibert, R. Picorel, A. B. Rubin, J. S. Connolly, Spectral, photophysical, and stability properties of isolated photosystem II reaction center, *Plant Physiol.* 87 (2) (1988) 303–306.
- [116] M. Eppard, E. Rhiel, The genes encoding light-harvesting subunits of *Cyclotella*

- cryptica (Bacillariophyceae) constitute a complex and heterogeneous family, *Mol. Gen. Genet.* 260 (4) (1998) 335–345.
- [117] O. Kilian, P. G. Kroth, Identification and characterization of a new conserved motif within the presequence of proteins targeted into complex diatom plastids, *Plant J.* 41 (2) (2005) 175–183.
- [118] S. Savikhin, Ultrafast optical spectroscopy of photosystem I, in: J. H. Golbeck (Ed.), *Photosystem I The Light-Driven Plastocyanin:Ferredoxin Oxidoreductase*, Vol. 24, Springer Netherlands, 2006, Ch. 12, pp. 155–175.
- [119] A. S. Sun, K. Sauer, Pigment systems and electron transport in chloroplasts I. Quantum requirements for the two light reactions in spinach chloroplasts, *Biochim. Biophys. Acta* 234 (3) (1971) 399–414.
- [120] E. G. Andrizhiyevskaya, T. M. E. Schwabe, M. Germano, S. D’Haene, J. Kruij, R. van Grondelle, J. P. Dekker, Spectroscopic properties of PSI-IsiA supercomplexes from the cyanobacterium *Synechococcus* PCC 7942, *Biochim. Biophys. Acta* 1556 (2-3) (2002) 265 – 272.
- [121] N. V. Karapetyan, A. R. Holzwarth, M. Rögner, The photosystem I trimer of cyanobacteria: molecular organization, excitation dynamics and physiological significance, *FEBS Lett.* 460 (3) (1999) 395–400.
- [122] M. Byrdin, I. Rimke, E. Schlodder, D. Stehlik, T. A. Roelofs, Decay kinetics and quantum yields of fluorescence in photosystem I from *Synechococcus elongatus* with P700 in the reduced and oxidized state: are the kinetics of excited state decay trap-limited or transfer-limited?, *Biophys J* 79 (2) (2000) 992–1007.
- [123] R. Croce, G. Zucchelli, F. M. Garlaschi, R. Bassi, R. C. Jennings, Excited state equilibration in the photosystem I-light-harvesting I complex: P700 is almost isoenergetic with its antenna, *Biochemistry* 35 (26) (1996) 8572–8579.

- [124] L.-O. Pålsson, J. P. Dekker, E. Schlodder, R. Monshouwer, R. Grondelle, Polarized site-selective fluorescence spectroscopy of the long-wavelength emitting chlorophylls in isolated photosystem I particles of *Synechococcus elongatus*, *Photosynth. Res.* 48 (1) (1996) 239–246.
- [125] M. Rätsep, T. W. Johnson, P. R. Chitnis, G. J. Small, The red-absorbing chlorophyll a antenna states of photosystem I: A hole-burning study of *Synechocystis* sp. PCC 6803 and its mutants, *J. Phys. Chem. B* 104 (4) (2000) 836–847.
- [126] B. Gobets, I. H. van Stokkum, M. Rögner, J. Kruij, E. Schlodder, N. V. Karapetyan, J. P. Dekker, R. van Grondelle, Time-resolved fluorescence emission measurements of photosystem I particles of various cyanobacteria: A unified compartmental model, *Biophys. J.* 81 (1) (2001) 407 – 424.
- [127] R. Croce, T. Morosinotto, J. A. Ihalainen, A. Chojnicka, J. Breton, J. P. Dekker, R. van Grondelle, R. Bassi, Origin of the 701-nm fluorescence emission of the lhca2 subunit of higher plant photosystem I, *J. Biol. Chem.* 279 (47) (2004) 48543–48549.
- [128] J. A. Ihalainen, F. Klimmek, U. Ganeteg, I. H. M. van Stokkum, R. van Grondelle, S. Jansson, J. P. Dekker, Excitation energy trapping in photosystem I complexes depleted in lhca1 and lhca4, *FEBS Lett.* 579 (21) (2005) 4787–4791.
- [129] B. Gobets, R. van Grondelle, Energy transfer and trapping in photosystem I, *Biochim. Biophys. Acta* 1507 (1-3) (2001) 80–99.
- [130] J. A. Ihalainen, B. Gobets, K. Sznee, M. Brazzoli, R. Croce, R. Bassi, R. van Grondelle, J. E. I. Korppi-Tommola, J. P. Dekker, Evidence for two spectroscopically different dimers of light-harvesting complex I from green plants, *Biochemistry* 39 (29) (2000) 8625–8631.

- [131] M. Mimuro, T. Ookubo, D. Takahashi, T. Sakawa, S. Akimoto, I. Yamazaki, H. Miyashita, Unique fluorescence properties of a cyanobacterium *Gloeobacter violaceus* PCC 7421: Reasons for absence of the long-wavelength PSI Chl a fluorescence at -196 °C, *Plant Cell Physiol.* 43 (6) (2002) 587–594.
- [132] Z. Gardian, L. Bumba, A. Schrofel, M. Herbstova, J. Nebesarova, F. Vacha, Organisation of photosystem I and photosystem II in red alga *Cyanidium caldarium*: encounter of cyanobacterial and higher plant concepts, *Biochim. Biophys. Acta* 1767 (6) (2007) 725–731.
- [133] S. Kereiche, R. Kouril, G. T. Oostergetel, F. Fusetti, E. J. Boekema, A. B. Doust, C. D. van der Weij-de Wit, J. P. Dekker, Association of chlorophyll a/c2 complexes to photosystem I and photosystem II in the cryptophyte *Rhodomonas* CS24, *Biochim. Biophys. Acta* 1777 (9) (2008) 1122–1128.
- [134] C. Tack, Isolation und Charakterisierung von Photosystem II-Komplexen aus der Diatomee *Cyclotella meneghiniana*, Diploma Thesis, University of Frankfurt (2008).
- [135] Y. Fujita, K. Ohki, On the 710 nm fluorescence emitted by the diatom *Phaeodactylum tricornutum* at room temperature, *Plant Cell Physiol.* 45 (4) (2004) 392–397.
- [136] R. F. Strzepek, P. J. Harrison, Photosynthetic architecture differs in coastal and oceanic diatoms, *Nature* 431 (7009) (2004) 689–692.
- [137] M. Westermann, E. Rhiel, Localisation of fucoxanthin chlorophyll a/c-binding polypeptides of the centric diatom *Cyclotella cryptica* by immuno-electron microscopy, *Protoplasma* 225 (3-4) (2005) 217–223.
- [138] F. Savard, C. Richard, M. Guertin, The *Chlamydomonas reinhardtii* LI818 gene

- represents a distant relative of the *cabl/II* genes that is regulated during the cell cycle and in response to illumination, *Plant Mol. Biol.* 32 (3) (1996) 461–473.
- [139] A. Oeltjen, J. Marquardt, E. Rhiel, Differential circadian expression of genes *fcp2* and *fcp6* in *Cyclotella cryptica*, *Int. Microbiol.* 7 (2) (2004) 127–131.
- [140] D. Elrad, A. R. Grossman, A genome's-eye view of the light-harvesting polypeptides of *Chlamydomonas reinhardtii*, *Curr. Genet.* 45 (2) (2004) 61–75.
- [141] J. Lavaud, B. Rousseau, H. J. van Gorkom, A.-L. Etienne, Influence of the diadinoxanthin pool size on photoprotection in the marine planktonic diatom *Phaeodactylum tricornutum*, *Plant Physiol.* 129 (3) (2002) 1398–1406.
- [142] E. G. Andrizhiyevskaya, A. Chojnicka, J. A. Bautista, B. A. Diner, R. van Grondelle, J. P. Dekker, Origin of the F685 and F695 fluorescence in photosystem II, *Photosynth. Res.* 84 (1-3) (2005) 173–180.
- [143] E. Krausz, J. L. Hughes, P. J. Smith, R. J. Pace, S. P. Arsköld, Assignment of the low-temperature fluorescence in oxygen-evolving photosystem II, *Photosynth. Res.* 84 (1-3) (2005) 193–199.
- [144] E. Krausz, J. L. Hughes, P. Smith, R. Pace, S. P. Arsköld, Oxygen-evolving photosystem II core complexes: a new paradigm based on the spectral identification of the charge-separating state, the primary acceptor and assignment of low-temperature fluorescence, *Photochem. Photobiol. Sci.* 4 (9) (2005) 744–753.

7 Acknowledgements

First of all I would like to thank Prof. Dr. C. Büchel for giving me the opportunity to do my thesis in her group. Her constant support, understanding, advice, and her trust especially before my start laid the grounds not only for this work but for one of my most important decisions, so far.

I would also like to express my thanks to Prof. Dr. E. Schleiff for accepting to co-review this thesis.

Additionally, the whole Plant Cell Physiology crew, including former members should be mentioned here. The friendly and positive atmosphere created a nice environment to work. At this point I would like to emphasise the efforts of C. van Oijen, Dr. M. Schmidt, and K. Pieper who keep (not only) the lab running.

Furthermore, staff and administration should be included in this list, especially Dr. M. Fauth, L. Jung, A. Meier, and Dr. M. Weil.

I will not forget former and present TEM specialists M. Basoglu and S. Münzner. After hours in the dark in front of lenses and a screen your help and invitations to coffee and/or (scientific) chat were always welcome.

Of course I would like to express my gratitude to my former PhD mates Anja, Dario, Kathi and Holger. Whether in the lab, office or beside the barbeque - it was a pleasure

to spend my time with you. Here, I also want to acknowledge the "new" PhD students Anja and Jidnyasa. I thank all of you.

Thanks also to all the students I had the opportunity to work with. Probably I learned more from you than you from me.

Special thanks go out to Dr. P. Lambrev and Dr. W. Keegstra for their help and work on the GRIP installation.

Last but definitely not least I would like to express my deepest gratitudes to Sabine. For everything...

I dedicate this thesis to my parents.

8 Curriculum vitae

Personal information

Surname	Veith
First name	Thomas
Adress	Saalburgstraße 30, 60385 Frankfurt am Main
Phone	+49-(0) 69-15 04 91 19
E-Mail	thomasveith@email.de
Nationality	German
Birth	25 July 1978, Frankfurt am Main, Germany

Employment

Since 03/2009	Postdoctoral position at the Institute of Molecular Biology, Johann Wolfgang Goethe–University, Frankfurt under supervision of Prof. Dr. Jens Wöhnert (RNA-structure biology)
01/2005 – 02/2009	Research associate at the Institute of Molecular Biology, Johann Wolfgang Goethe–University, Frankfurt and start of my PhD thesis about "Biochemical Characterisation of Photosystem I Complexes in Diatoms" under supervision of Prof. Dr. C. Büchel (Plant Cell Physiology)
01/2004 – 11/2004	Research associate at the Institute of Molecular Biology, Johann Wolfgang Goethe–University, Frankfurt un-

der supervision of Prof. Dr. H. D. Osiewacz (Molecular Developmental Biology and Biotechnology)

2002 – 2003 Students' tutor at the department of Biological Sciences of Johann Wolfgang Goethe–University, Frankfurt

2000 – 2003 Tutor at "Schülerhilfe" (a tutoring centre) for Natural Sciences, German, and English

Education

January 2007 Attendance on the Intro2 practical course on single particle analysis at the University of Groningen, Netherlands

September 2005 Attendance on the EMBO practical course on image processing for cryo–electron microscopy at the ISMB, Birkbeck College in London, England

11/2003 – 12/2003 Practical course at the Max Planck Institute of Biophysics, department of "Structural Biology" under supervision of Dr. C. Büchel

July 2003 Achievement of the academical grade "'Diplom-Biologe'" at the Johann Wolfgang Goethe–University (final grade: 1.8) under supervision of Prof. Dr. J. Feierabend

1998 – 2003 Student of biology science at Johann Wolfgang Goethe–University in Frankfurt

June 1998 Abitur (A-levels) at Ziehen Gymnasium (final grade: 2.4)

1989 – 1998 Higher education at the Ziehen Gymnasium in Frankfurt

1985 – 1989

Heinrich Seliger Elementary School in Frankfurt

Alternative service

1996 – 2003

Engagement at Technisches Hilfswerk (THW) (public technical aid and civil protection)

Publications

journals

T. Veith, C. Büchel, The monomeric photosystem I-complex of the diatom *Phaeodactylum tricornutum* binds specific fucoxanthin chlorophyll proteins (FCPs) as light-harvesting complexes, *Biochim. Biophys. Acta* 1767 (12) (2007) 1428–1435.

poster

Veith, T and Büchel, C: Isolation and characterisation of a PSI-FCP complex of the diatom *Phaeodactylum tricornutum*; P002, 2nd Joint German/UK Bioenergetics Conference - Integration of structures, spectroscopies and mechanisms, University of Edinburgh, UK, 2 - 4 April 2008.

Sonja Werner, Thomas Veith, Ansgar Gruber, Peter Kroth, Claudia Büchel, Harald Paulsen and Martin Lohr: Characterization of a Transgenic Diatom That Accumulates Chlorophyll b; P14: 3, 125 Jahre Deutsche Botanische Gesellschaft - Botanikertagung - 3 - 7 Sep 2007

Veith, T and Büchel, C: The monomeric photosystem I-complex of the diatom *Phaeodactylum tricornutum* binds specific fucoxanthin chlorophyll proteins (FCPs) as light-

harvesting complexes; published in: *Photosynth Res*; Volume: 91 Issue: 2-3, Feb-Mar 2007, Pages: 164-165, Meeting Abstract: PS331

Beer, A and Veith, T: Towards the Determination of the Structures of FCP and PSI Complexes in Diatoms; 3rd International Conference on Structure, Dynamics and Function of Proteins in Biological Membranes, Monte Verita, Ascona, Switzerland, 14 - 19 May 2006.